UNIVERSITATEA DIN BUCUREȘTI

NU XU

Doctor Honoris Causa

NU XU
DOCTOR HONORIS CAUSA

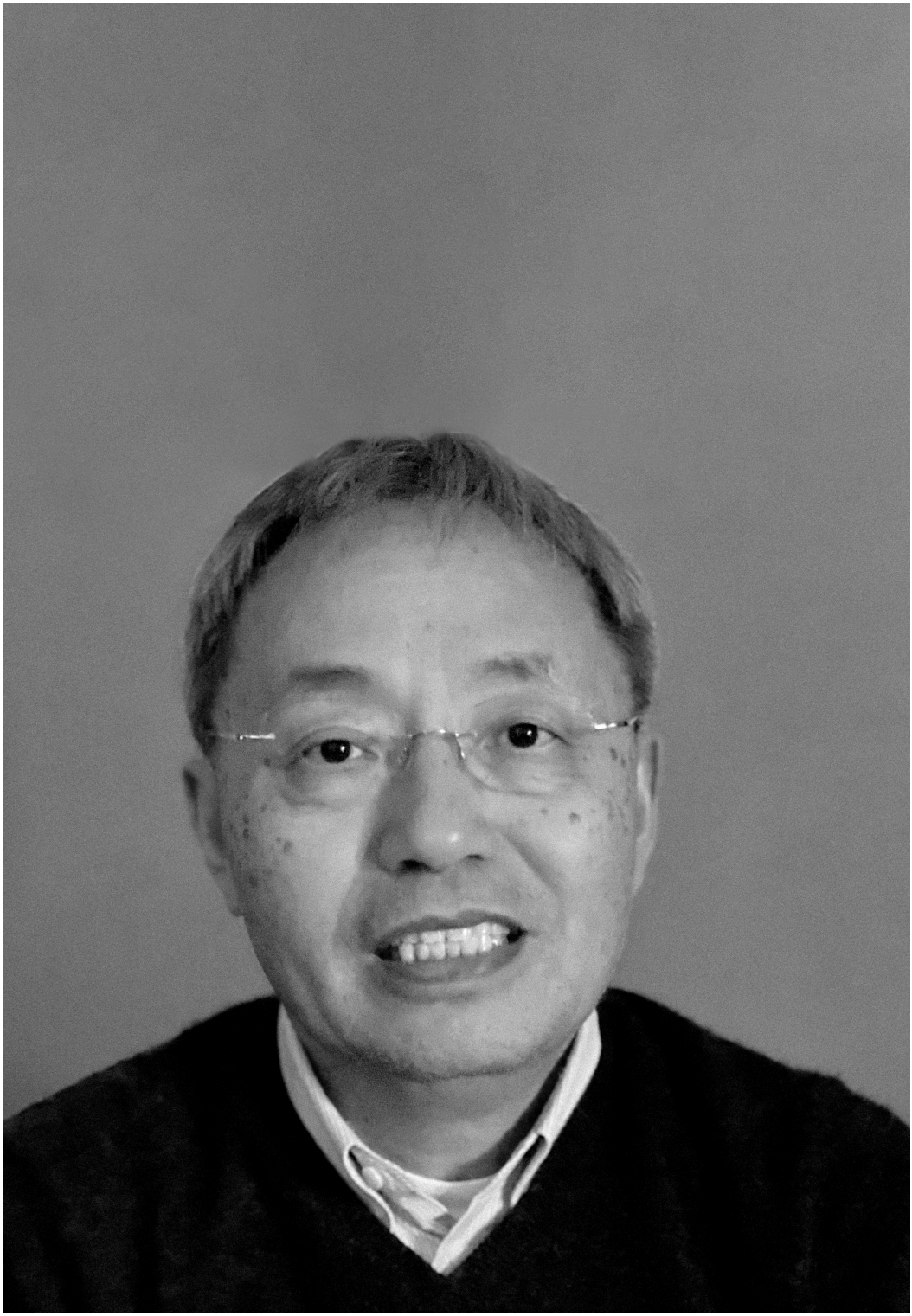

Profesorul Nu XU a contribuit semnificativ la dezvoltarea și testarea experimentală a predicțiilor modelului standard al fizicii particulelor pentru formarea plasmei de cuarci și gluoni, conexiuni dintre scenariul „Exploziei primordiale" (Big Bang) pentru Universul nostru și comportarea materiei nucleare extrem de fierbinți și de dense formată în regiunea de suprapunere a nucleelor care se ciocnesc la energii relativiste și ultrarelativiste, precum și a altor perspective moderne și teorii în fizica nucleară și a particulelor elementare, contribuind semnificativ la succesul diferitelor modele în descrierea structurii subnucleare și evoluțiilor cosmologice.

Laudatio | Profesor univ. dr. Nu Xu

Stimate Domnule Profesor Nu Xu,

Stimate Domnule Rector,

Stimate Domnule Președinte al Senatului Universității din București,

Stimați colegi,

Doamnelor și domnilor,

Dragi prieteni,

Profesorul **Nu XU** este una dintre personalitățile proeminente și remarcabile ale fizicii contemporane, activitatea sa având un impact substanțial în dezvoltarea fizicii nucleare relativiste și fizicii particulelor elementare, atât prin rezultate proprii prestigioase, cât și prin contribuții majore la dezvoltarea acestor domenii în SUA, China și în întreaga lume.

Profesorul Nu XU a absolvit Universitatea de Științe și Tehnologie din China, în anul 1982. A obținut titlul de Doctor în Fizică la Universitatea de Stat din New York la Stony Brook (SUA), în anul 1990, după un stagiu de cinci ani, început în anul 1985, sub îndrumarea Profesorului David Fossan.

În anii care au urmat susținerii tezei de doctorat, a făcut studii postdoctorale la Universitatea de Stat din New York la Stony Brook (SUA), între 1990 și 1994. După acest stagiu de studii postdoctorale, domnia sa și-a continuat activitatea de cercetare științifică în SUA. Între 1994 și 1997 a fost „Director Fellow" la Laboratorul Național din Los Alamos, SUA. În anul 1997, a devenit „Divisional Fellow" la Laboratorul Național „Lawrence" din Berkeley. Din anul 2001 este cercetător științific „superior" (gradul I) la același laborator național.

Din anul 2001 până în prezent, domnia sa a ocupat diferite funcții în instituții de prestigiu. De exemplu, din anul 2002, profesorul Nu XU este profesor adjunct la Universitatea de Știință și Tehnologie din China, evaluator extern al Academiei Chineze de Științe, din 2004, profesor invitat la Institutul de Fizică Aplicată din Shanghai, membru CAS, China, din 2008.

Din anul 2010, până în prezent, Profesorul Nu XU este decan la Colegiul de Științe Fizice și Tehnologie, Universitatea Normală din China Centrală, iar

din 2015 este profesor adjunct la Institutul Național de Educație Științifică și Cercetare din India.

Rezultatele excelente obținute în activitatea de cercetare științifică și academică au făcut ca domnia sa să fie membru în comitetele editoriale ale mai multor reviste de prestigiu din domeniul fizicii. Profesorul Nu XU este membru în comitetele editoriale ale unor reviste precum *Journal of Physics G: Nuclear and Particle Physics, IoP*, UK (2004–2014), *Nuclear Physics A* ș.a.m.d. Este membru al comitetului editorial al Editurii „Elsevier", fiind editor supervizor/ supraveghetor din 2014 până în prezent.

Calitățile științifice, precum și abilitățile administrative i-au permis domnului profesor Nu XU să ocupe funcția de coordonator responsabil al unei colaborări/ *spokesperson*. Printre cele mai importante colaborări la care a deținut această funcție este colaborarea STAR de la *Collider-ul de Ioni Grei Relativiști* (**R**elativistic **H**eavy **I**on **C**ollider (RHIC), Brookhaven National Laboratory (BNL), SUA, între 2008 și 2014.

De asemenea, profesorul Nu XU este membru al comitetelor de organizare sau științifice ale unor conferințe internaționale de prestigiu din domeniul fizicii nucleare relativiste și ultrarelativiste, inclusiv în cel al celei mai importante dintre ele, și anume: *Quark Matter Conference* (din 2008, până în prezent).

Cunoașterea profundă a domeniului, experiența, calitățile științifice remarcabile, integritatea și echilibrul au fost apreciate în mod deosebit de comunitatea științifică internațională. De aceea, a fost inclus în comitete internaționale de avizare ale celor mai importante institute internaționale, și anume: Centrul Internațional Helmholtz pentru FAIR (Helmholtz International Center for FAIR (HIC for FAIR), Germania (2009 – prezent); Comitetul de Avizare, Centrul de Analiză și Teorie pentru Experimente cu Ioni Grei, BNL, SUA (Advisory Board, Center for Analysis and Theory of Heavy Ion Experiments, BNL), SUA (2007 – prezent); Comitetul Internațional de Evaluare a Experimentelor de Fizica energiilor Înalte, de la IUCN Dubna (PAC, High Energy Physics, Joint Institute for Nuclear Research, Russia), din 2009 până în prezent, Comitetul de Avizare de pe lângă Comitetul de Știință și Tehnologie pentru HIAF (Advisory Board,

Committee of Science and Technology for HIAF), din 2016 până astăzi.

În întreaga sa carieră științifică, domnul profesor univ. dr. Nu XU a fost un participant activ la soluționarea problemelor comunității științifice internaționale. De aceea, a fost ales în diferite funcții în asociații internaționale ale fizicienilor. De exemplu, în anul 2017 a fost ales Președintele Organizației Internaționale a Fizicienilor și Astronomilor Chinezi. Este și în prezent președintele acestei organizații.

Profesorul Nu XU a contribuit semnificativ la dezvoltarea și testarea experimentală a predicțiilor modelului standard al fizicii particulelor pentru formarea plasmei de cuarci și gluoni, conexiuni dintre scenariul „Exploziei primordiale" (Big Bang) pentru Universul nostru și comportarea materiei nucleare extrem de fierbinți și de dense formată în regiunea de suprapunere a nucleelor care se ciocnesc la energii relativiste și ultrarelativiste, precum și a altor perspective moderne și teorii în fizica nucleară și a particulelor elementare, contribuind semnificativ la succesul diferitelor modele în descrierea structurii subnucleare și evoluțiilor cosmologice.

Activitatea științifică a domnului Profesor Nu XU a fost recunoscută prin publicarea unui număr impresionant de lucrări în cele mai prestigioase reviste de fizică din domeniu. Până în prezent, Profesorul Nu XU a publicat peste 500 de lucrări în reviste cotate ISI, domnia sa având un indice Hirsh de 88, având peste 31,425 citări. De aceea, Profesorul Nu XU este una dintre cele mai productive personalități în domeniul fizicii nucleare la energii înalte din lume.

Rezultatele de excepție obținute de profesorul Nu XU au fost foarte apreciate și, de aceea, domnia sa a primit numeroase premii și a fost ales în diferite organizații profesionale de prestigiu. Câteva dintre acestea sunt următoarele:

– 2004: membru al Institutului de Fizică (*The Institute of Physics*), Marea Britanie
– 2009: membru al Societății American de Fizică, SUA
– 2010: 1000 – Talent Plan, China
– 2018: membru ales al Academiei Europene

De asemenea, este referent al celor mai importante reviste de specialitate din domeniu, cum ar fi: *Physical Review Letters, Physics Letters B, Physical Review C.* Este editor al *Progress in Particle and Nuclear Physics* (Elsevier), *Science China Physics, Mechanics and Astronomy* (CAS, China), dar și membru al Comitetului Editorial de Avizare pentru Știință și Tehnici Nucleare din China (CAS, China).

De-a lungul timpului, prof. univ. dr. Nu XU a colaborat în cadrul diferitelor experimente cu fizicieni români, cum ar fi marile experimente de la RICH-BNL (SUA) și FAIR-GSI (Germania). În aceste colaborări, fizicieni români de la Facultatea de Fizică a Universității din București, Institutul de Științe Spațiale, Institutul de Fizică și Inginerie Nucleară „Horia Hulubei" s-au implicat profund, ceea ce a permis publicarea unui număr mare de articole științifice în reviste de prestigiu din domeniul fizicii, în particular din domeniul fizicii nucleare și particulelor elementare.

Profesor univ. dr. Nu XU a susținut continuu cercetarea științifică din România în domeniul fizicii nucleului și particulelor elementare. Ca purtător de cuvânt al câtorva colaborări internaționale, și președinte al CBM Experiment Collaboration Board la FAIR-GSI Darmstadt (Germania), Profesorul Nu XU a încurajat permanent prezență fizicienilor români în aceste colaborări și instituții. De aceea, fizicieni români, membri ai corpului didactic al Universității din București și studenți la diferite cicluri de studii universitare, au făcut vizite la aceste institute, au avut stagii de lucru și/ sau au prezentat seminarii. Profesor univ. dr. Nu XU și grupul său au contribuit la organizarea unor școli de vară și conferințe în domeniul fizicii nucleare și particulelor elementare și prin calitatea cursurilor și a lucrărilor prezentate, care au contribuit semnificativ la prestigiul științific al acestor școli și conferințe din domeniu.

Întreaga activitate științifică și administrativă a profesorului Nu XU este caracterizată de o creativitate profundă, intuiție în rezolvarea unor probleme științifice, concentrare continuă pe concepte fundamentale, simple, dar esențiale pentru înțelegerea proceselor și fenomenelor fizice. Contribuția sa fundamentală și profundă la dezvoltarea fizicii nucleare relativiste și fizicii particulelor este legată de combinația dintre abilități experimentale de

excepție, înțelegerea profundă a aspectelor teoretice implicate și o intuiție remarcabilă.

Acordarea titlului de *Doctor Honoris Causa* al Universității din București domnului profesor univ. dr. Nu XU reprezintă o recunoaștere simbolică a marilor sale merite științifice și un pas înainte în direcția creșterii colaborărilor științifice și educaționale dintre Universitatea din București, universități din China, institute americane și europene, precum și cele dintre oamenii de știință din întreaga lume.

Director de Departament,
Prof. unv. dr. Alexandru JIPA

Dear Professor Nu Xu,
Dear Rector,
Dear President of the University Senate,
Dear colleagues,
Ladies and gentlemen,
Dear friends,

Professor **Nu XU** is one of the most prominent and remarkable personalities of contemporary Physics, his activities had a substantial impact on the development of Relativistic Nuclear Physics and Particle Physics, both through his own prestigious results and major contributions to the scientific development in the USA, China and in the world.

Professor Nu XU graduated from the University of Science and Technology of China, in 1982. He obtained his Ph.D. title from the State University of New York at Stony Brook (USA) in 1990 under the supervision of Professor David Fossan, after five years of study beginning in 1985. In the following years, he was a Postdoctoral Fellow at the State University of New York at Stony Brook, USA, from 1990 to 1994. After this stage, he continued his research activities in the USA, serving as Director Fellow at Los Alamos National Laboratory from 1994 to 1997 and as Divisional Fellow at Lawrence Berkeley National Laboratory from 1997 to 2001. Since 2001, Professor Nu XU has been a Senior Staff Scientist at Lawrence Berkeley National Laboratory, USA.

Since 2001 he has occupied different positions. For example, since 2002, Professor Nu XU has been an Adjunct Professor at the University of Science and Technology of China, an Overseas Assessor at the Chinese Academy of Sciences of China since 2004, and a Guest Professor at the Shanghai Institute of Applied Physics, CAS, China since 2008. Since 2010, Professor Nu XU has been Dean at the College of Physical Science and Technology, Central China Normal University, and since 2015 he has been an Adjunct Professor at the National Institute of Science Education and Research, India.

The excellent results obtained from his research and academic activities recommended Professor Nu XU as a member of the Editorial Boards of some prestigious Physics journals. It is important to mention here the Journal of Physics G: Nuclear and Particle Physics, IoP, UK (2004-2014), Nuclear Physics A. Since 2014, he has been a member and Supervisory Editor of the Editorial Board, Elsevier.

The scientific qualities, as well as the administrative abilities allowed Professor Nu XU to occupy the spokesperson position at one of the most important collaborations from the Relativistic Heavy Ion Collider (RHIC), Brookhaven National Laboratory (BNL), USA, namely: the STAR Experiment (2008–2014).

Professor Nu XU is a member of the boards of some important conferences in the Relativistic and Ultrarelativistic Heavy Ion Physics field: member of International Advisory Committee for Quark Matter Conference (2008 – present).

The deep knowledge of the field, expertise, outstanding scientific qualities, probity, and equilibrium were very well appreciated by the international scientific community. Therefore, he was included in international advisory committees at the most important international institutes, namely: Helmholtz International Center for FAIR (HIC for FAIR), Germany (2009 – present); Advisory Board, Center for Analysis and Theory of Heavy Ion Experiments, BNL, USA, (2007 – now); PAC, High Energy Physics, Joint Institute for Nuclear Research, Russia (2009 – present), Advisory Board, Committee of Science and Technology for HIAF (2016 – now).

In his entire scientific career, Professor Nu XU has been an active participant in the solving of the problems of the scientific community. Therefore, he was elected in different positions in international associations of physicists. For example, since 2017, he has been President of the International Organization of Chinese Physicists and Astronomers.

Professor Nu XU has contributed significantly to the development and experimental testing of the predictions of the Standard Model for quark-gluon plasma formation, connections among the Big Bang scenario for our Universe with the behaviour of the very hot and very dense nuclear matter formed in the overlapping region of the colliding nuclei at relativistic and ultrarelativistic energies, as well as at other modern perspectives and theories in Nuclear and Particle Physics, contributing significantly to the success of different models in the description of the subnuclear structure and cosmological descriptions.

The scientific activity of Professor Nu XU has been published in many prestigious Physics journals. Professor Nu XU has published over 503 papers in ISI-cited journals. Professor Nu XU has a Hirsh Index of 88 and over 31,425 citations. Therefore, he is one of the most productive personalities in the field of Nuclear and Particle Physics at high energies in the World.

The outstanding results obtained by Professor Nu XU were very well appreciated and he received many awards. A few of these awards are the following:

– 2004: Fellow of the Institute of Physics, UK;
– 2009: Fellow of the American Physical Society Fellow;
– 2010: 1000-Talent Plan, China;
– 2018: Elected Member of the Academia Europaea.

Also, he is the referee for the most important journals in the field, such as “Physical Review Letters”, “Physics Letters B”, “Physical Review C”, or editor of “Progress in Particle and Nuclear Physics” (Elsevier), “Science China Physics, Mechanics and Astronomy” (CAS, China), member of Advisory Editor Board of “Nuclear Science and Techniques” (CAS, China)

During this time, Professor Nu XU collaborated in the frame of different experiments with Romanian physicists, including large experiments from RHIC-BNL and FAIR-GSI. In these collaborations, Romanian

physicists from the Faculty of Physics, University of Bucharest, Institute of Space Science, "Horia Hulubei" National Institute for Nuclear Physics and Engineering were involved, and large numbers of papers have been published in prestigious Physics journals.

Professor Nu XU permanently sustained the Nuclear and Particle Physics research in Romania. As the spokesperson of some international collaborations, and president of the CBM Experiment Collaboration Board, at FAIR-GSI, Germany, Professor Nu XU permanently encouraged the presence of Romanian physicists in these collaborations and institutes. Therefore, Romanian physicists, members of the academic staff at the University of Bucharest, and researchers visited, had work stages and presented seminars there. Professor Nu XU and his groups have contributed, during this time, to the organization of summer schools and conferences in the Nuclear and Particle Physics field, and by the quality of the lectures and works presented here, which have contributed significantly to the scientific prestige of these schools and conferences in Nuclear and Particle Physics.

The entire scientific and administrative activity of Professor Nu XU is characterized by great and profound creativity, scientific intuition, permanently focused on fundamental concepts, simple but essential for the understanding of physical phenomena and processes. His fundamental and profound contribution to the development of Relativistic Nuclear Physics and Particle Physics is related to the unique combination of outstanding experimental skills with deep theoretical understanding and remarkable intuition.

The awarding of the title of *Doctor Honoris Causa* by the University of Bucharest to Professor Nu XU represents a symbolic recognition of his great scientific merits and further promotes scientific and teaching collaborations between the University of Bucharest and Chinese Universities, American European institutes and the global scientific community.

Director of Department,
Prof. unv. dr. Alexandru JIPA

Curriculum vitae | Profesor univ. dr. Nu Xu

Lawrence Berkeley National Laboratory
http://www-rnc.lbl.gov/~nxu/

EDUCATION

1978 – 1982: B.S., University of Science and Technology of China, China
1985 – 1990: Ph.D., State University of New York at Stony Brook, USA

EXPERIENCE

1990–1994: Postdoctoral Fellow, State University of New York at Stony Brook, USA 1994 – 1997: Director Fellow, Los Alamos National Laboratory, USA
1997–2001: Divisional Fellow, Lawrence Berkeley National Laboratory, USA 2001 – now: Senior Scientist, Lawrence Berkeley National Laboratory, USA
2010 – now: Adjunct Professor, University of Science and Technology of China, China 2015 – now: Adjunct Professor, National Institute of Science Education and Research, India
2008–2014: Spokesperson, STAR Experiment at RHIC, USA
2009–2018: PAC, High Energy Physics, Joint Institute for Nuclear Research, Russia 2009 – 2018: IPAC, Helmholtz International Center for FAIR (HIC for FAIR), Germany
2017–2018: President, "International Organization of Chinese Physicists and Astronomer" 2017–2022: PAC, High Energy Physics, J-PARC, Japan
2018 – now: Chair, Institutional Board, CBM Experiment at FAIR, Germany

AWARDS

2004: Fellow of The Institute of Physics, UK 2009: American Physical Society Fellow, USA 2018: Member of the Academia Europaea, UK
2022: Humboldt Prize, Alexander von Humboldt Foundation of Germany

SERVICE WORK

– **Referee:** Phys. Rev. Lett.; Phys. Rev. **C**; Phys. Lett. **B**.
– **Editor:** Progress in Particle and Nuclear Physics, Elsevier
– Supervisory Editor, Nuclear Physics **A** Editorial Board, Elsevier

Publications | Profesor univ. dr. Nu Xu

MS70R0319, Nuclear Science Division, Lawrence Berkeley National Laboratory

1 Cyclotron Road, Berkeley, CA 94720, USA

Publications

† Principle Author, Proceedings are not included

1. Collective oblate band in ^{131}La due to the rotational alignment of $h_{11/2}$ neutrons
E.S. Paul, C.W. Beausang, D.B. Fossan, R. Ma, W.F. Piel, Jr., N. Xu, L. Hildingsson, and G.A. Leander, Phys. Rev. Lett. **58**, 984(1987).
2. Band-crossings in the γ-soft nucleus ^{136}Nd
E.S. Paul, C.W.Beausang, D.B. Fossan, R. Ma, W.F. Piel, Jr., and N. Xu, Phys. Rev. **C36**, 153(1987).
3. Collective band structures in the odd-proton nuclei ^{135,137}Pm
C.W. Beausang, D.B. Fossan, L. Hildingsson, E.S. Paul, W.F. Piel, Jr., P.K. Weng, and N. Xu, Phys. Rev. **C36**, 602(1987).
4. Observation of both $h_{11/2}$ proton and neutron alignments in ^{139}Pm
† N. Xu, C.W. Beausang, D.B. Fossan, E.S. Paul, W.F. Piel, Jr., P.K. Weng, E. Gülmez, and J.A. Cizewski, Phys. Rev. **C36**, R 1649(1987).
5. Collective bands in the doubly-odd nuclei ^{136}Pm and ^{134}Pr
† C.W. Beausang, L. Hildingsson, E.S. Paul, W.F. Piel, Jr., P.K. Weng, N. Xu, and D.B. Fossan, Phys. Rev. **C36**, 1810(1987).
6. High-spin states in doubly-odd ^{130}La
† E.S. Paul, C.W. Beausang, D.B. Fossan, R. Ma, W.F. Piel, Jr., N. Xu and L. Hildingsson, Phys. Rev. **C36**, 1853(1987).
7. Rotational bands in ^{133}Ce
R. Ma, E.S. Paul, C.W. Beausang, S. Shi, N. Xu, and D.B. Fossan, Phys. Rev. **C36**, 2322(1987).
8. Band-crossings in even-even ^{138}Sm and ^{134}Nd
E.S. Paul, S. Shi, C.W. Beausang, D.B. Fossan, R. Ma, W.F. Piel, Jr., and N. Xu, Phys. Rev. **C36**, 2380(1987).
9. High-spin states of ^{99}Ag and ^{100}Cd
W.F. Piel, Jr., C.W. Beausang, D.B. Fossan, R. Ma, E.S. Paul, G. Scharff-Goldhaber, and N. Xu, Phys, Rev. **C37**, 1067(1988).
10. Band-structures in doubly-odd ^{132}Pr
S. Shi, C.W. Beausang, D.B. Fossan, R. Ma, E.S. Paul, N. Xu, and A.J. Kreiner, Phys. Rev. **C37**, 1478(1988).
11. Band-structures in doubly-odd ^{130}Pr
R. Ma, E.S. Paul, S. Shi, C.W. Beausang, W.F. Piel, Jr., N. Xu, D.B. Fossan, T. Chapuran, D.P. Balamuth, and J. Arrison, Phys. Rev. **C37**, 1926(1988).
12. Deformation-driving properties of the $\nu_{13/2}(660)1/2^+$ intruder orbital for A$\sim$130 nuclei
† E.S. Paul, R. Ma, C.W. Beausang, D.B. Fossan, W.F. Piel, Jr., S. Shi, N. Xu, and J.-y Zhang, Phys. Rev. Lett. **61**, 42(1988).
13. High spin states in ^{172}Ta and additivity of odd-N and odd-Z effects
A.J. Kreiner, D. Hojman, J. Davidson, M. Davidson, M. Debray, G. Facone, D. Santos, C.W. Beausang, D.B. Fossan, E.S. Paul, R. Ma, S. Shi, and N. Xu, Phys. Lett. **B215**, 629(1988).
14. The yrast band in doubly-odd ^{138}Eu
Y. Liang, K. Ahn, R. Ma, E.S. Paul, N. Xu, and D.B. Fossan, Phys. Rev. **C38**, 2432(1988).
15. Rotational bands in ^{140}Gd: Systematics of triaxial N = 76 isotones
E.S. Paul, K. Ahn, D.B. Fossan, Y. Liang, R. Ma, and N. Xu, Phys. Rev. **C39**, 153(1989).
16. Properties of shape-driving orbitals: Rotational bands in ^{131}La
L. Hildingsson, C.W. Beausang, D.B. Fossan, R. Ma, E.S. Paul, W.F. Piel, Jr., and N. Xu, Phys. Rev. **C39**, 471(1989).
17. Rotational states in neutron-deficient ^{139}Gd
R. Ma, K. Ahn, Y. Liang, E.S. Paul, N. Xu, and D.B. Fossan, Phys. Rev. **C39**, 530(1989).
18. Nilsson parameter set in the A $\approx$ 120 - 140 region
† Jing-ye Zhang, N. Xu, D.B. Fossan, Y. Liang, R. Ma, and E.S. Paul, Phys. Rev. **C39**, 714(1989).
19. High spin states in ^{137}Pr
† N. Xu, C.W. Beausang, R. Ma, E.S. Paul, D.B. Fossan, and L. Hildingsson, Phys. Rev. **C39**, 1799(1989).

20. High spin structure in ^{137}Sm: Role of the $\beta-$driving $\nu_{13/2}$ intruder in deformation enhancement
R. Ma, C.W. Beausagn, E.S. Paul, W.F. Piel, Jr., S. Shi, N. Xu, D.B. Fossan, J. Burde, M.A. Deleplanque, R.M. Diamond, A.O. Macchiavelli, and F.S. Stephens, Phys. Rev. **C40**, 156(1989).

21. Rotational bands in doubly-odd ^{128}Cs
E.S. Paul, D.B. Fossan, Y. Liang, R. Ma, and N. Xu, Phys. Rev. **C40**, 619(1989).

22. Band-crossings in ^{132}Ba
E.S. Paul, D.B. Fossan, Y. Liang, R. Ma, and N. Xu, Phys. Rev. **C40**, 1255(1989).

23. Coexistence of low-K prolate and high-K oblate $\pi h_{11/2}$ orbitals
Y. Liang, R. Ma, E.S. Paul, N. Xu, D.B. Fossan, Jing-ye Zhang, F. Dönau, Phys. Rev. Lett. **64**, 29(1990).

24. Competing proton and neutron rotational alignment: Band structures in ^{131}Ba
R. Ma, Y. Liang, E.S. Paul, N. Xu, D.B. Fossan, L. Hildingsson and R.A. Wyss, Phys. Rev. **C41**, 717(1990).

25. High-spin structure of N = 51 ^{96}Rh and ^{97}Pd: A shell-model study
W.F. Piel, Jr., D.B. Fossan, R. Ma, E.S. Paul, N. Xu, and J.B. McGrory, Phys. Rev. **C41**, 1223(1990).

26. High-spin states in ^{136}Ce: Systematics of collective oblate rotation
E.S. Paul, D.B. Fossan, Y. Liang, R. Ma, N. Xu, R. Wadsworth, I. Jenkins, and P.J. Nolan, Phys. Rev. **C41**, 1576(1990).

27. Evidence for the onset of reflection asymmetry in ^{216}Fr
M.E. Debary, J. Davidson, M. Davidson, A.J. Kreiner, D. Hojman, D. Santos, K. Ahn, D.B. Fossan, Y. Liang, R. Ma, E.S. Paul, W.F. Piel, Jr., and N. Xu, Phys. Rev. **C41**, R1895(1990).

28. Rotational bands in ^{135}Ce: Collective prolate and oblate rotation
R. Ma, E.S. Paul, D.B. Fossan, Y. Liang, N. Xu, R. Wadsworth, I. Jenkins, and P.J. Nolan, Phys. Rev. **C41**, 2624(1990).

29. High spin states in doubly-odd ^{122}Cs
† N. Xu, H.M. Latvakoski, Y. Liang, R. Ma, E.S. Paul, and D.B. Fossan, Phys. Rev. **C41**, 2681(1990).

30. An $i_{13/2}$ intruder band in ^{139}Gd
R. Ma, D.B. Fossan, E.S. Paul, N. Xu, P.H. Regan, R. Wadsworth, Y.-J. He, I. Jenkins, M. Metcalfe, S.M. Mullins, and P.J. Nolan, J. Phys., **G16**, 1233(1990).

31. Rotational band structures in doubly-odd ^{138}Pm
C.W. Beausang, P.K. Weng, R. Ma, E.S. Paul, W.F. Piel, Jr., N. Xu and D.B. Fossan, Phys. Rev. **C42**, 541(1990).

32. Rotational band structures in ^{127}Cs: Shape changes induced by $h_{11/2}$ neutron alignment
Y. Liang, R. Ma, E.S. Paul, N. Xu, and D.B. Fossan, Phys. Rev. **C42**, 890(1990).

33. Electro-magnetic properties of N = 75 isotones: evidence for triaxiality at low spin
E.S. Paul, R. Ma, C.W. Beausang, S.A. Forbes, D.B. Fossan, J. Gizon, J.R. Hughes, Y. Liang, S.M. Mullins, P.J. Nolan, W.F. Piel,Jr., P.J. Poynter, P.H. Regan, R. Wadsworth, and N. Xu, J. Phys. G:Nucl. Part. Phys. **17**, 605(1990).

34. Further evaluation of the fitted Nilsson parameters in the A $\approx$ 120 – 140 mass region
† N. Xu, Jing-ye Zhang, Y. Liang, R. Ma, E.S. Paul, and D.B. Fossan, Phys. Rev. **C42**, 1394(1990).

35. Lifetime measurements in ^{135}Sm: Large deformation in the N = 6 intruder band and evidence of quenched proton paring
P.H. Regan, R. Wadsworth, R. Wyss, D.B. Fossan, Y.-J. He, J.R. Hughes, I. Jenkins, R. Ma, M.S. Metcalfe, S.M. Mullins, P.J. Nolan, E.S. Paul, R.J. Poynter, and N. Xu, Phys. Rev. **C42**, 1805(1990).

36. High spin states in ^{141}Eu
† N. Xu, Y. Liang, R. Ma, E.S. Paul, and D.B. Fossan, Phys. Rev. **C43**, 2189(1991).

37. The neutron $i_{13/2}$ in A = 120 – 140 mass region
† Jing-ye Zhang and N. Xu, Phys. Rev. **C43**, 2449(1991).

38. Band termination in ^{121}I
Y. Liang, D.B. Fossan, J.R. Hughes, D.R. LaFosse, T. Lauritsen, R. Ma, E.S. Paul, P. Vaska, M.P. Waring, N. Xu, and R.A. Wyss, Phys. Rev. **C44**, R578(1991).

39. Collective properties of ^{129}Cs
L. Hildingsson, W. Klamra, Th. Lindblad, F. Liden, Y. Liang, R. Ma, E.S. Paul, N. Xu, D.B. Fossan, and J. Gascon, Z. Phys. **A340**, 29(1991).

40. High-spin spectroscopy of ^{119,121}I: prolate and oblate shape coexistence
Y. Liang, D.B. Fossan, J.R. Hughes, D.R. LaFosse, T. Lauritsen, R. Ma, E.S. Paul, P. Vaska, M.P. Waring, and N. Xu, Phys. Rev. **C45**, 1041(1992).

41. Electro-magnetic dissociation of relativistic ^{28}Si into $p+^{27}$Al
J. Barrette, *et al.*, [E814 Collaboration], Phys. Rev. **C45**, 2427(1992).

42. Measurement of the intrinsic quadrupole moments in the $\nu i_{13/2}$ bands of ^{135,137}Sm
P.H. Regan, R. Wadsworth, S.M. Mullins, J. Nyberg, A. Atac, S.A. Forbes, D.B. Fossan, Y.-J. He, J.R. Hughes, I. Jenkins, R. Ma, M.S. Metcalfe, P.J. Nolan, E.S. Paul, R.J. Poynter, D. Santonicio, A. Virtanen, and N. Xu, J. Phys. **G:** Nucl. Part. Phys., **18**, 847(1992).

43. Charged particle multiplicity in ^{28}Si + Al, Cu, and Pb reactions at E_{lab} = 14.6 GeV/u
J. Barrette, *et al.*, [E814 Collaboration], Phys. Rev. **C46**, 312(1992).

44. Prolate and oblate rotational bands in ^{136}Sm
E.S. Paul, S. Davis, P. Vaska, P.J. Bishop, S.A. Forbes, D.B. Fossan, Y-J He, J.R. Hughes, I. Jenkins, Y. Liang, R. Ma, M.S. Metcalfe, S.M. Mullins, P. Nolan, P.J. Poynter, P.H. Regan, R. Wadsworth, and N. Xu, J. Phys. **G:** Nucl. Part. Phys., **19**, 861(1993).

45. Anti-proton production in relativistic Si-Nucleus collisions
J. Barrette, *et al.*, [E814 Collaboration], Phys. Rev. Lett. **70**, 1763(1993).

46. E_T production in reactions with 11.4 AGeV ^{197}Au and 14.6 AGeV ^{28}Si beams
† J. Barrette, *et al.*, [E814 Collaboration], Phys. Rev. Lett. **70**, 2296(1993).

47. Baryon distributions in ultra-relativistic nucleus–nucleus collisions
† J. Barrette, *et al.*, [E814 Collaboration], Z. Physik, **C59**, 211(1993).

48. Near yrast states in doubly odd ^{214}Fr
M.E. Debray, A.J. Kreiner, J.M. Kesque, M. Ozafran, A. Romo, H. Somacal, M.E. Vazquez, J. Davidson, M. Davidson, D.B. Fossan, Y. Liang, E.S. Paul, R. Ma, W.F. Piel, Jr., and N. Xu, Phys. Rev. **C48**, 2246(1993).

49. Two charged particle and transverse energy correlations in the $Si + Pb$ collisions at 14.6 AGeV
J. Barrette, *et al.*, [E814 Collaboration], Phys. Rev. **C49**, 1669(1994).

50. Production of light nuclei in relativistic heavy-ion collisions
J. Barrette, *et al.*, [E814 Collaboration], Phys. Rev. **C50**, 1077(1994).

51. Evidence for expansion of a hot fireball from two-pion correlation for $Si + Pb$ collisions at AGS energy
† J. Barrette, *et al.*, [E814 Collaboration], Phys. Lett. **B333**, 33(1994).

52. Observation of anisotropic event shapes and directed flow in $Au + Au$ collisions at AGS energy
J. Barrette, *et al.*, [E877 Collaboration], Phys. Rev. Lett. **73**, 2532(1994).

53. Centrality dependence of baryon distributions in ultra-relativistic nuclear collisions
† J. Barrette, *et al.*, [E814 Collaboration], Phys. Rev. **C50**, 3047(1994).

54. m_T dependence of Boson interferometry in heavy ion collisions at the CERN SPS
† H. Beker, *et al.*, [NA44 Collaboration], Phys. Rev. Lett. **74**, 3340(1995).

55. Thermal equilibration and expansion in nucleus-nucleus collisions at the AGS
† P. Braun-Munzinger, J. Stachel, J. Wessels, and N. Xu, Phys. Lett. **B344**, 43(1995).

56. Electro-magnetic dissociation of relativistic ^{28}Si
J. Barrette, *et al.*, [E814 Collaboration], Phys. Rev. **C51**, 865(1995).

57. Production of neutron-rich isotopes from the fragmentation of ^{28}Si projectiles at p_{lab} = 14.6 GeV/c per nucleon
J. Barrette, *et al.*, [E814 Collaboration], Phys. Rev. **C52**, 956(1995).

58. The relationship between correlation function fit parameters and source distributions
† D.E. Fields, J.P. Sullivan, J. Simon-Gillo, H. van Hecke, B.V. Jacak, and N. Xu, Phys. Rev. **C52**, 986(1995).

59. Charged particle pseudo-rapidity distributions in $Au + Al$, Cu, Au, and U collisions at 10.8 AGeV
J. Barrette, *et al.*, [E877 Collaboration], Phys. Rev. **C51**, 3309(1995).

60. Performance of a prototype RICH detector using a CsI hotocathode readout
B. Surrow, T.K. Hemmick, B. Hong, T. Piazza, N. Xu, A.D. Frawley, L. Wright, Y. Akiba, H. Hamagaki, R. Hayano, and K. Itahashi, NIM **A355**, 342(1995).

61. Measurements of pion enhancement at low transverse momentum and of the Δ resonance abundance in Si-nucleus collisions
† J. Barrette, *et al.*, [E814 Collaboration], Phys. Lett. **B351**, 93(1995).

62. Search for pion-neutron bound states in 14.6 AGeV Si + nucleus collisions
J. Barrette, *et al.*, [E814 Collaboration], Phys. Rev. **C52**, 2679(1995).

63. Hadron distributions - recent results from the CERN experiment NA44
† N. Xu *et al.*, [NA44 Collaboration], Nucl. Phys. **A610**, 175c(1996).

64. Thermal and hadrochemical equilibration in nucleus-nucleus collisions at the SPS
† P. Braun-Munzinger, J. Stachel, J. Wessels, and N. Xu, Phys. Lett. **B365**, 1(1996).

65. Low pt phenomena in A+A and p+A collisions
† H. Bøggild, *et al.*, [NA44 Collaboration], Z. Phys. **C69**, 621(1996).

66. Coulomb effect in single particle distributions
† H. Böggild, *et al.*, [NA44 Collaboration], Phys. Lett. **B372**, 399(1996).

67. Mid-rapidity protons in 158 AGeV Pb+Pb collisions
† H. Böggild, *et al.*, [NA44 Collaboration], Phys. Lett. **B388**, 431(1996).

68. On the m_T-dependence of Bose-Einstein correlation radii
† B.R. Schlei and N. Xu, Phys. Rev. **C54**, R2155(1996).

69. Energy and charged particle flow in Ultra-relativistic $Au + Au$ collisions
J. Barrette, *et al.*, [E877 Collaboration], Phys. Rev. **C55**, 1420(1997).

70. Collective expansion in high energy heavy ion collisions
† I.G. Bearden, *et al.*, [NA44 Collaboration] , Phys. Rev. Lett. **78**, 2080(1997).

71. Transverse flow at the SPS
† S. Esumi, S. Chapman, H. van Hecke, and N. Xu, Phys. Rev. **C55** R2161(1997).

72. Collective flow or random walk?
† S. Esumi, U. Heinz, and N. Xu, Phys. Lett. **B403**, 145(1997).

73. Two-pion correlations in $Au + Au$ collisions at 10.8 GeV per nucleon
J. Barrette, *et al.*, [E814/E877 Collaboration], Phys. Rev. Lett. **78**, 2916(1997).

74. Multiplicity dependence of the pion source in $S + A$ collisions at the CERN SPS
K. Kaimi, *et al.*, [NA44 Collaboration], Z. Phys., **C75**, 619(1997).

75. Proton and pion production relative to the reaction plane in $Au + Au$ collisions at ASG energies
J. Barrette, *et al.*, [E814/E877 Collaboration], Phys. Rev. **C56**, 3254(1997).

76. Relative space-time asymmetries in pion and nucleon production in non-central nucleus-nucleus collisions at high energies
† S. Voloshin, R. Lednicky, S. Panitkin, and Nu Xu, Phys. Rev. Lett. **79**, 4766(1997).

77. Linear correlation coefficient vs. cross term in Bose-Einstein correlations
† B. Schlei, D. Strottman, and N. Xu, Phys. Lett. **B420**, 1(1998).

78. Ξ productions in Central $Pb + Pb$ Collisions at 158 GeV per Nucleon
H. Appelsh'auser, *et al.* [NA49 Collaboration], Phys. Lett. **B444**, 523(1998).

79. Proton and anti-proton distributions at mid-rapidity in proton-nucleus and sulphur-nucleus collisions
I.G. Bearden, *et al.*, [NA44 Collaboration], Phys. Rev. **C57**, 837(1998).

80. On the equation of state of nuclear matter in 158 AGeV $Pb + Pb$ collisions
† B. Schlei, D. Strottman, and N. Xu, Phys. Rev. Lett. **80**, 3467(1998).

81. Evidence of early multi-strange hadron freeze-out in high energy nuclear collisions
† H. van Hecke, H. Sorge, and N. Xu, Phys. Rev. Lett. **81**, 5764(1998).

82. High energy $Pb + Pb$ collisions viewed by pion interferometry
I.G. Bearden, *et al.*, [NA44 Collaboration], Phys. Rev. **C58**, 1656(1998).

83. Event anisotropy in high energy nucleus-nucleus collisions
† H. Liu, S. Panitkin, and N. Xu, Phys. Rev. **C59**, 348(1999).

84. Baryon Stopping and Charged Particle Distributions in Central $Pb + Pb$ Collisions at 158 GeV per Nucleon
H. Appelshauser, *et al.* [NA49 Collaboration], Phys. Rev. Lett. **82**, 2471(1999).

85. Directed flow of light nuclei in $Au + Au$ collisions at 10.8 GeV/nucleon
J. Barrette, *et al.*, [E877 Collaboration], Phys. Rev. **C59**, 884(1999).

86. Thermal analysis of particle yields from RQMD
† J. Sollfrank, U. Heinz, H. Sorge, and N. Xu, J. Phys. **G25**, 363(1999).

87. Final conditions in ultra-relativistic heavy ion collisions
† Yu. M. Sinyukov, S.V. Akkelin, and N. Xu, Phys. Rev. **C59**, 3437(1999).

88. Two-Proton correlations near mid-rapidity in $p + Pb$ and $S + Pb$ collisions at the CERN SPS
H. Boggild, *et al.*, [NA44 Collaboration], Phys. Lett. **B458**, 181(1999).

89. Thermal analysis of hadron multiplicities from relativistic quantum molecular dynamics
† J. Sollfrank, U. Heinz, H. Sorge, and N. Xu, Phys. Rev. **C59**, 1637(1999).

90. Event-by-event fluctuations of averaged transverse momentum in central $Pb + Pb$ collisions at 158 GeV per nucleon
H. Appelshauser, *et al.*, [NA49 Collaboration], Phys. Lett. **B459**, 679(1999).

91. Two-proton correlations from 14.6 AGeV $Si + Pb$ and 11.5 AGeV $Au + Au$ central collisions
J. Barrette, *et al.*, [E877 Collaboration], Phys. Rev. **C60**, 054905(1999).

92. Deuterons and space-momentum correlation in high energy nuclear collisions
† B. Monreal *et al.*, Phys. Rev. **C60**, R31903(1999).

93. Proton and deuteron distributions as signatures for collective particle dynamics and event shape geometries at the RHIC
† B. Monreal, W.J. Llope, R. Mattiello, S.Y.Panitkin, H.Sorge, N. Xu, Phys. Rev. **C60**, R51902(1999).

94. Two-proton correlations from 158 AGeV $Pb + Pb$ central collisions
H. Appelshauser, *et al.*, [NA49 Collaboration], Phys. Lett. **B467**, 21(1999).

95. Strange meson enhancement in $Pb + Pb$ collisions
I. Bearden, *et al.*, [NA44 Collaboration], Phys. Lett. **B471**, 6(1999).

96. Light fragment yields from $Au + Au$ collisions at 11.5AGeV
J. Barrette, *et al.*, [E877 Collaboration], Phys. Rev. **C61**, 044906(2000).

97. Novel rapidity dependence of directed flow in high energy heavy ion collisions
† R.J.M. Snellings, H. Sorge, S. Voloshin, F.Q. Wang, and N. Xu, Phys. Rev. Lett. **84**, (2000).

98. Proton and pion production in $Au + Au$ collisions at 10.8 AGeV
J. Barrette, *et al.*, [E877 Collaboration], Phys. Rev. **C62**, 024901(2000).

99. Baryon phase-space density in heavy ion collisions
† Fuqiang Wang and N. Xu, Phys. Rev. **C61**, R021904(2000).

100. A systematic study of the kaon to pion multiplicity ratios in heavy ion collisions
† Fuqiang Wang, H. Liu, H. Sorge, J. Yang, and N. Xu, Phys. Rev. **C61**, 4904(2000).

101. Global observables and secondary interactions in central $Au + Au$ collisions at $\sqrt{s_{\rm NN}} = 200$ GeV
† M.J. Bleicher, S.A. Bass, L.V. Bravina, W. Greiner, S. Soff, H. Stöcker, N. Xu, and E.E. Zabrodin, Phys. Rev. **C62**, 024904(2000).

102. Directed flow of antiprotons in $Au + Au$ collisions at AGS
J. Barrette, *et al.* [E877 Collaboration], Phys. Lett. **B485**, 319(2000).

103. Strangeness enhancement from strong color fields at RHIC
† M. Bleicher, W. Greiner, H. Stocker, and N. Xu, Phys. Rev. **C62**, 1901R(2000).

104. Deuteron production in central $Pb + Pb$ collisions at 158 AGeV
S.V. Afanasiev, *et al.*, [NA49 Collaboration], Phys. Lett. **B486**, 22(2000).

105. Production of Φ mesons in $p + p$, $p + Pb$, and central $Pb + Pb$ collisions at $E_{beam} = 158$ AGeV
S.V. Afanasiev, *et al.*, [NA49 Collaboration], Phys. Lett. **B491**, 59(2000).

106. Antideuteron production in 158 AGeV $Pb + Pb$ collisions
I.G. Bearden, *et al.*, [NA44 Collaboration], Phys. Rev. Lett. **85**, 2681(2000).

107. Space-time evolution of the hadronic source in peripheral to central $Pb + Pb$ collisions
† I.G. Bearden *et al.*, [NA44 Collaboration], Eur. Phys. J., **C18**, 317(2000).

108. Enhancement of ϕ-mesons in p+Pb and Pb+Pb collisions at 158 AGeV
† B.H. Sa, A. Faessler, C. Fuchs, A. Tai, X.R. Wang, N. Xu and E. Zaborodin, Phys. Lett. **B507**, 104(2001).

109. Lambda production and flow in $Au + Au$ collisions at 11.5 AGeV
J. Barrette, *et al.* [E877 Collaboration], Phys. Rev. **C63**, 4902(2001).

110. Elliptic flow in $Au + Au$ collisions at $\sqrt{s_{\rm NN}} = 130$ GeV
K.H. Ackermann, *et al.*, [STAR Collaboration], Phys. Rev. Lett. **86**, 402(2001).

111. K/π e-by-e fluctuations in Central $Pb + Pb$ Collisions at 158 GeV per Nucleon
H. Appelshäuser, *et al.*, [NA49 Collaboration], Phys. Rev. Lett. **86**, 1695(2001).

112. Mid-rapidity anti-proton over proton ratio in $Au + Au$ Collisions at $\sqrt{s_{\rm NN}} = 130$ GeV
C. Adler, *et al.*, [STAR Collaboration], Phys. Rev. Lett. , **86**, 4778(2001).

113. Enhancement of ϕ mesons in $p + Pb$ and $Pb + Pb$ collisions at 158 AGeV
† Ben-Hao Sa, Amand Faessler, Xiao-Rong Wang, C. Fuchs, An Tai, N. Xu, and E. Zabrodin, Phys. Lett. **B507**, 104(2001).

114. Pion interferometry of $\sqrt{s_{\rm NN}} = 130$ GeV $Au + Au$ collisions at RHIC
C. Adler, *et al.*, [STAR Collaboration], Phys. Rev. Lett. **87**, 9007(2001).

115. One and two dimensional analysis of 3π correlations measured in $Pb + Pb$ interactions
I.G. Bearden, *et al.*, [NA44 Collaboration], Phys. Lett. **B517**, 25(2001).

116. Multiplicity distribution and spectra of negatively charged hadrons in $Au + Au$ collisions at $\sqrt{s_{\rm NN}} = 130$ GeV
C. Adler, *et al.*, [STAR Collaboration], Phys. Rev. Lett. **87**, 112303(2001).

117. Identified particle elliptic flow in $Au + Au$ collisions at $\sqrt{s_{\rm NN}} = 130$ GeV
C. Adler, *et al.*, [STAR Collaboration], Phys. Rev. Lett. **87**, 182301(2001).

118. HBT parameters and space-momentum correlations in relativistic heavy-ion collisions
† Jing-Bo Zhang, Lei Huo, Wei-Ning Zhang, Xin-Hua Li, Nu Xu, Yi-Ming Liu, Chin. Phys. Lett. **18**, 1568(2001).

119. Measurement of inclusive antiprotons from $Au + Au$ collisions at $\sqrt{s_{\rm NN}} = 130$ GeV
C. Adler, *et al.*, [STAR Collaboration], Phys. Rev. Lett. **87**, 262302-1(2001).

120. Antideuteron and Antihelium production in $Au + Au$ collisions at $\sqrt{s_{\rm NN}} = 130$ GeV
C. Adler, *et al.*, [STAR Collaboration], Phys. Rev. Lett. **87**, 262301-1(2001).

121. Two-Kaon correlations in central $Pb + Pb$ collisions at 158 AGeV
I.G. Bearden *et al.*, [NA44 Collaboration], Phys. Rev. Lett. **87**, 112301(2001).

122. Event texture search for phase transitions in $Pb + Pb$ collisions
I.G. Bearden, *et al.*, [NA44 Collaboration], Phys. Rev. **C65**, 044903(2002).

123. Deuteron and triton production with high energy S and Pb beams
I.G. Bearden, *et al.*, [NA44 Collaboration], Eur. Phys. J. **C23**, 237(2002).

124. Mid-rapidity ϕ production in $Au + Au$ collisions at $\sqrt{s_{\rm NN}} = 130$ GeV
† C. Adler, *et al.*, [STAR Collaboration], Phys. Rev. **C65**, Rapid Communications, 041901(2002).

125. Mid-rapidity Λ and $\bar{\Lambda}$ production in $Au + Au$ collisions at $\sqrt{s_{\rm NN}} = 130$ GeV
C. Adler, *et al.*, [STAR Collaboration], Phys. Rev. Lett. **89**, 092301(2002).

126. Azimuthal anisotropy of K^0_S and $\Lambda + \bar{\Lambda}$ production at mid-rapidity from $Au + Au$ collisions at $\sqrt{s_{\rm NN}} = 130$ GeV
† C. Adler, *et al.*, [STAR Collaboration], Phys. Rev. Lett. **89**, 132301(2002).

127. Erratum: Azimuthal anisotropy of K^0_S and $\Lambda + \bar{\Lambda}$ production at mid-rapidity from Au+Au collisions at $\sqrt{s_{\rm NN}}$ =130 GeV [Phys. Rev. Lett. **89**, 132301 (2002)]
C. Adler, *et al.*, [STAR Collaboration], Phys. Rev. Lett. **127**, 089901(2021).

128. Elliptic flow from two- and four-particle correlations in $Au + Au$ collisions at $\sqrt{s_{\rm NN}} = 130$ GeV
C. Adler, *et al.*, [STAR Collaboration], Phys. Rev. **C66**, 034904(2002).

129. Centrality dependence of high p_T hadron suppression in $Au + Au$ collisions at $\sqrt{s_{\rm NN}} = 130$ GeV
C. Adler, *et al.*, [STAR Collaboration], Phys. Rev. Lett. **89**, 202301(2002).

130. Effects of strong color fields on baryon dynamics
† S. Soff, J. Randrup, H. Stöcker, N Xu, Phys. Lett. **B551**, 115(2003).

131. $K^{*0}(892)$ Production in relativistic heavy ion collisions at $\sqrt{s_{\rm NN}} = 130$ GeV
C. Adler, *et al.*, [STAR Collaboration], Phys. Rev. **C66**, 061901R(2002).

132. Particle production in central $Pb + Pb$ collisions at 158 AGeV
I.G. Bearden, *et al.*, [NA44 Collaboration], Phys. Rev. **C66**, 044907(2002).

133. Coherent ρ^0 production in ultra-peripheral heavy ion collisions
C. Adler, *et al.*, [STAR Collaboration], Phys. Rev. Lett. **89**, 272302(2002).

134. Azimuthal anisotropy and correlations in the hard scattering regime at RHIC
C. Adler, *et al.*, [STAR Collaboration], Phys. Rev. Lett. **90**, 032301(2003).

135. Strange anti-particle to particle ratios at mid-rapidity in $\sqrt{s_{\rm NN}} = 130$ GeV $Au + Au$ collisions
J. Adams, *et al.*, [STAR Collaboration], Phys. Lett. **B567**, 167(2003).

136. Disappearance of back-to-back high p_T hadron correlations in central $Au + Au$ collisions at $\sqrt{s_{\rm NN}} = 200$ GeV
J. Adams, *et al.*, [STAR Collaboration], Phys. Rev. Lett. **90**, 082302(2003).

137. Evidence from $d + Au$ measurements for final-state suppression of high pT hadrons in $Au + Au$ collisions at RHIC
C. Adams, *et al.*, [STAR Collaboration], Phys. Rev. Lett. **91**, 072304(2003).

138. Transverse expansion in ^{197}Au + ^{197}Au collisions at relativistic energies
† Y. Cheng, F. Liu, K. Schweda, and N. Xu, Phys. Rev. **C68**, 034910(2003).

139. Transverse momentum and collision energy dependence of high p_T hadron suppression in $Au + Au$ collisions at ultra-relativistic energies
C. Adler, *et al.*, [STAR Collaboration], Phys. Rev. Lett. **91**, 172302(2003).

140. Global systematics of charged particle production in pp and AA collisions at RHIC energies
† V. Topor Pop, M. Gyulassy, J. Barrette, C. Gale, S. Vance, X.N. Wang, N. Xu, and K. Filimonov, Phys. Rev. **C68**, 054902(2003).

141. Three-pion HBT correlations in relativistic heavy-ion collisions from the STAR experiment
C. Adler, *et al.*, [STAR Collaboration], Phys. Rev. Lett. **91**, 262301(2003).

142. Pion-kaon correlations in $Au + Au$ collisions at $\sqrt{s_{\rm NN}} = 130$ GeV
J. Adams, *et al.*, [STAR Collaboration], Phys. Rev. Lett. **91**, 262302(2003).

143. Particle dependence of azimuthal anisotropy and nuclear modification of particle production at moderate p$_T$ in $Au + Au$ collisions at $\sqrt{s_{\rm NN}} = 200$ GeV
C. Adler, *et al.*, [STAR Collaboration], Phys. Rev. Lett. **92**, 052302(2004).

144. Energy and centrality dependence of deuteron and proton production in $Pb + Pb$ collisions at relativistic energies
T. Anticic, *et al.*, [NA49 Collaboration], Phys. Rev. **C69**, 024902(2004).

145. Azimuthal anisotropy at RHIC: the first and fourth harmonics
C. Adler, *et al.*, [STAR Collaboration], Phys. Rev. Lett. **92**, 062301(2004).

146. ρ^0 production and possible modification in $Au + Au$ and $p + p$ collisions at $\sqrt{s_{\rm NN}}$ = 200 GeV
C. Adler, *et al.*, [STAR Collaboration], Phys. Rev. Lett. **92**, 092301(2003).

147. Cross sections and transverse single-spin asymmetries in forward neutral pion production from proton collisions at $\sqrt{s_{\rm NN}}$ = 200 GeV
J. Adams, *et al.*, [STAR Collaboration], Phys. Rev. Lett. **92**, 171801(2003).

148. Azimuthally sensitive HBT in $Au + Au$ collisions at $\sqrt{s_{\rm NN}}$ = 200 GeV
J. Adams, *et al.*, [STAR Collaboration], Phys. Rev. Lett. **93**, 012301(2003).

149. Multi-strange baryon production in $Au + Au$ collisions at $\sqrt{s_{\rm NN}}$ = 130 GeV
† J. Adams, *et al.*, [STAR Collaboration], Phys. Rev. Lett. **92**, 182301(2004).

150. Resonance decay effects on anisotropy parameters
† X. Dong, S. Esumi, P. Sorensen, N. Xu , Z. Xu, Phys. Lett. **B597**, 328(2004).

151. Pion, Kaon, proton and anti-proton transverse momentum distributions from $p + p$ and $d + Au$ collisions at $\sqrt{s_{\rm NN}}$ = 200 GeV
J. Adams, *et al.*, [STAR Collaboration], Phys. Rev. Lett. **92**, 112301(2004).

152. Rapidity and centrality dependence of proton and anti-proton production from $Au + Au$ collisions at $\sqrt{s_{\rm NN}}$ = 130 GeV
J. Adams, *et al.*, [STAR Collaboration], Phys. Rev. **C70**, R041901(2004).

153. Kaon production and Kaon to pion ratio in $Au + Au$ collisions at $\sqrt{s_{\rm NN}}$ = 130 GeV
C. Adler, *et al.*, [STAR Collaboration], Phys. Lett. **B595**, 143(2004).

154. Centrality and pseudorapidity dependence of charged hadron production at intermediate p_T in $Au + Au$ collisions at $\sqrt{s_{\rm NN}}$ = 130 GeV
J. Adams, *et al.*, [STAR Collaboration], Phys. Rev. **C70**, 044901(2004).

155. Photon and neutral pion production in $Au + Au$ collisions at $\sqrt{s_{\rm NN}}$ =130 GeV
J. Adams, *et al.*, [STAR Collaboration], Phys. Rev. **C70**, 044902(2004).

156. Production of $e^+ + e^-$ pairs accompanied by nuclear dissociation in ultra-peripheral heavy ion collisions
J. Adams, *et al.*, [STAR Collaboration], Phys. Rev. **C70**, R031902(2004).

157. ϕ-meson production at RHIC: Strong color field and intrinsic transverse momenta
† S. Soff, S. Kesavan, J. Randrup, H. Stocker, N. Xu, J. Phys. **G30**: Nucl. Part. Phys., L35(2004).

158. Global systematics of charged particle production in pp and AA collisions at RHIC energies
† V. Topor Pop, M. Gyulassy, J. Barrette, C. Gale, X.N. Wang, and N. Xu, Phys. Rev. **C70**, 064906(2004).

159. Study of Bulk Properties at High Energy Nuclear Collisions – The search for the partonic equation of state at RHIC
N. Xu, Proceedings *International School of Nuclear Physics*, Erice, Italy, Sept. 2003; Prog. Part. Nucl. Phys. **53** 165(2004).

160. J/Ψ transport in QGP and p_T distribution at SPS and RHIC
† Xiang-lei Zhu, Peng-fei Zhuang, N. Xu, Phys. Lett. **B607**, 107(2005).

161. Open charm yields in d + Au collisions at $\sqrt{s_{\rm NN}}$ = 200 GeV
J. Adams, *et al.*, [STAR Collaboration], Phys. Rev. Lett. **94**, 062301(2005).

162. ϕ meson production in $Au + Au$ and $p + p$ collisions at $\sqrt{s_{\rm NN}}$ = 200 GeV
J. Adams, *et al.*, [STAR Collaboration], Phys. Lett. **B612**, 181(2005).

163. Collective flow of open and hidden charm in $Au + Au$ collisions at $\sqrt{s_{\rm NN}}$ = 200 GeV
† E. L. Bratkovskaya, W. Cassing, H. Stöcker, N. Xu, Phys. Rev. **C71**, 044901(2005).

164. Transverse-momentum dependent modification of dynamic texture in central $Au + Au$ collisions at $\sqrt{s_{\rm NN}}$ = 200 GeV
J. Adams, *et al.*, [STAR Collaboration], Phys. Rev. **C71**, 031901(R)(2005).

165. Pion, kaon, proton and anti-proton transverse momentum distributions from $p + p$ and $d + Au$ collisions at $\sqrt{s_{\rm NN}}$ = 200 GeV
J. Adams, *et al.*, [STAR Collaboration], Phys. Lett. **B616**, 8(2005).

166. Centrality dependence of thermal parameters deduced from hadron multiplicity in $Au + Au$ collisions at $\sqrt{s_{\rm NN}}$ = 130 GeV
† J. Cleymans, B. Kampfer, M. Kaneta, S. Wheaton, N. Xu, Phys. Rev. **C71**, 054901(2005).

167. K(892)* resonance production in $Au + Au$ and $p + p$ collisions at $\sqrt{s_{\rm NN}}$ = 200 GeV at STAR
J. Adams, *et al.*, [STAR Collaboration], Phys. Rev. **C71**, 064902(2005).

168. Pion interferometry in $Au + Au$ collisions at $\sqrt{s_{\rm NN}}$ = 200 GeV
J. Adams, *et al.*, [STAR Collaboration], Phys. Rev. **C71**, 044906(2005).

169. Experimental and theoretical challenges in the search for the Quark Gluon Plasma: The STAR Collaboration's critical assessment of the evidence from RHIC collisions
† J. Adams, *et al.*, [STAR Collaboration], Nucl. Phys. **A757**, 102(2005).

170. Partonic collectivity in high-energy nuclear collisions
† K. Schweda and N. Xu, Acta Phys. Hung. **A22**, 103(2005).

171. Multiplicity and pseudorapidity distributions of photons in $Au + Au$ collisions at $\sqrt{s_{\rm NN}} = 62.4$ GeV
J. Adams, *et al.*, [STAR Collaboration], Phys. Rev. Lett. **95**, 062301(2005).

172. Multi-strange baryon elliptic flow in $Au + Au$ collisions at $\sqrt{s_{\rm NN}} = 200$ GeV
J. Adams, *et al.*, [STAR Collaboration], Phys. Rev. Lett. **95**, 122301(2005).

173. Incident energy dependence of p_T correlations at RHIC
J. Adams, *et al.*, [STAR Collaboration], Phys. Rev. **C72**, 044902(2005).

174. Distributions of Charged Hadrons Associated with High Transverse Momentum Particles in $p + p$ and $Au + Au$ Collisions at $\sqrt{s_{\rm NN}} = 200$ GeV
J. Adams, *et al.*, [STAR Collaboration], Phys. Rev. Lett. **95** , 152301(2005).

175. Event-wise ($\rm p_t$) fluctuations in $Au + Au$ collisions at $\sqrt{s_{\rm NN}} = 130$ GeV
J. Adams, *et al.*, [STAR Collaboration], Phys. Rev. **C71**, 064906(2005).

176. Collective expansion in high-energy nuclear collisions: the search for the partonic EOS at RHIC
N. Xu, Nucl. Phys. **A751**, 109c(2005).

177. Identified hadron spectra at large transverse momentum in $p + p$ and $d + Au$ collisions at $\sqrt{s_{\rm NN}} = 200$ GeV
J. Adams, *et al.*, [STAR Collaboration], Phys. Lett. **B637**, 161(2006).

178. Multiplicity and Pseudorapidity Distributions of Charged Particles and Photons at Forward Pseudorapidity in $Au + Au$ Collisions at $\sqrt{s_{\rm NN}} = 62.4$ GeV
J. Adams, *et al.*, [STAR Collaboration], Phys. Rev. **C73**, 034906(2006).

179. Directed flow in $Au + Au$ collisions at $\sqrt{s_{\rm NN}} = 62.4$ GeV
J. Adams, *et al.*, [STAR Collaboration], Phys. Rev. **C73**, 034903(2006).

180. Transverse-momentum p_T correlations on (η,ϕ) from mean-p_T fluctuations in $Au + Au$ collisions at $\sqrt{s_{\rm NN}} = 200$ GeV
J. Adams, *et al.*, [STAR Collaboration], J. Phys. **G32**, L37(2006).

181. Anisotropic flow at RHIC: How unique is the number-of-constituent-quark scaling?
† Y. Lu, M. Bleicher, F. Liu, Z. Kiu, P. Sorensen, H. Stocker, N. Xu, X. Zhu, J. of Phys. G: Nucl. Part. Phys. **32**, 1121(2006).

182. Strange baryon resonance production in $\sqrt{s_{\rm NN}} = 200$ GeV $p + p$ and $Au + Au$ collisions
J. Adams, *et al.*, [STAR Collaboration], Phys. Rev. Lett. **97**, 132301(2006).

183. Proton-Λ correlations in central $Au + Au$ collisions at $\sqrt{s_{\rm NN}} = 200$ GeV
J. Adams, *et al.*, [STAR Collaboration], Phys. Rev. **C74**, 064906(2006).

184. Direct observation of dijets in central $Au + Au$ collisions at $\sqrt{s_{\rm NN}} = 200$ GeV
J. Adams, *et al.*, [STAR Collaboration], Phys. Rev. Lett. **97**, 162301(2006).

185. Identified baryon and meson distributions at large transverse momenta from $Au + Au$ collisions at $\sqrt{s_{\rm NN}} = 200$ GeV
J. Adams, *et al.*, [STAR Collaboration], Phys. Rev. Lett. **97**, 152301(2006).

186. Forward neutral pion production in $p + p$ and $d + Au$ collisions at $\sqrt{s_{\rm NN}} = 200$ GeV
J. Adams, *et al.*, [STAR Collaboration], Phys. Rev. Lett. **97**, 152302(2006).

187. J/ψ Production in Quark-Gluon Plasma
† L. Yan, P. Zhuang, N. Xu, Phys. Rev. Lett. **97**, 232301(2006).

188. Neutral kaon interferometry in $Au + Au$ collisions at $\sqrt{s_{\rm NN}} = 200$ GeV
B.I. Abelev, *et al.*, [STAR Collaboration], Phys. Rev. **C74**, 054902(2006).

189. The multiplicity dependence of inclusive p_T spectra from p-p collisions at $\sqrt{s_{\rm NN}} = 200$ GeV
J. Adams, *et al.*, [STAR Collaboration], Phys. Rev. **D74**, 032006(2006).

190. Partonic equation of state in high-energy nuclear collisions
N. Xu, J. Phys. G**32**, S123(2006).

191. Scaling properties of hyperon production in $Au + Au$ collisions at $\sqrt{s_{\rm NN}} = 200$ GeV
J. Adams, *et al.*, [STAR Collaboration], Phys. Rev. Lett. **98**, 060301(2007).

192. Mass, quark-number, and $\sqrt{s_{\rm NN}}$ dependence of the second and fourth flow harmonics in ultra-relativistic nucleus-nucleus collisions
J. Adams, *et al.*, [STAR Collaboration], Phys. Rev. **C75**, 54906(2007).

193. Transverse Momentum and Centrality Dependence of High-p_T Nonphotonic Electron Suppression in $Au + Au$ Collisions at $\sqrt{s_{\rm NN}} = 200$ GeV
J. Adams, *et al.*, [STAR Collaboration], Phys. Rev. Lett. **98**, 192301(2007).

194. Strange particle production in p + p collisions at $\sqrt{s_{\rm NN}} = 200$ GeV
B.I. Abelev, *et al.*, [STAR Collaboration], Phys. Rev. **C75**, 064901(2007).

195. D and $\bar{D}$ correlations as a sensitive probe for thermalization in high-energy nuclear collisions
† X. Zhu, M. Bleicher, S.L. Huang, K. Schweda, Horst Stoecker, N. Xu and P. Zhuang, Phys. Lett. **B647**, 366(2007).

196. Strangelet search in $Au + Au$ collisions at $\sqrt{s_{\rm NN}} = 200$ GeV
B.I. Abelev, *et al.*, [STAR Collaboration], Phys. Rev. **C76**, 011901(2007).

197. Partonic flow and ϕ-meson production in $Au + Au$ collisions at $\sqrt{s_{\rm NN}} = 200$ GeV
† B.I. Abelev, *et al.*, [STAR Collaboration], Phys. Rev. Lett. **99**, 112301(2007).

198. Energy dependence of charged pion, proton and anti-proton transverse momentum spectra for $Au + Au$ collisions at $\sqrt{s_{\rm NN}} = 62.4$ and 200 GeV
B.I. Abelev, *et al.*, [STAR Collaboration], Phys. Lett. **B655**, 104(2007).

199. Rapidity and species dependence of particle production at large transverse momentum for $d + Au$ collisions at $\sqrt{s_{\rm NN}} = 200$ GeV
B.I. Abelev, *et al.*, [STAR Collaboration], Phys. Rev. **C76**, 054903(2007).

200. Measurement of Transverse Single-Spin Asymmetries for bottom Production in Proton-Proton Collisions at $\sqrt{s_{\rm NN}} = 200$ GeV
B.I. Abelev, *et al.*, [STAR Collaboration], Phys. Rev. Lett. **99**, 142003(2007).

201. Global polarization measurement in $Au + Au$ collisions
B.I. Abelev, *et al.*, [STAR Collaboration], Phys. Rev. **C76**, 024915(2007).

202. Forward Λ production and nuclear stopping power in $d + Au$ collisions at $\sqrt{s_{\rm NN}} = 200$ GeV
B.I. Abelev, *et al.*, [STAR Collaboration], Phys. Rev. **C76**, 64904(2007).

203. Enhanced strange baryon production in $Au + Au$ collisions compared to $p + p$ at $\sqrt{s_{\rm NN}} = 200$ GeV
B.I. Abelev, *et al.*, [STAR Collaboration], Phys. Rev. **C77**, 44908(2008).

204. Energy dependence of charged pion, proton and anti-proton transverse momentum spectra for $Au + Au$ collisions at $\sqrt{s_{\rm NN}} = 62.4$ and 200 GeV
B.I. Abelev, *et al.*, [STAR Collaboration], Phys. Lett. **B655**, 104(2007).

205. Charm quark thermalization in quark-gluon plasma
† L. Yan, P.F. Zhuang, N. Xu, Int. J. Mod. Phys. **E16**, 2048(2007).

206. J/ψ continuous regeneration and suppression in quark-gluon plasma
† P.F. Zhuang, L. Yan, N. Xu, J. Phys. **G34**, S487(2007).

207. Longitudinal double-spin asymmetry for inclusive jet production in $\vec{p} + \vec{p}$ collisions at $\sqrt{s_{\rm NN}} = 200$ GeV
B.I. Abelev, *et al.*, [STAR Collaboration], Phys. Rev. Lett. **100**, 232003(2008).

208. The effect of partonic wind on charm quark correlations in high-energy nuclear collisions.
† X. Zhu, N. Xu, P. Zhuang, Phys. Rev. Lett. **100**, 152301(2008).

209. ρ^0 Photoproduction in Ultra-Peripheral Relativistic Heavy Ion Collisions with STAR
B.I. Abelev, *et al.*, [STAR Collaboration], Phys. Rev. **C77**, 34910(2008).

210. Forward Neutral Pion Transverse Single Spin Asymmetries in $p + p$ Collisions at $\sqrt{s_{\rm NN}} = 200$ GeV
B.I. Abelev, *et al.*, [STAR Collaboration], Phys. Rev. Lett. **101**, 222001(2008).

211. System-size independence of directed flow at the Relativistic Heavy-Ion Collider
B.I. Abelev, *et al.*, [STAR Collaboration], Phys. Rev. Lett. **101**, 252301(2008).

212. Hadronic resonance production in $d + Au$ collisions at 200 GeV at RHIC
B.I. Abelev, *et al.*, [STAR Collaboration], Phys. Rev. **C78**, 44906(2008).

213. Spin alignment measurements of the K* and phi vector meson at RHIC
B.I. Abelev, *et al.*, [STAR Collaboration], Phys. Rev. **C77**, 61902(2008).

214. Centrality dependence of charged hadron and strange hadron elliptic flow from $\sqrt{s_{\rm NN}} = 200$ GeV $Au + Au$ collisions
B.I. Abelev, *et al.*, [STAR Collaboration], Phys. Rev. **C77**, 54901(2008).

215. Observation of Two-source Interference in the Photoproduction Reaction $AuAu \to AuAu\rho^0$
B.I. Abelev, *et al.*, [STAR Collaboration], Phys. Rev. Lett. **102**, 112301(2009).

216. Energy and system size dependence of ϕ meson production in $Cu + Cu$ and $Au + Au$ collisions
† B.I. Abelev, *et al.*, [STAR Collaboration], Phys. Lett. **B673**, 183(2009).

217. Indications of Conical Emission of Charged Hadrons at RHIC
B.I. Abelev, *et al.*, [STAR Collaboration], Phys. Rev. Lett. **102**, 052302(2009).

218. Beam-Energy and System-Size Dependence of Dynamical Net Charge
B.I. Abelev, *et al.*, [STAR Collaboration], Phys. Rev. **C79**, 024906(2009).

219. Systematic Measurements of Identified Particle Spectra in pp, $d + Au$ and $Au + Au$ Collisions at the STAR detector
B.I. Abelev, *et al.*, [STAR Collaboration], Phys. Rev. **C79**, 034909(2009).

220. Measurements of ϕ meson production in relativistic heavy-ion collisions at RHIC
B.I. Abelev, *et al.*, [STAR Collaboration], Phys. Rev. **C79**, 64903(2009).

221. Space-time evolution of J/ψ production in high-energy nuclear collisions
† Y.P. Liu, Z. Qu, N. Xu, P.F. Zhuang, J. Phys. **G36**, 064057(2009).

222. J/ψ Transverse momentum distribution in high-energy nuclear collisions at RHIC
† Yun-peng Liu, Zhen Qu, Nu Xu and Peng-fei Zhuang, Phys. Lett. **B678**, 72(2009).

223. Measurement of D* mesons in jets from $p + p$ collisions at $\sqrt{s_{\rm NN}} = 200$ GeV
B.I. Abelev, *et al.*, [STAR Collaboration], Phys. Rev. **D79**, 112006(2009).

224. K/pi fluctuations at relativistic energies
B.I. Abelev, *et al.*, [STAR Collaboration], Phys. Rev. Lett. **103**, 92301(2009).

225. Pion interferometry in $Au + Au$ and $Cu + Cu$ collisions at RHIC
B.I. Abelev, *et al.*, [STAR Collaboration], Phys. Rev. **C80**, 24905(2009).

226. Predictions of elliptic flow and nuclear modification factor from 200 GeV U + U collisions at RHIC
† H. Masui, B. Mohanty and N. Xu, Phys. Lett. **B679**, 440(2009).

227. Initial eccentricity in deformed ^{197}Au+^{197}Au and ^{238}U+^{238}U collisions
† P. Filip, R. Lednicky, H. Masui and N. Xu, Phys. Rev. **C80**, 054903(2009).

228. J/Ψ production at high transverse momentum in $p + p$ and $Cu + Cu$ collisions at $\sqrt{s_{\rm NN}} = 200$ GeV
B.I. Abelev, *et al.*, [STAR Collaboration], Phys. Rev. **C80**, 041902(2009).

229. Long range rapidity correlations and jet production in high energy nuclear collisions
B.I. Abelev, *et al.*, [STAR Collaboration], Phys. Rev. **C80**, 064912(2009).

230. Azimuthal charged-particle correlations and possible local strong parity violation
B.I. Abelev, *et al.*, [STAR Collaboration], Phys. Rev. Lett. **103**, 251601(2009).

231. Topology studies of hydrodynamics using two-particle correlation analysis
† J. Takahashi, B. M. Tavares, W. L. Qian, R. Andrade, F. Grassi, and Y. Hama, T. Kodama, and N. Xu, Phys. Rev. Lett. **103**, 242301(2009).

232. Longitudinal spin transfer to Λ and $\overline{\Lambda}$ hyperons in polarized proton-proton collisions at $\sqrt{s} = 200$ GeV
B.I. Abelev, *et al.*, [STAR Collaboration], Phys. Rev. **D80**, 111102(2009).

233. Longitudinal double-spin asymmetry and cross section for inclusive neutral pion production in polarized proton collisions at $\sqrt{s} = 200$ GeV
B.I. Abelev, *et al.*, [STAR Collaboration], Phys. Rev. **D80**, (Rapid Communications), 111108(2009).

234. Center of mass energy and system-size dependence of photon production at forward rapidity at RHIC
B.I. Abelev, *et al.*, [STAR Collaboration], Nucl. Phys. **A832**, 134(2009).

235. Neutral pion production in $Au + Au$ collisions at $\sqrt{s_{\rm NN}} = 200$ GeV
B.I. Abelev, *et al.*, [STAR Collaboration], Phys. Rev. **C80**, 44905(2009).

236. Growth of Long Range Forward-Backward Multiplicity Correlations with Centrality in $Au + Au$ Collisions at $\sqrt{s_{\rm NN}} = 200$ GeV
B.I. Abelev, *et al.*, [STAR Collaboration], Phys. Rev. Lett. **103**, 172301(2009).

237. D and anti-D correlation as signature of strongly coupled quark matter
† X.L. Zhu, N. Xu, P.F. Zhuang, J. Phys. **G36**, 064025 (2009).

238. Identified particle production, azimuthal anisotropy, and interferometry measurements in $Au + Au$ collisions at $\sqrt{s_{\rm NN}} = 9.2$ GeV
B.I. Abelev, *et al.*, [STAR Collaboration], Phys. Rev. **C81**, 024911(2010).

239. Observation of charge-dependent azimuthal correlations and possible local strong parity violation in heavy ion collisions
B.I. Abelev, *et al.*, [STAR Collaboration], Phys. Rev. **C81**, 054908(2010).

240. System size dependence of associated yields in hadron-triggered jets
B.I. Abelev, *et al.*, [STAR Collaboration], Phys. Lett. **B683**, 123(2010).

241. Spectra of identified high-p_T $\pi^{\pm}$ and $p(\bar{p})$ in $Cu + Cu$ collisions at $\sqrt{s_{\rm NN}} = 200$ GeV
B.I. Abelev, *et al.*, [STAR Collaboration], Phys. Rev. **C81**, 054907(2010).

242. Rapidity dependence of J/ψ production at RHIC and LHC
Yun-peng Liu, Zhen Qu, Nu Xu and Peng-fei Zhuang, J. of Phys. **G37**, 075110(2010).

243. Observation of $\pi^+\pi^-\pi^+\pi^-$ photoproduction in ultra-peripheral heavy ion collisions at STAR
B.I. Abelev, *et al.*, [STAR Collaboration], Phys. Rev. **C81**, 44901(2010).

244. Charged particle and strange hadron elliptic flow from $\sqrt{s_{\rm NN}}$ = 62.4 and 200 GeV $Cu + Cu$ collisions
B.I. Abelev, *et al.*, [STAR Collaboration], Phys. Rev. **C81**, 44902(2010).

245. Balance functions from $Au + Au$, $d + Au$, and $p + p$ collisions at $\sqrt{s_{\rm NN}}$ = 200 GeV
B.I. Abelev, *et al.*, [STAR Collaboration], Phys. Rev. **C82**, 024905(2010).

246. Observation of an Antimatter Hypernucleus
B.I. Abelev, *et al.*, [STAR Collaboration], **Science, 328**, 58(2010).

247. Azimuthal di-hadron correlations in $d + Au$ and $Au + Au$ collisions at $\sqrt{s_{\rm NN}}$ = 200 GeV from STAR
B.I. Abelev, *et al.*, [STAR Collaboration], Phys. Rev. **C82**, 024912(2010).

248. Parton energy loss in heavy-ion collisions via direct-photon and charged-particle azimuthal correlations
B.I. Abelev, *et al.*, [STAR Collaboration], Phys. Rev. **C82**, 034909(2010).

249. Three-particle coincidence of the long range pseudorapidity correlation in high energy nucleus-nucleus collisions
B.I. Abelev, *et al.*, [STAR Collaboration], sub. to Phys. Rev. Lett. **105**, 22301(2010).

250. Higher moments of net-proton distributions at RHIC
† B.I. Abelev, *et al.*, [STAR Collaboration], Phys. Rev. Lett. **105**, 22302 (2010).

251. Transverse Momentum Distribution as a Probe of J/ψ Production Mechanism in Heavy Ion Collisions
† K. Zhou, N. Xu and P.F. Zhuang, Nucl. Phys. **A834**, 249c(2010).

252. Hadron Production in Heavy Ion Collisions
† H. Oeschler, H.-G. Ritter and N. Xu, *Relativistic Heavy Ion Physics*, R. Stöck (ed.), Springer Materials, 2010.

253. Υ Production as a probe for early state dynamics in high-energy nuclear collisions at RHIC.
† Yun-peng Liu, Zhen Qu, Nu Xu and Peng-fei Zhuang, Phys. Lett. **B697**, 32(2011).

254. Dilepton production and de-confinement phase transition in heavy ion collisions
† Jian Deng, Qun Wang, Nu Xu, Pengfei Zhuang, Phys. Lett. **B701**, 581(2011).

255. Observation of the Antimatter Helium-4 Nucleus
† B.I. Abelev, *et al.*, [STAR Collaboration], **Nature, 473**, 353(2011).

256. Experimental studies of di-jet survival and surface emission bias in $Au + Au$ collisions via angular correlations with respect to back-to-back leading hadrons
B.I. Abelev, *et al.*, [STAR Collaboration], Phys. Rev. **C83**, 061901(2011).

257. Effect of final state interactions on particle production in $d + Au$ collisions at energies available at the BNL Relativistic Heavy Ion Collider
† X.P. Zhang, J.H. Chen, Z.Z. Ren, N. Xu, Z.B. Xu, Q. Zheng, X.L. Zhu, Phys. Rev. **C84**, 031901(R)(2011).

258. Evolution of the differential transverse momentum correlation function with centrality in $Au + Au$ collisions at $\sqrt{s_{\rm NN}}$ = 200 GeV
G. Agakishiev, *et al.*, [STAR Collaboration], Phys. Lett. **B704**, 467(2011).

259. System size and energy dependence of near-side dihadron correlations
G. Agakishiev, *et al.*, [STAR Collaboration], Phys. Rev. **C85**, 014903(2012).

260. The Scale for QCD
† S. Gupta, X.F. Luo, B. Mohanty, H.G. Ritter, and N. Xu, **Science**, **332**, 1525(2011).

261. Strangeness enhancement in $Cu + Cu$ and $Au + Au$ $\sqrt{s_{\rm NN}}$ = 200 GeV collisions
B.I. Abelev, *et al.*, [STAR Collaboration], Phys. Rev. Lett. **108**, 72301(2012).

262. ρ^0 photo-production in $Au + Au$ collisions at $\sqrt{s_{\rm NN}}$ = 62.4 GeV measured with the STAR detector
G. Agakishiev, *et al.*, [STAR Collaboration], Phys. Rev. **C85**, 64902(2012).

263. Directed and elliptic flow of charged particles in $Cu + Cu$ collisions at $\sqrt{s_{\rm NN}}$ = 22.4 GeV
G. Agakishiev, *et al.*, [STAR Collaboration], Phys. Rev. **C85**, 014901(2012).

264. System size and energy dependence of near-side dihadron correlations
G. Agakishiev, *et al.*, [STAR Collaboration], Phys. Rev. **C85**, 014903(2012).

265. Measurement of the $W \to e\nu$ and $Z/\gamma* \to e^+e^-$ production cross sections at mid-rapidity in proton-proton collisions at $\sqrt{s}$ = 500 GeV
L. Adamczyk, *et al.*, [STAR Collaboration], Phys. Rev. **D85**, 092010(2012).

266. Identified hadron compositions in $p + p$ and $Au + Au$ collisions at high transverse momenta at $\sqrt{s_{\rm NN}}$ = 200 GeV
G. Agakishiev, *et al.*, [STAR Collaboration], Phys. Rev. Lett. **108**, 072302(2012).

267. Di-electron spectrum at mid-rapidity in $p + p$ collisions at $\sqrt{s}$ = 200 GeV
L. Adamczyk, *et al.*, [STAR Collaboration], Phys. Rev. **C86**, 024906(2012).

268. Measurements of D^0 and D^* production in $p + p$ collisions at $\sqrt{s}$ = 200 GeV
L. Adamczyk, *et al.*, [STAR Collaboration], Phys. Rev. **D86**, 72013(2012).

269. Transverse single-spin asymmetry and cross-section for π^0 and η mesons at large Feynman-x in $p^{\uparrow} + p$ collisions at $\sqrt{s} = 200$ GeV
L. Adamczyk, *et al.*, [STAR Collaboration], Phys. Rev. **D86**, 51101(2012).

270. Inclusive charged hadron elliptic flow in $Au + Au$ collisions at $\sqrt{s_{\rm NN}} = 7.7$ - 39 GeV
L. Adamczyk, *et al.*, [STAR Collaboration], Phys. Rev. **C86**, 54908(2012).

271. Directed flow of identified particles in $Au + Au$ collisions at $\sqrt{s_{\rm NN}} = 200$ GeV at RHIC
L. Adamczyk, *et al.*, [STAR Collaboration], Phys. Rev. Lett. **108**, 202301(2012).

272. Anomalous centrality evolution of two-particle angular correlations from $Au + Au$ collisions at $\sqrt{s_{\rm NN}} = 62.4$ and 200 GeV
G. Agakishiev, *et al.*, [STAR Collaboration], Phys. Rev. **C86**, 64902(2012).

273. Velocity dependence of Quarkonium dissociation temperature in high-energy nuclear collisions
† Yunpeng Liu, N. Xu, Pengfei Zhuang, Phys. Lett. **B724**, 73(2013).

274. Elliptic flow of ϕ mesons as a sensitive probe for the onset of the de-confinement transition in high energy heavy-ion collisions
† Md. Nasim, N. Xu, and B. Mohanty, Phys. Rev. **C87**, 014903(2013).

275. Single spin asymmetry A_N in polarized proton-proton elastic scattering at $\sqrt{s} = 200$ GeV
L. Adamczyk, *et al.*, [STAR Collaboration], Phys. Lett. **B719**, 62 (2013).

276. Observation of an energy-dependent difference in elliptic flow between particles and antiparticles in relativistic heavy ion collisions
L. Adamczyk, *et al.*, [STAR Collaboration], Phys. Rev. Lett. **110**, 142301(2013).

277. System-size dependence of transverse momentum correlations at $\sqrt{s_{\rm NN}} = 62.4$ and 200 GeV at the BNL Relativistic Heavy Ion Collider
L. Adamczyk, *et al.*, [STAR Collaboration], Phys. Rev. **C87**, 64902(2013).

278. J/ψ production at high transverse momenta in $p + p$ and $Au + Au$ collisions at $\sqrt{s_{\rm NN}} = 200$ GeV
L. Adamczyk, *et al.*, [STAR Collaboration], Phys. Lett. **B722**, 55(2013).

279. Elliptic flow of identified hadrons in $Au + Au$ collisions at $\sqrt{s_{\rm NN}} = 7.7$ - 62.4 GeV
L. Adamczyk, *et al.*, [STAR Collaboration], Phys. Rev. **C88**, 14902(2013).

280. Third harmonic flow of charged particles in $Au + Au$ collisions at $\sqrt{s_{\rm NN}} = 200$ GeV
L. Adamczyk, *et al.*, [STAR Collaboration], Phys. Rev. **C88**, 14904(2013).

281. Freeze-out dynamics via charged Kaon femtoscopy in $\sqrt{s_{\rm NN}} = 200$ GeV central $Au + Au$ collisions
G. Agakishiev, *et al.*, [STAR Collaboration], Phys. Rev. **C88**, 34906(2013).

282. Conserved number fluctuations in a hadron resonance gas model
† P. Garg, D.K. Mishra, P.K. Netrakanti, B. Mohanty, A.K. Mohanty, B.K. Singh, and N. Xu, Phys. Lett. **B726**, 136(2013).

283. Fluctuations of charge separation perpendicular to the event plane and local parity violation in $\sqrt{s_{\rm NN}} = 200$ GeV $Au + Au$ collisions at RHIC
L. Adamczyk, *et al.*, [STAR Collaboration], Phys. Rev. **C88**, 64911(2013).

284. Neutral pion cross section and spin asymmetries at intermediate pseudorapidity in polarized proton collisions at $\sqrt{s_{\rm NN}} = 200$ GeV
L. Adamczyk, *et al.*, [STAR Collaboration], Phys. Rev. **D89**, 012001(2014).

285. Energy dependence of moments of net-proton multiplicity distributions at RHIC
† L. Adamczyk, *et al.*, [STAR Collaboration], Phys. Rev. Lett. **112**, 032302 (2014).

286. Jet-hadron correlations in $\sqrt{s_{\rm NN}} = 200$ GeV $Au + Au$ and $p + p$ collisions
L. Adamczyk, *et al.*, [STAR Collaboration], Phys. Rev. Lett. **112**, 122301(2014).

287. Measurement of charge multiplicity asymmetry correlations in high energy nucleus-nucleus collisions at 200 GeV
L. Adamczyk, *et al.*, [STAR Collaboration], Phys. Rev. **C89**, 044908(2014).

288. Suppression of Upsilon production in $d + Au$ and $Au + Au$ collisions at $\sqrt{s_{\rm NN}} = 200$ GeV
L. Adamczyk, *et al.*, [STAR Collaboration], Phys. Lett. **B735**, 127(2014).

289. Dielectron mass spectra from $Au + Au$ Collisions at $\sqrt{s_{\rm NN}} = 200$ GeV
L. Adamczyk, *et al.*, [STAR Collaboration], Phys. Rev. Lett. **113**, 22301(2014).

290. Even-plane-dependent dihadron correlations with harmonic v_n subtraction in $Au + Au$ collisions at $\sqrt{s_{\rm NN}} = 200$ GeV
H. Agakishiev, *et al.*, [STAR Collaboration], Phys. Rev. **C89**, 04190R(2014).

291. J/ψ production at low p_T in $Au + Au$ and $Cu + Cu$ collisions at $\sqrt{s_{\rm NN}} = 200$ GeV with the STAR detector
H. Agakishiev, *et al.*, [STAR Collaboration], Phys. Rev. **C90**, 24906(2014).

292. J/ψ polarization in $p+p$ collisions at $\sqrt{s_{\rm NN}}$ = 200 GeV in STAR
H. Agakishiev, *et al.*, [STAR Collaboration], Phys. Lett. **B739**, 180(2014).

293. Probing nuclear symmetry energy at high densities using pion, kaon, eta and photon productions in heavy-ion collisions
† Zhi-Gang Xiao, Gao-Chan Yong, Lie-Wen Chen, Bao-An Li, Ming Zhang, Guo-Qing Xiao and Nu Xu, Eur. Phys. J. **A50**, 37(2014).

294. Beam-Energy Dependence of Directed Flow of Protons, antiprotons and pions in $Au+Au$ Collisions
† L. Adamczyk, *et al.*, [STAR Collaboration], Phys. Rev. Lett. **112**, 162301(2014).

295. Measurement of longitudinal spin asymmetries for weak boson production in polarized proton-proton collisions at RHIC
L. Adamczyk, *et al.*, [STAR Collaboration], Phys. Rev. Lett. **113**, 072301(2014).

296. Medium effects on charmonium production at LHC
† K. Zhou, N. Xu, Z. Xu, P.F. Zhuang, Phys. Rev. **C89**, 054911(2014).

297. Beam energy dependence of moments of the net-charge multiplicity distributions in $Au+Au$ collisions at RHIC
L. Adamczyk, *et al.*, [STAR Collaboration], Phys. Rev. Lett. **113**, 92301(2014).

298. Observation of D^0 meson nuclear modifications in $Au+Au$ collisions at $\sqrt{s_{\rm NN}}$ = 200 GeV
L. Adamczyk, *et al.*, [STAR Collaboration], Phys. Rev. Lett. **113**, 142301(2014).

299. Beam-energy dependence of charge separation along the magnetic field in $Au+Au$ collisions at RHIC
L. Adamczyk, *et al.*, [STAR Collaboration], Phys. Rev. Lett. **113**, 52302(2014).

300. Charmonium transverse momentum distribution in high energy nuclear collisions
† Z.B. Tang, N. Xu, K. Zhou and P.F. Zhuang, J. Phys. **G41**, 124004(2014).

301. Dielectron azimuthal anisotropy at mid-rapidity in $Au+Au$ collisions at 200 GeV
L. Adamczyk, *et al.*, [STAR Collaboration], Phys. Rev. **C90**, 64904(2014).

302. Υ production in heavy ion collisions at LHC
† K. Zhou, N. Xu, P.F. Zhuang, Nucl. Phys. **A931**, 654c(2014).

303. An Overview of STAR Results
N. Xu, [STAR Collaboration], Nucl. Phys. **A931**, 1c(2014).

304. The lambda-lambda correlation function in $Au+Au$ collisions at $\sqrt{s_{\rm NN}}$ = 200 GeV
L. Adamczyk, *et al.*, [STAR Collaboration], Phys. Rev. Lett. **114**, 22301(2015).

305. Effect of event selection on jet-like correlation measurement in $d+Au$ collisions at 200 GeV
L. Adamczyk, *et al.*, [STAR Collaboration], Phys. Lett. **B743**, 333(2015).

306. Isolation of flow and non-flow correlations by two- and four-particle cumulant measurements of azimuthal harmonics in $\sqrt{s_{\rm NN}}$ = 200 GeV $Au+Au$ collisions
L. Adamczyk, *et al.*, [STAR Collaboration], Phys. Lett. **B745**, 40(2015).

307. Magnetic field effect on Charmonium production in high-energy nuclear collisions
† X.Y. Guo, S.Z. Shi, N. Xu, Z. Xu, P.F. Zhuang, Phys. Lett. **B751**, 215(2015).

308. Di-Hadron correlations with identified leading hadrons in 200 GeV $Au+Au$ and $d+Au$ collisions at STAR
L. Adamczyk, *et al.*, [STAR Collaboration], Phys. Lett. **B751**, 233 (2015).

309. The Hot QCD White Paper: Exploring the Phases of QCD at RHIC and the LHC
† Y. Akiba, A. Angerami, H. Caines, T. Frawley, U. Heinz, B. Jacak, J.Y. Jia, T. Lappi, W. Li, A. Majumder, D. Morrison, M. Ploskon, J. Putschke, K. Rajagopal, R. Rapp, G. Roland, P. Sorensen, U. Wiedemann, N. Xu, W.A. Zajc arXiv: 1502.02730

310. Charged-to-neutral correlation at forward rapidity in $Au+Au$ collisions at 200 GeV
L. Adamczyk, *et al.*, [STAR Collaboration], Phys. Rev. **C91**, 34905(2015).

311. Energy dependence of K-pi, p-pi and K-p Fluctuations in Au+Au collisions from $\sqrt{s_{\rm NN}}$ = 7.7 to 200 GeV
L. Adamczyk, *et al.*, [STAR Collaboration], Phys. Rev. **C92**, 21901(2015).

312. Precision measurement of the longitudinal double-spin asymmetry for inclusive Jet production in polarized proton collisions at $\sqrt{s}$ = 200 GeV
L. Adamczyk, *et al.*, [STAR Collaboration], Phys. Rev. Lett. **115**, 92002(2015).

313. Beam energy dependent two-pion interferometry and the freeze-out eccentricity in heavy ion collisions at STAR
L. Adamczyk, *et al.*, [STAR Collaboration], Phys. Rev. **C92**, 14904(2015).

314. Energy dependence of acceptance-corrected dielectron excess mass spectrum at mid-rapidity in $Au+Au$ collisions at $\sqrt{s_{\rm NN}}$ = 19.6 and 200 GeV
L. Adamczyk, *et al.*, [STAR Collaboration], Phys. Lett. **B750**, 64(2015).

315. Long-range pseudorapidity dihadron correlations in $d+Au$ collisions at $\sqrt{s_{\rm NN}}$ = 200 GeV
L. Adamczyk, *et al.*, [STAR Collaboration], Phys. Lett. **B747**, 265 (2015).

316. Measurements of Dielectron Production in Au+Au Collisions at $\sqrt{s_{\rm NN}}$ = 200 GeV from the STAR Experiment
L. Adamczyk, *et al.*, [STAR Collaboration], Phys. Rev. **C92**, 24912(2015).

317. Observation of charge asymmetry dependence of pion elliptic flow and the possible chiral magnetic wave in heavy-ion collisions
L. Adamczyk, *et al.*, [STAR Collaboration], Phys. Rev. Lett. **114**, 252302(2015).

318. Azimuthal anisotropy in U+U and Au+Au collisions at RHIC
L. Adamczyk, *et al.*, [STAR Collaboration], Phys. Rev. Lett. **115**, 222301(2015).

319. Measurement of interaction between antiprotons
L. Adamczyk, *et al.*, [STAR Collaboration], Nature, **527**, 345(2015).

320. Observation of Transverse Spin-Dependent Azimuthal Correlations of Charged Pion Pairs in p(trans) + p at $\sqrt{s}$ = 200 GeV
L. Adamczyk, *et al.*, [STAR Collaboration], Phys. Rev. Lett. **115**, 242501(2015).

321. Energy dependence of K/π, p/π, and K/p fluctuations in $Au + Au$ collisions from $\sqrt{s_{NN}}$ = 7.7 to 200 GeV
L. Adamczyk, *et al.*, [STAR Collaboration], Phys. Rev. **C92**, 21901(2015).

322. Baseline measures for net-proton distributions in high energy heavy-ion collisions
† P.K. Netrakanti, X.F. Luo, D.K. Mishra, B. Mohanty, A. Mohanty, and N. Xu, Nucl. Phys. **A947**, 248(2016).

323. Centrality dependence of identified particle elliptic flow in relativistic heavy ion collisions at $\sqrt{s_{\rm NN}}$ = 7.7 - 62.4 GeV
L. Adamczyk, *et al.*, [STAR Collaboration], Phys. Rev. **C93**, 014907(2016).

324. Centrality and transverse momentum dependence of elliptic flow of multi-strange hadrons and phi-meson in Au+Au Collisions at $\sqrt{s_{\rm NN}}$ = 200 GeV
† L. Adamczyk, *et al.*, [STAR Collaboration], Phys. Rev. Lett. **116**, 062301(2016).

325. Probing parton dynamics of QCD matter with Omega and phi production
† L. Adamczyk, *et al.*, [STAR Collaboration], Phys. Rev. **C93**, 021903(R)(2016).

326. Measurement of the transverse single-spin asymmetry in p+p $\rightarrow W^{\pm}/Z^0$ at RHIC
L. Adamczyk, *et al.*, [STAR Collaboration], Phys. Rev. Lett. **116**, 132301 (2016).

327. Beam-energy dependence of charged balance functions from Au + Au collisions at energies available at the BNL Relativistic Heavy Ion Collider
L. Adamczyk, *et al.*, [STAR Collaboration], Phys. Rev. **C94**, 024909 (2016).

328. Beam energy dependence of the third harmonic of azimuthal correlations in Au+Au collisions at RHIC
L. Adamczyk, *et al.*, [STAR Collaboration], Phys. Rev. Lett. **116**, 112302 (2016).

329. Measurement of elliptic flow of light nuclei at $\sqrt{s_{\rm NN}}$ = 200, 62.4, 39, 27, 19.6, 11.5, and 7.7 GeV at RHIC
L. Adamczyk, *et al.*, [STAR Collaboration], Phys. Rev. **C94**, 034908 (2016).

330. J/ψ production at low transverse momentum in $p + p$ and $d + Au$ collisions at $\sqrt{s_{\rm NN}}$ = 200 GeV
L. Adamczyk, *et al.*, [STAR Collaboration], Phys. Rev. **C93**, 64904 (2016).

331. Jet-like Correlations with Direct-Photon and Neutral-Pion Triggers at $\sqrt{s_{\rm NN}}$ = 200 GeV
L. Adamczyk, *et al.*, [STAR Collaboration], Phys. Lett. **B760**, 689 (2016).

332. Near-side azimuthal and pseudorapidity correlations using neutral strange baryons and mesons in d+Au, Cu+Cu and Au+Au collisions at $\sqrt{s_{\rm NN}}$ = 200 GeV
L. Adamczyk, *et al.*, [STAR Collaboration], Phys. Rev. **C94**, 14910(2016).

333. Effects of Nuclear Potential on the Cumulants of Net-Proton and Net-Baryon Multiplicity Distributions in Au+Au Collisions at $\sqrt{s_{\rm NN}}$ = 5 GeV
S. He, X.F, Luo, Y. Nara, S. Esumi and N. Xu, Phys. Lett. **B762**, 296 (2016).

334. Conceptual design of the HIRFL-CSR external-target experiment
† L.M. Lü, H. Yi, Z.G. Xiao, M. Shao, S. Zhang, G.Q. Xiao and N. Xu, Sci China Phys.Mech.Astro, **60**, 012021(2017).

335. Upsilon production in $U + U$ collisions at $\sqrt{s_{\rm NN}}$ = 193 GeV with the STAR experiment
L. Adamczyk, *et al.*, [STAR Collaboration], Phys. Rev. **C94**, 064904(2016).

336. Heavy quark and quarkonium transport in high-energy nuclear collisions
Kai Zhou, Wei Dai, N. Xu, P.F. Zhuang, Nucl. Phys. **A956**, 120(2016).

337. Charge-dependent directed flow in $Cu + Au$ collisions at $\sqrt{s_{\rm NN}}$ = 200 GeV
L. Adamczyk, *et al.*, [STAR Collaboration], Phys. Rev. Lett. **118**, 012301 (2017).

338. Challenges in QCD matter physics - The scientific programme of the Compressed Baryonic Matter experiment at FAIR
T. Ablyazimov *et al.*, [CBM Collaboration], Eur. Phys. J. **A53**, 60 (2017).

339. Elliptic flow of non-phonic electrons in Au + Au collisions at $\sqrt{s_{\rm NN}}$ = 200, 62.4, and 39 GeV
L. Adamczyk *et al.*, [STAR Collaboration], Phys. Rev. **C95**, 34907 (2017).

340. Heavy-flavor production and medium properties in high-energy nuclear collisions - What next?
† G. Aarts, *et al.*, Eur. Phys. J. **A53**, 93(2017).

341. Measurement of D^0 azimuthal anisotropy at mid-rapidity in Au+Au collisions at $\sqrt{s_{NN}} = 200$ GeV
L. Adamczyk *et al.*, [STAR Collaboration], Phys. Rev. Lett. **118**, 212301(2017).

342. Measurement of the cross section and longitudinal double-spin asymmetry for di-jet production in polarized *pp* collisions at $\sqrt{s_{NN}} = 200$ GeV
L. Adamczyk, *et al.*, [STAR Collaboration], Phys. Rev. **D95** , 71103 (2017).

343. Direct virtual photon production in $Au + Au$ collisions at $\sqrt{s_{NN}} = 200$ GeV
L. Adamczyk, *et al.*, [STAR Collaboration], Phys. Lett. **B770**, 451(2017).

344. 16th International Conference on Strangeness in Quark Matter (SQM 2016)
† H.Z. Huang, R. Seto, J. Thäder and N. Xu, Editor, J. Phys. Conf. Ser. **779**, 1(2017).

345. Search for the QCD Critical Point with Fluctuations of Conserved Quantities in Relativistic Heavy-Ion Collisions at RHIC : An Overview
† X.F. Luo and N. Xu, Nucl. Sci. Tech., **28**, 112(2017).

346. Energy dependence of J/ψ production in Au+Au collisions at $\sqrt{s_{NN}} = 39$, 62.4 and 200 GeV
L. Adamczyk, *et al.*, [STAR Collaboration], Phys. Lett. **B771**, 13 (2017).

347. Di-jet imbalance measurements at $\sqrt{s_{NN}} = 200$ GeV at STAR
L. Adamczyk, *et al.*, [STAR Collaboration], Phys. Rev. Lett. **119**, 62301 (2017).

348. Bulk properties of the medium produced in relativistic heavy-ion collisions from the beam energy scan program
L. Adamczyk *et al.*, [STAR Collaboration], Phys. Rev. **C96**, 44904 (2017).

349. Constraining the initial conditions and temperature dependent transport with three-particle correlations in Au+Au collisions
L. Adamczyk *et al.*, [STAR Collaboration], Phys. Lett. **B790**, 81(2019).

350. Harmonic decomposition of three-particle azimuthal correlations at RHIC
L. Adamczyk *et al.*, [STAR Collaboration], Phys. Rev. **C98**, 34918(2018).

351. Measurement of jet-quenching with semi-inclusive hadron+jet distributions in Au+Au collisions at $\sqrt{s_{NN}} = 200$ GeV
L. Adamczyk *et al.*, [STAR Collaboration], Phys. Rev. **C96**, 24905 (2017).

352. Coherent diffractive photo production of ρ^0 mesons on gold nuclei at RHIC
L. Adamczyk *et al.*, [STAR Collaboration], Phys. Rev. **C96**, 54904 (2017).

353. Global Lambda Hyperon Polarization in Nuclear Collisions: Evidence for the most Vortical Fluid
L. Adamczyk *et al.*, [STAR Collaboration], Nature **548**, 62 (2017).

354. Beam Energy Dependence of Directed Flow of Λ, $\overline{\Lambda}$, $K^{\pm}$, K^0_S and ϕ in Au+Au collisions
† L. Adamczyk *et al.*, [STAR Collaboration], Phys. Rev. Lett. **120**, 62301 (2018).

355. Azimuthal transverse single-spin asymmetries of inclusive jets and charged pions within jets from polarized-proton collisions at $\sqrt{s} = 500$ GeV
L. Adamczyk *et al.*, [STAR Collaboration], Phys. Rev. **D97**, 32004 (2018).

356. Transverse spin-dependent azimuthal correlations of charged pion pairs measured in p+p collisions at $\sqrt{s} = 500$ GeV
L. Adamczyk *et al.*, [STAR Collaboration], Phys. Lett. **B780**, 332 (2018).

357. Global polarization of Lambda hyperons in Au+Au collisions at $\sqrt{s_{NN}} = 200$ GeV
L. Adamczyk *et al.*, [STAR Collaboration], Phys. Rev. **C98**, 014910(2018).

358. Collision Energy Dependence of Moments of Net-Kaon Multiplicity Distributions at RHIC
† L. Adamczyk *et al.*, [STAR Collaboration], Phys. Lett. **B785**, 551 (2018).

359. Measurement of hyper triton lifetime in Au+Au collisions at the Relativistic Heavy-Ion Collider
L. Adamczyk *et al.*, [STAR Collaboration], Phys. Rev. **C97**, 54909(2018).

360. Azimuthal anisotropy in Cu+Au collisions at $\sqrt{s_{NN}} = 200$ GeV
L. Adamczyk *et al.*, [STAR Collaboration], Phys. Rev. **C98**, 014915(2018).

361. Correlation measurements between flow harmonics in Au+Au collisions at RHIC
L. Adamczyk *et al.*, [STAR Collaboration], Phys. Lett. **B338**, 50(2018).

362. Longitudinal double-spin asymmetries for Dijets production at intermediate pseudo rapidity in polarized pp collisions at $\sqrt{s} = 200$ GeV
L. Adamczyk *et al.*, [STAR Collaboration], Phys. Rev. **D98**, 032011(2018).

363. Beam Energy Dependence of Jet-Quenching Effects in Au+Au Collisions at $\sqrt{s_{NN}} = 7.7$, 11.5, 14.5, 19.6, 27, 39, and 62.4 GeV
L. Adamczyk *et al.*, [STAR Collaboration], Phys. Rev. Lett. **121**, 32301(2018)

364. Longitudinal double-spin asymmetries for π^0s in the forward directions for 510 GeV polarized pp collisions
L. Adamczyk *et al.*, [STAR Collaboration], Phys. Rev. **D98**, 32013 (2018).

365. Low-p_T $e + e^-$ pair production in Au+Au collisions at $\sqrt{s_{NN}}$ = 200 GeV and U+U collisions at $\sqrt{s_{\rm NN}}$ = 193 GeV at STAR
L. Adamczyk *et al.*, [STAR Collaboration], Phys. Rev. Lett. **121**, 132301(2018).

366. Collision energy dependence of p_T correlations in Au+Au collisions at RHIC
J. Adam *et al.*, [STAR Collaboration], Phys. Rev. **C99**, 44918(2019).

367. Centrality and transverse momentum dependence of D0-meson production at mid-rapidity in Au+Au collisions at $\sqrt{s_{\rm NN}}$ = 200 GeV
J. Adam *et al.*, [STAR Collaboration], Phys. Rev. **C99**, 34908(2019).

368. Measurement of the longitudinal spin asymmetries for weak boson production in proton-proton collisions at $\sqrt{s}$ = 510 GeV
J. Adam *et al.*, [STAR Collaboration], Phys. Rev. **D99**, 51102(2019).

369. Transverse spin transfer to Λ and $\overline{\Lambda}$ hyperons in polarized proton-proton collisions at $\sqrt{s}$ = 200 GeV
L. Adamczyk *et al.*, [STAR Collaboration], Phys. Rev. **D98**, 91103(2018).

370. Improved measurement of the longitudinal spin transfer to Λ and $\overline{\Lambda}$ hyperons in polarized proton-proton collisions at $\sqrt{s}$ = 200 GeV
L. Adamczyk *et al.*, [STAR Collaboration], Phys. Rev. **D98**, 112009(2018).

371. The proton-Omega correlation function in Au+Au collisions at $\sqrt{s_{\rm NN}}$ = 200 GeV
J. Adam *et al.*, [STAR Collaboration], Phys. Lett. **B790**, 490(2019).

372. J/ψ production cross section and its dependence on charged-particle multiplicity in p+p collisions at $\sqrt{s}$ = 200 GeV
L. Adamczyk *et al.*, [STAR Collaboration], Phys. Lett. **B786**, 87(2018).

373. Global polarization of Lambda hyperons in Au+Au collisions at $\sqrt{s_{\rm NN}}$ = 200 GeV
J. Adam *et al.*, [STAR Collaboration], Phys. Rev. **C98**, 14910(2018).

374. Azimuthal Harmonics in Small and Large Collision Systems at RHIC Top Energies
J. Adam *et al.*, [STAR Collaboration], Phys. Rev. Lett. **122**, 172301(2019).

375. Collision-energy dependence of second-order off-diagonal and diagonal cumulants of net-charge, net-proton, and net-kaon multiplicity distributions in Au + Au collisions
J. Adam *et al.*, [STAR Collaboration], Phys. Rev. **C100**, 014902(2019).

376. Longitudinal double-spin asymmetry for inclusive jet and dijet production in *pp* collisions at $\sqrt{s}$ = 510 GeV
J. Adam *et al.*, [STAR Collaboration], Phys. Rev. **D100**, 052005(2019).

377. Measurements of the transverse-momentum-dependent cross sections of J/ψ production at mid-rapidity in proton+proton collisions at $\sqrt{s}$ = 510 and 500 GeV with the STAR detector
J. Adam *et al.*, [STAR Collaboration], Phys. Rev. **D100**, 052009(2019).

378. Measurement of inclusive J/ψ suppression in Au+Au collisions at $\sqrt{s_{\rm NN}}$ = 200 GeV through the dimuon channel at STAR
J. Adam *et al.*, [STAR Collaboration], Phys. Lett. **B797**, 134917(2019).

379. Polarization of Λ ($\overline{\Lambda}$) Hyperons along the Beam Direction in Au+Au Collisions at $\sqrt{s_{\rm NN}}$ = 200 GeV
J. Adam *et al.*, [STAR Collaboration], Phys. Rev. Lett. **123**, 132301(2019).

380. Charge-dependent pair correlations relative to a third particle in p+Au and d+Au collisions at RHIC
J. Adam *et al.*, [STAR Collaboration], Phys. Lett. **B798**, 134975(2019).

381. First observation of the directed flow of D^0 and $\overline{D^0}$ in Au+Au collisions at $\sqrt{s_{\rm NN}}$ = 200 GeV
† J. Adam *et al.*, [STAR Collaboration], Phys. Rev. Lett. **123** , 162301(2019).

382. Observation of excess J/ψ yield at very low transverse momenta in Au+Au collisions at $\sqrt{s_{\rm NN}}$ = 200 GeV and U+U collisions at $\sqrt{s_{\rm NN}}$ = 193 GeV
J. Adam *et al.*, [STAR Collaboration], Phys. Rev. Lett. **123**, 132302(2019).

383. Beam energy dependence of (anti)deuteron production in Au+Au collisions at RHIC
† J. Adam *et al.*, [STAR Collaboration], Phys. Rev. **C99**, 64905(2019).

384. Azimuthal harmonics in small and large collision systems at RHIC top energies
J. Adam *et al.*, [STAR Collaboration], Phys. Rev. Lett. **122**, 172301(2019).

385. Collision Energy Dependence of p_T Correlations in Au+Au collisions at RHIC
J. Adam *et al.*, [STAR Collaboration], Phys. Rev. **C99**, 44918(2019).

386. Measurement of the mass difference and the binding energy of hypertriton and antihypertriton
J. Adam *et al.*, [STAR Collaboration], Nature Physics, **16**, 409(2020).

387. Beam-energy dependence of identified two-particle angular correlations in $\sqrt{s_{\rm NN}}$ = 7.7 - 200 GeV Au + Au collisions J. Adam *et al.*, [STAR Collaboration], Phys. Rev. **C101**, 014916(2020).

388. Bulk Properties of the System Formed in Au+Au Collisions at $\sqrt{s_{\rm NN}}$ = 14.5 GeV at STAR
J. Adam *et al.*, [STAR Collaboration], Phys. Rev. **C101**, 024905 (2020).

389. Mapping the Phases of Quantum Chromodynamics with Beam Energy Scan
† A. Bzdak, S. Esumi, V. Koch, M. Stephanov, and N. Xu, Physics Report **853**, 1 (2020).

390. Underlying event measurements in p+p collisions at $\sqrt{s}$ = 200 GeV at RHIC
J. Adam *et al.*, [STAR Collaboration], Phys. Rev. **D101**, 052004(2020).

391. First measurement of Λ_c baryon production in Au+Au collisions at $\sqrt{s_{\rm NN}}$ = 200 GeV
† J. Adam *et al.*, [STAR Collaboration], Phys. Rev. Lett. **124**, 172301(2020).

392. A next-generation LHC heavy-ion experiment
D. Adamova, *et al.*, May, (2019).
arXiv: 1902.01211 v2

393. Electron - Ion Collider in China (in Chinese)
† Xu Cao *et al.*, Nucl. Sci. and Tech., **43**, 020001(2020).

394. Study of the Properties of the QCD Phase Diagram in High-Energy Nuclear Collisions
† Xiaofeng Luo, Shusu Shi, Nu Xu and Yifei Zhang, Particle **3**, 278(2020).

395. Charm and beauty isolation from heavy flavor decay electrons in Au+Au collisions at $\sqrt{s_{\rm NN}}$ = 200 GeV at RHIC
Fan Si, Xiao-Long Chen, Long Zhou, Yo-Fei Zhang, Sheng-Hui Zhang, Xin-Yue Li, Sing Dong, N. Xu, Phys. Lett. **B805**, 135465(2020).

396. Huizhou accelerator complex facility and its future development
† H.W. Zhao *et al.*, Science in China, **50**, 112006 (2020).

397. Physics Cases in EicC
† X. Cao *et al.*, Science in China, **50**, 112005 (2020).

398. Study of the QCD Phase Structure at HIAF
† Y.G. Ma, N. Xu and F. Liu, Science in China, **50**, 112009 (2020).

399. Beam-Energy Dependence of the Directed Flow of Deuterons in Au+Au Collisions
† J. Adam *et al.*, [STAR Collaboration], Phys. Rev. **C102**, 044906 (2020).

400. The Little-Bang and the Femto-Nova in Nucleus-Nucleus Collisions
† N. Xu, K. Fukushima and B. Mohanty, AAPPS Bulletin, **31**, 1 (2021).

401. Probing thermal nature of matter formed at RHIC via fluctuations
† S. Gupta, D. Mallick, D.K. Mishra, B. Mohanty and N. Xu, Nucl. Phys. **A1005**, 121987(2021).

402. Measurements of W and Z/γ^* cross sections and their ratios in $p+p$ collisions at RHIC
J. Adam *et al.*, [STAR Collaboration], Phys. Rev. **D103**, 012001 (2021).

403. The 28th International Conference on Ultra-relativistic Nucleus-Nucleus Collisions: Quark Matter 2019
† F.Liu, E.K. Wang, X.N. Wang, N. Xu and B.W. Zhang, Editors, Proceedings of *Quark Matter 2019*, November 4 - 11, 2019, Wuhan, China, Nucl. Phys. **A1005**, 1(2021).

404. Non-monotonic energy dependence of net-proton number fluctuations
† J. Adam *et al.*, [STAR Collaboration], Phys. Rev. Lett. **126**, 092301 (2021).

405. Comparison of transverse single-spin asymmetries for forward π^0 production in polarized pp, pAl and pAu collisions at nucleon pair c.m. energy $\sqrt{s_{\rm NN}}$ = 200 GeV
J. Adam *et al.*, [STAR Collaboration], Phys. Rev. **D103**, 072005 (2021).

406. Flow and interferometry results from Au+Au collisions at $\sqrt{s_{\rm NN}}$ = 4.5 GeV
J. Adam *et al.*, [STAR Collaboration], Phys. Rev. **C103**, 034908(2021).

407. EIC Physics from An All-Silicon Tracking Detector
† J. Arrington, *et al.* February, (2021).
arXiv:2102.08337

408. Global polarization of Ξ and Ω hyperons in Au+Au collisions at $\sqrt{s_{\rm NN}}$ = 200 GeV
J. Adam *et al.*, [STAR Collaboration], Phys. Rev. Lett. **126**, 162301(2020).

409. Measurement of transverse single-spin asymmetries of π^0 and electromagnetic jets at forward rapidity in 200 and 500 GeV transversely polarized proton-proton collisions
J. Adam *et al.*, [STAR Collaboration], Phys. Rev. **D103**, 092009 (2021).

410. Methods for a blind analysis of isobar data collected by the STAR collaboration
J. Adam *et al.*, [STAR Collaboration], NST **32**, 48 (2021).

411. Measurement of inclusive J/ψ polarization in p+p collisions at 200 GeV by the STAR experiment
J. Adam *et al.*, [STAR Collaboration], Phys. Rev. **D 102**, 92009 (2020).

412. Observation of $D_S^{\pm}/D^0$ enhancement in Au+Au collisions at $\sqrt{s_{\rm NN}}$ = 200 GeV
J. Adam *et al.*, [STAR Collaboration], Phys. Rev. Lett. **127**, 092301 (2021).

413. Measurement of e+e- Momentum and Angular Distributions from Linearly Polarized Photon Collisions
J. Adam *et al.*, [STAR Collaboration], Phys. Rev. Lett. **127**, 052302 (2021).

414. Cumulants and correlation functions of net-proton, proton, and antiproton multiplicity distributions in Au+Au collisions at energies available at the BNL Relativistic Heavy Ion Collider
† M.S. Abdallah *et al.*, [STAR Collaboration], Phys. Rev. **C104**, 024902 (2021).

415. Electron-Ion Collider in China (EicC)
† D.P. Anderle *et al.* Frontier of Physics, **16**, 64701(2021).

416. Longitudinal double-spin asymmetry for inclusive jet and dijet production in polarized proton collisions at $\sqrt{s}$ = 200 GeV
M.S. Abdallah *et al.*, [STAR Collaboration], Phys. Rev. **D103**, L0911003 (2021).

417. Azimuthal anisotropy measurements of strange and multi-strange hadrons in U+U collisions at 193 GeV at RHIC
M.S. Abdallah *et al.*, [STAR Collaboration], Phys. Rev. **C103**, 064907 (2021).

418. Erratum: Azimuthal anisotropy at the relativistic heavy ion collider: The first and fourth harmonics [Phys. Rev. Lett. **92**, 062301 (2004)]
J. Adam *et al.*, [STAR Collaboration], Phys. Rev. Lett. **127**, 069901(2021).

419. Measurement of the sixth-order cumulant of net-proton multiplicity distributions in Au+Au collisions at 27, 54.4, and 200 GeV at RHIC
† M.S. Abdallah *et al.*, [STAR Collaboration], Phys. Rev. Lett. **127**, 262301(2021).

420. Search for the chiral magnetic effect via charge-dependent azimuthal correlations relative to spectator and participant planes in Au+Au collisions at $\sqrt{s_{\rm NN}}$ = 200 GeV
M.S. Abdallah *et al.*, [STAR Collaboration], Phys. Rev. Lett. **128**, 92301 (2022).

421. Invariant jet mass measurements in pp collisions at $\sqrt{s}$ = 200 GeV at RHIC
M.S. Abdallah *et al.*, [STAR Collaboration], Phys. Rev. **D104**, 052007(2021).

422. Global Λ-hyperon polarization in Au+Au collisions at $\sqrt{s_{\rm NN}}$ = 3 GeV
M.S. Abdallah *et al.*, [STAR Collaboration], Phys. Rev. **C104**, 61901(2021).

423. Measurement of cold nuclear matter effects for inclusive J/ψ in p+Au collisions at 200 GeV
M.S. Abdallah *et al.*, [STAR Collaboration], Phys. Lett. **B825**, 136865 (2021).

424. Search for the Chiral Magnetic Effect with Isobar Collisions at $\sqrt{s_{\rm NN}}$ = 200 GeV by the STAR Collaboration at RHIC
M.S. Abdallah *et al.*, [STAR Collaboration], Phys. Rev. **C105**, 014901(2022).

425. Light Nuclei Collectivity from 3 GeV Au+Au Collisions at RHIC
† M.S. Abdallah *et al.*, [STAR Collaboration], Phys. Lett. **B827**, 136941(2022).

426. Measurement of inclusive electrons from open heavy-flavor hadron decays in p+p collisions at $\sqrt{s}$ = 200 GeV with the STAR detector
M.S. Abdallah *et al.*, [STAR Collaboration], Phys. Rev. **D105**, 032007(2022).

427. Search for the chiral magnetic effect via charge-dependent azimuthal correlations relative to spectator and participant planes in Au+Au collisions at $\sqrt{s_{\rm NN}}$ = 200 GeV
M.S. Abdallah *et al.*, [STAR Collaboration], Phys. Rev. Lett. **128**, 092301(2022).

428. Probing the Gluonic Structure of the Deuteron with J/ψ Photoproduction in d+Au Ultra-peripheral Collisions
M.S. Abdallah *et al.*, [STAR Collaboration], Phys. Rev. Lett. **128**, 122303(2022).

429. Differential measurements of jet substructure and partonic energy loss in Au+Au collisions at $\sqrt{s_{\rm NN}}$ = 200 GeV
M.S. Abdallah *et al.*, [STAR Collaboration], Phys. Rev. **C105**, 29901(2022).

430. Disappearance of partonic collectivity in $\sqrt{s_{\rm NN}}$ = 3 GeV Au+Au Collisions at RHIC
† M.S. Abdallah *et al.*, [STAR Collaboration], Phys. Lett. **B827**, 137003(2021).

431. Limits of thermalization in relativistic heavy ion collisions
S. Gupta, D. Mallick, D.K. Mishra, B. Mohanty and N. Xu, Phys. Lett. **B829**, 137021 (2021).

432. Longitudinal double-spin asymmetry for inclusive jet and dijet production in polarized proton collisions at $\sqrt{s}$ = 510 GeV
M.S. Abdallah *et al.*, [STAR Collaboration], Phys. Rev. **D105**, 92011 (2022).

433. Measurements of ${}^3_{\Lambda}$H and ${}^3_{\bar{\Lambda}}\bar{\rm H}$ Lifetimes and Yields in Au+Au Collisions in the High Baryon Density Region
M.S. Abdallah *et al.*, [STAR Collaboration], Phys. Rev. Lett. **128**, 202301 (2021).

434. Probing Strangeness Canonical Ensemble with K^-, $\phi(1020)$ and Ξ^- Production in Au+Au Collisions at $\sqrt{s_{\rm NN}} = 3$ GeV
M.S. Abdallah *et al.*, [STAR Collaboration], Phys. Lett. **B831**, 137152(2022).

435. Azimuthal transverse single-spin asymmetries of inclusive jets and identified hadrons within jets from polarized pp collisions $\sqrt{s} = 200$ GeV
M.S. Abdallah *et al.*, [STAR Collaboration], Phys. Rev. **D106**, 072010 (2022).

436. Measurements of Proton High Order Cumulants in $\sqrt{s_{\rm NN}} = 3$ GeV Au+Au Collisions and Implications for the QCD Critical Point
† M.S. Abdallah *et al.*, [STAR Collaboration], Phys. Rev. Lett. **128**, 202303 (2022).

437. Evidence for Nonlinear Gluon Effects in QCD and Their Mass Number Dependence at STAR
M.S. Abdallah *et al.*, [STAR Collaboration], Phys. Rev. Lett. **129**, 092501 (2022).

438. Pair invariant mass to isolate background in the search for the chiral magnetic effect in Au+Au collisions at $\sqrt{s_{\rm NN}} =$ 200 GeV
J. Adam *et al.*, [STAR Collaboration], Phys. Rev. **C106**, 034908 (2020).

439. Projections of two-particle correlations onto transverse rapidity in Au+Au collisions at $\sqrt{s_{\rm NN}} = 200$ GeV at STAR
M.S. Abdallah *et al.*, [STAR Collaboration], Phys. Rev. **C106**, 044906 (2022).

440. Evidence of Mass Ordering of Charm and Bottom Quark Energy Loss in Au+Au Collisions at RHIC
M.S. Abdallah *et al.*, [STAR Collaboration], Eur. J. Phys. **C82**, 1150 (2022).

441. Collision-system and beam-energy dependence of anisotropic flow fluctuations
M.S. Abdallah *et al.*, [STAR Collaboration], Phys. Rev. Lett. **129**, 252301(2022).

442. Measurement of ${}^4_\Lambda$H and ${}^4_\Lambda$He binding energy in Au+Au collisions at $\sqrt{s_{\rm NN}} = 3$ GeV
M.S. Abdallah *et al.*, [STAR Collaboration], Phys. Lett. **B834**, 137449 (2022).

443. Centrality and transverse momentum dependence of higher-order flow harmonics of identified hadrons in Au+Au collisions at $\sqrt{s_{\rm NN}} = 200$ GeV
M.S. Abdallah *et al.*, [STAR Collaboration], Phys. Rev. **C105**, 64911 (2022).

444. Pattern of global spin alignment of ϕ and K^{*0} mesons in heavy-ion collisions
M.S. Abdallah *et al.*, [STAR Collaboration], Nature, **6144**, 244 (2023).

445. K^{*0} production in Au+Au collisions at $\sqrt{s_{\rm NN}} = 7.7$, 11.5, 14.5, 19.6, 27 and 39 GeV from the RHIC beam energy scan
M.S. Abdallah *et al.*, [STAR Collaboration], Phys. Rev. **C107**, 034907 (2023).

446. Azimuthal transverse single-spin asymmetries of inclusive jets and identified hadrons within jets from polarized *pp* collisions at $\sqrt{s_{\rm NN}} = 200$ GeV
M.S. Abdallah *et al.*, [STAR Collaboration], Phys. Rev. **C106**, 72010 (2022).

447. Measurement of Sequential Υ Suppression in Au+Au Collisions at $\sqrt{s_{\rm NN}} = 200$ GeV With the STAR Experiment
B.E. Aboona *et al.*, [STAR Collaboration], Phys. Rev. Lett. **130**, 112301 (2023).

448. Search for the Chiral Magnetic Effect in Au+Au collisions at $\sqrt{s_{\rm NN}}$ =27 GeV with the STAR forward Event Plane Detectors
B.E. Aboona *et al.*, [STAR Collaboration], Phys. Lett. **B839**, 137779 (2023).

449. Azimuthal anisotropy measurement of (multi-)strange hadrons in Au+Au collisions at $\sqrt{s_{\rm NN}} = 54.4$ GeV
M.S. Abdallah *et al.*, [STAR Collaboration], Phys. Rev. **C**, accepted, (2023).

450. Higher-Order Cumulants and Correlation Functions of Proton Multiplicity Distributions in $\sqrt{s_{\rm NN}} = 3$ GeV Au+Au Collisions by the STAR Experiment
† M.S. Abdallah *et al.*, [STAR Collaboration], Phys. Rev. **C107**, 024908(2023).

451. Beam energy dependence of the linear and mode-coupled flow harmonics in Au+Au collisions
B.E. Aboona *et al.*, [STAR Collaboration], Phys. Lett. **B839**, 137755 (2023).

452. The Present and Future of QCD
† P. Achenbach *et al.*, arXiv: 2303.02579

453. Beam Energy Dependence of Fifth and Sixth-Order Net-proton Number Fluctuations in Au+Au Collisions at RHIC
† M.S. Abdallah *et al.*, [STAR Collaboration], Phys. Rev. Lett. , accepted, (2023).

454. First Observation of Directed Flow of Hypernuclei ${}^3_\Lambda$H and ${}^4_\Lambda$H in $\sqrt{s_{\rm NN}} = 3$ GeV Au+Au Collisions at RHIC
† M.S. Abdallah *et al.*, [STAR Collaboration], Phys. Rev. Lett. , accepted, (2023).

455. Pion, Kaon, and (Anti-)Proton Production in U+U Collisions at $\sqrt{s_{\rm NN}} = 193$ GeV in STAR
M.S. Abdallah *et al.*, [STAR Collaboration], Phys. Rev. **C107**, 024901 (2023).

456. Beam Energy Dependence of Triton Production and Yield Ratios ($N_t \times N_p/N_d^2$) in Au+Au Collisions at RHIC
† M.S. Abdallah *et al.*, [STAR Collaboration], Phys. Rev. Lett. **130**, 202301(2023).

457. Measurements of the elliptic and triangular azimuthal anisotropies in central 3He+Au, d+Au and p+Au collisions at $\sqrt{s_{\rm NN}} = 200$ GeV
M.S. Abdallah *et al.*, [STAR Collaboration], Phys. Rev. Lett. , accepted, (2023).

Article | Nu Xu

The Little-Bang and the femto-nova in nucleus-nucleus collisions

Nu Xu[1,2,3*], Kenji Fukushima[4] and Bedangadas Mohanty[1,5]

Abstract

We make a theoretical and experimental summary of the state-of-the-art status of hot and dense QCD matter studies on selected topics. We review the Beam Energy Scan program for the QCD phase diagram and present the current status of the search for the QCD critical point, particle production in high baryon density region, hypernuclei production, and global polarization effects in nucleus-nucleus collisions. The available experimental data in the strangeness sector suggests that a grand canonical approach in the thermal model at high collision energy makes a transition to the canonical ensemble behavior at low energy. We further discuss future prospects of nuclear collisions to probe properties of baryon-rich matter. Creation of a quark-gluon plasma at high temperature and low baryon density has been called the "Little-Bang" and, analogously, a femtometer-scale explosion of baryon-rich matter at lower collision energy could be called the "femto-nova", which could possibly sustain substantial vorticity and a magnetic field for non-head-on collisions.

1 Introduction

Nuclei are bound states of protons and neutrons via the strong interaction. The fundamental theory of the strong interaction is quantum chromodynamics (QCD). In QCD, gluons are massless due to gauge symmetry; up (u) quarks are as light as $m_u = 3 - 4\,\mathrm{MeV}$ and down (d) quarks are heavier than u-quarks, i.e., $m_u/m_d \sim 0.5$ (see Ref. [1] for a recent review of quark masses from the lattice-QCD). The strange (s) quark mass is comparable to the typical QCD energy scale, that is, $m_s = 80 - 90\,\mathrm{MeV}$ of the same order as $\Lambda_{\mathrm{QCD}} = 100 - 200\,\mathrm{MeV}$. Since charm ($c$) and bottom ($b$) quarks are much heavier than Λ_{QCD}, they would make only small contributions to bulk thermodynamics and they serve as external probes. Here, we focus on two puzzling QCD features for the nucleons which are composed of N_c valence quarks (where $N_c = 3$ is the number of colors in QCD) and have a mass, $m_N \simeq 940\,\mathrm{MeV} \sim N_c\Lambda_{\mathrm{QCD}}$. The first question is how can almost massless particles form a bound state with a positive binding energy? The second question is how can the nucleons become so extremely massive out of almost massless particles? The former question on the existence of bound states is referred to as *confinement* and the latter on the origin of the mass is via *spontaneous chiral symmetry breaking*.

The key to resolve these puzzles lies in QCD vacuum structure. The vacuum in quantum field theory is not empty in general but is full of quantum fluctuations dictated by fundamental interactions. Thus, the QCD vacuum is regarded as a "medium" in analogy to condensed matter physics. Just like spin systems for example, the QCD vacuum structure may be either an ordered/disordered state according to external environments such as the temperature T, the baryon density ρ_{B} (or the baryon chemical potential μ_{B}), the magnetic field $\boldsymbol{B}$, and the vorticity $\boldsymbol{\omega}$, etc. The idea of using the relativistic nucleus-nucleus collisions or heavy-ion collisions is to shake the QCD vacuum with high energy density to observe new states of matter out of quarks and gluons and to seek for traces of phase transitions associated with confinement and/or chiral symmetry breaking (see Ref. [2] for historical backgrounds).

*Correspondence: nxu@lbl.gov
[1] Institute of Modern Physics, Chinese Academy of Sciences, 509 Nanchang Road, Lanzhou 730000, China
[2] College of Physical Science and Technology, Central China Normal University, Wuhan 430079, China
Full list of author information is available at the end of the article

The saturation density around the center of heavy nuclei is $\rho_0 \simeq 0.16\,\text{nucleons/fm}^3$ corresponding to the energy density $\epsilon_0 \simeq 0.15\,\text{GeV/fm}^3$. At the initial stage of the heavy-ion collisions, the energy density can reach hundreds times larger than the saturation density depending on the collision energy per nucleon, $\sqrt{s_{NN}}$. The thermodynamic relation between the energy density ϵ and the temperature T (i.e., the Stefan-Boltzmann law) converts $\epsilon = 0.8 - 1.0\,\text{GeV/fm}^3$ to $T = 150 - 160\,\text{MeV}$ which is comparable to *LQCD*, above which a quark-gluon plasma (QGP) is realized. In the history of the Universe such high-T matter should have existed shortly (on the order of μs) after the Big Bang. In this sense, the QGP physics can be regarded as an emulation of the Big Bang in the laboratory on the Earth, which may well be called the *Little Bang*.

Now that we have learnt intriguing properties of the QGP in the regime at high T and low μ_B, a next direction of the relativistic heavy-ion collision physics is expanding toward the regime at high baryon density. The phase structures could have much richer contents in these high-density regions, see Refs. [3–5] for reviews on the QCD phase diagrams. We have already known that symmetric nuclear matter has a first-order phase transition at $\mu_B \approx 923\,\text{MeV}$, that is, the nucleon mass minus the binding energy $\sim 16\,\text{MeV}$. Then, a terminal point of the first-order phase boundary, namely, a critical point of liquid-gas phase transition in nuclear matter exists around $T = (10 - 20)\,\text{MeV}$ (see Ref. [6] for a comprehensive review including experimental signatures). The question is what new state of matter is anticipated for nuclear matter at higher baryon density. The central core of a neutron star could exhibit the most baryon-rich and equilibrated state of matter in the Universe, where the density could be as large as $\sim 5\rho_0$ or even higher. The baryon density may become even larger in transient processes such as neutron star mergers. Analogously, by adjusting the collision energy in the heavy-ion collisions, the baryon density could transiently increase up to several times of ρ_0 according to numerical simulations [7]. Such a femtometer-scale explosion of baryon rich matter can be called the *femto-nova*. This concept is illustrated in Fig. 1.

Historically, studies with heavy-ion collisions started from low energy and we had to wait for high-energy colliders, the Relativistic Heavy Ion Collider (RHIC) and the Large Hadron Collider (LHC), to arrive at a definitive conclusion on the QGP formation. As for the low-energy regions, unfortunately, only little is known in theory about the phase structures in low-T and high-μ_B (or high-ρ_B) regions. There are some speculations on the ground state structures in such regimes which will be partially reviewed in this article. The most important landmark is the *QCD critical point*. In the same way as the critical point of the nuclear liquid-gas phase transition, deconfined QCD matter may have a first-order phase boundary and the QCD critical point appears at the terminal point of the first-order line. Its exact location is not well constrained yet, and the experimental efforts to discover the QCD critical point are still continuing.

This article is organized as follows. We will first describe the phase diagram, the QCD critical point, and properties of baryon-rich matter including strangeness degrees of freedom. We will then proceed to the current status of experimental data on these topics. After this, we will return to theory to cover speculations and challenges to be clarified in the future. Finally, we discuss the future directions of ongoing experimental projects as well as future experimental facilities.

2 Current status—theory

2.1 Theoretical background for the QCD phase diagram

It has been established that hadronic matter continuously changes into the QGP with increasing temperature T as long as μ_B is sufficiently smaller than T. Although this continuous change of matter takes place around $T = (156.5 \pm 1.5)\,\text{MeV}$ according to the lattice-QCD simulations [8], there is no strict phase transition. In the QCD community this transitional but still continuous change of matter is commonly referred to as a *crossover*.

If masses of u and d quarks are zero and other quarks are massive, such 2-flavor QCD, matter would go through a second-order phase transition for which various derivatives of thermodynamic quantities diverge with critical exponents belonging to the O(4) universality class (or a first-order transition if the axial anomaly is restored, see Ref. [9]). Physical values of m_u and m_d are much smaller than Λ_{QCD}, and it is conceivable to observe some remnants of the second-order phase transition. Indeed, in the lattice-QCD simulation [10], it has been numerically confirmed that the magnetic scaling follows consistently with the O(4) universality class, from which the "pseudo-critical" temperature, T_{pc}, can be deduced.

The pseudo-critical temperature should be a function of the density. Generally, $T_{pc}(\mu_B)$ is a decreasing function with increasing μ_B due to the Pauli blocking of quarks in phase space. Because of the notorious sign problem in the Monte-Carlo algorithm, expectation values of observables cannot be computed and the first-principles lattice-QCD simulation cannot access a region with a substantial value of baryon density, and so there is no reliable theoretical prediction for $T_{pc}(\mu_B)$ at μ_B much larger than T.

Instead, a phenomenologically determined boundary on the μ_B-T plane is known, called the line of the *chemical freeze-out*, which has been identified from a hybrid approach of theory and experiment. The chemical freeze-out literally means that inelastic reactions stop and chemical compositions are fixed there. In QCD matter hadrons interact and particle species can change

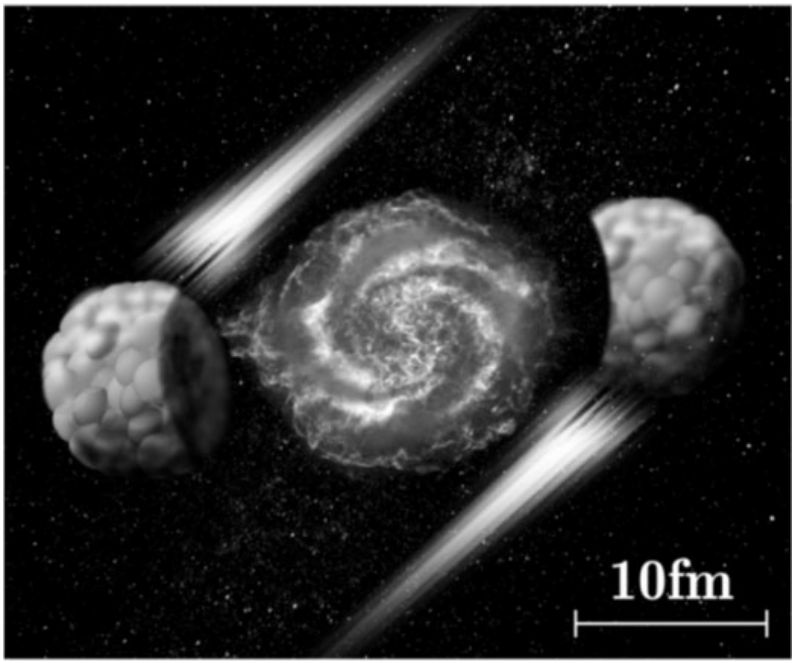

Fig. 1 Schematic illustration of a femto-nova as a femtometer-scale explosion of baryon-rich matter in relativistic heavy-ion collisions

like chemical reactions. In heavy-ion collision the physical system is expanding and the temperature rapidly drops down. Therefore, the average inter-particle distance would increase as the temperature gets lowered. In particular, around $T_{\rm pc}$, the entropy density significantly falls down, and correspondingly the degrees of freedom in thermal excitations decrease [11]. Since the average inter-particle distance becomes large, the interaction among hadrons is considered to be diminished. In this way, the observed particle yields keep the footprint of the hot and dense hadronic matter when the interaction was turned off at a temperature $T_{\rm ch}$, that is presumably close to the temperature when the matter underwent a crossover at $T_{\rm pc}$. As observed experimentally, relative abundances of hadrons obey the thermal distribution at common T and $\mu_{\rm B}$, so that the thermal fit can fix T and $\mu_{\rm B}$, or a line of chemical freeze-out, $T = T_{\rm ch}(\mu_{\rm B})$ [12]. We note that the charge chemical potential μ_Q is fixed from the proton/neutron ratio and the strangeness chemical potential μ_S is fixed from the strangeness free condition. With various center-of-mass colliding energies, we can change accessible $\mu_{\rm B}$ to sample $T_{\rm ch}(\mu_{\rm B})$ from the thermal fit [13, 14], see Fig. 2. Generally speaking, collisions at smaller $\sqrt{s_{NN}}$ have larger baryon stopping, leading to larger values of $\mu_{\rm B}$ (and smaller values of T) [15]. Thus, the line of chemical freeze-out on the $\mu_{\rm B}$-T plane should be regarded as an experimentally determined QCD phase diagram under the assumption that $T_{\rm ch}$ stays close to $T_{\rm pc}$, which has been verified by the lattice-QCD simulations for $\mu_{\rm B} \lesssim 0.3\,{\rm GeV}$ [8], as also displayed in Fig. 2. This underlies the idea of the beam energy scan (BES) program at RHIC. The thermal description is applicable for not only particle abundances but also thermodynamic quantities such as pressure and entropy density.

We note that the thermal models often assume the grand canonical ensemble (GCE) that is equivalent to the canonical ensemble (CE) in the thermodynamic (infinite volume) limit but is not so when the system size becomes small in the heavy-ion collision. We will discuss which of the GCE and the CE better fits the experimental data later.

2.2 Observables for the QCD critical point

It is known from the theoretical analysis that the QCD crossover has a general tendency to become closer to a first-order transition at larger $\mu_{\rm B}$ (see discussions in a review [16]). It is thus a natural anticipation that the

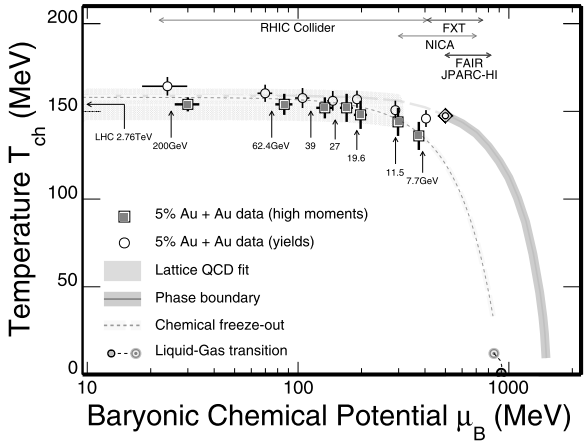

Fig. 2 Chemical freeze-out temperature $T_{\rm ch}(\mu_{\rm B})$ from the top 5% central Au+Au collisions at RHIC. Open-circles represent the parameters extracted from hadron yields [13], while the filled-squares are extracted from net-proton higher moments (up to third order) [14]. Representing the smooth crossover region is the lattice-QCD results shown by the green band. The empirical thermal fit results to global hadron yield data are shown as yellow line [15]. The coverage of the RHIC BES program, the STAR fixed target program (FXT), and future (FAIR, JPARC-HI, and NICA) experimental facilities are also indicated at the top of the figure. The liquid-gas transition region that features a second order critical point is shown by the red-circle, and a first-order transition line is shown by the black dashed line, which connects the critical point to the ground state of nuclear matter

QCD crossover may turn to a first order phase transition in a high-density regime. If this is the case, as suggested by some effective model studies, there must be a "critical" value of $\mu_{\rm B}$ above which a first-order phase transition occurs and below which only a crossover is found. This separating point is the QCD critical point and critical fluctuations associated with the second-order phase transition should be expected at this point. Its exact location is still under dispute, and the lattice-QCD results [17] disfavors the existence of the QCD critical point for $\mu_{\rm B}/T \lesssim 2$.

Interestingly, the QCD critical point emerges with nonzero physical quark masses, so that it belongs to not the O(4) but the Z(2) universality class. Moreover, the dynamical universality class has been also identified as the model H (dynamics of the liquid-gas critical point of a fluid) [18] (see a review [19] for detailed classification). The dynamical critical exponents are important inputs for simulations including the critical slowing down effects [20].

For experimental signatures, we can in principle seek for enhanced fluctuations coupled to the critical modes. Since the critical modes appear in a mixed scalar (i.e., chiral condensate) and vector (i.e., baryon density) channel at the QCD critical point [21], the baryon number fluctuations are sensitive to the criticality. Let us denote the baryon number fluctuation by $\delta N = N - \langle N \rangle$ where N is the number of net baryons at each collision event and $\langle \cdots \rangle$ stands for the ensemble average taken over collision events. At the critical point, generally, the correlation length ξ diverges, and it was pointed out in Ref. [22] that the non-Gaussian fluctuations behave as

$$\langle (\delta N)^k \rangle_c \sim \xi^{k(5-\eta)/2-3} . \tag{1}$$

Here, the subscript c represents a part of the correlation function corresponding to the connected diagrams (to extract non-Gaussian fluctuations) and η is the anomalous dimension (which is usually $\eta \ll 1$). Higher-order fluctuations are more sensitive to the criticality, but they need more statistics, in particular, to construct connected contributions. Now, the third order ($k = 3$) and the fourth order ($k = 4$), normalized by the $k = 2$ fluctuation (variance), $\sigma_B^2 = \langle (\delta N)^2 \rangle$, in Eq. (1) are common measures for the QCD critical point search; namely,

$$S_B = \frac{\langle (\delta N)^3 \rangle}{\sigma_B^3} , \qquad \kappa_B = \frac{\langle (\delta N)^4 \rangle_c}{\sigma^4} = \frac{\langle (\delta N)^4 \rangle}{\sigma_B^4} - 3 . \tag{2}$$

S_B and κ_B are called the skewness and the kurtosis with respect to the baryon number, and characterize how skewed and how sharp the distribution of δN appears, respectively. It is noted that, in the QCD-physics context, κ_B (or the fourth-order cumulant) was first considered in the lattice-QCD simulation to diagnose whether quarks are confined or deconfined [23].

This idea can be easily generalized to other observables coupled to the critical modes. Because observables in the heavy-ion collisions are integrated quantities over the whole dynamical evolution, we should look at fluctuations of conserved charges; otherwise, critical enhancement would be wiped off through the dynamical evolution. There are three representative candidates available in the heavy-ion collisions, i.e., the baryon number (B), the electric charge (Q), and the strangeness (S). In thermodynamics those fluctuations are defined by the derivatives of the pressure with respect to the chemical potentials corresponding to conserved charges, i.e., [24]

$$\chi_q^{(n)} = \frac{\partial^n [p(T,\mu_B,\mu_Q,\mu_S)/T^4]}{\partial(\mu_q/T)^n}, \tag{3}$$

where $q = B, Q, S$. In terms of these fluctuations the skewness and the kurtosis are represented as $S_q\sigma_q = \chi_q^{(3)}/\chi_q^{(2)}$ and $\kappa_q\sigma_q^2 = \chi_q^{(4)}/\chi_q^{(2)}$, respectively. Susceptibilities in mixed channels can also be defined in a similar fashion.

The baseline to be compared for the critical enhancement is estimated by an approximation of non-interacting and dilute hadronic gasses described by the Boltzmann distribution. Then, in this Boltzmann gas approximation, the chemical potential dependence is factored out, yielding,

$$S_q\sigma_q \simeq \tanh(\mu_q/T), \qquad \kappa_q\sigma_q^2 \simeq 1. \tag{4}$$

Since only the net charge is conserved, calculated as a difference between the particle and the anti-particle contributions, the above estimate is often referred to as the baseline by the *Skellam distribution* that is the probability distribution of two statistically independent variables. It is also possible to apply the Hadron Resonance Gas (HRG) model to estimate the baselines, and then, $S_q\sigma_q$ and $\kappa_q\sigma_q^2$ are generally suppressed by quantum statistical effects, that reflects deviations of the Bose and the Fermi distribution functions from the Boltzmann distribution. The major strategy for the QCD critical point search is to measure S_q and κ_q at various $\sqrt{s_{NN}}$ and look for enhancement as compared to the baseline (4).

2.3 Baryon-rich matter, an approximate triple point, and strangeness

From the HRG model estimate, the baryon number density along the chemical freeze-out line is maximized around $T \simeq 150$ MeV and $\mu_B \simeq 400$ MeV between $\sqrt{s_{NN}} = 3 - 19.6$ GeV. This has been experimentally confirmed through the K^+/π^+ ratio peaked around $\sqrt{s_{NN}} \simeq 8$ GeV. It is intuitively easy to understand that K^+/π^+ is sensitive to the baryon density, while K^-/π^- is not. In the heavy-ion collisions, the time scale is much shorter than the weak interaction, so the net strangeness should be vanishing. This means that the net chemical potential coupled to s quarks must be zero. Since s quarks have $S = -1$ and $B = 1/3$, the strangeness free condition leads to

$$\mu_S \simeq \frac{1}{3}\mu_B, \tag{5}$$

which means that the dense baryonic matter should contain strange baryons or *hyperons* that must be canceled by mesons involving $\bar{s}$ quarks such as K^+. Therefore, K^+ is enhanced at high density, while K^- is not.

In this sense, the point that is reached around $\sqrt{s_{NN}} \simeq 8$ GeV plays a special role to tell us about a regime transition: at smaller $\mu_B \lesssim 400$ MeV where physics is dominated by mesonic degrees of freedom, and at larger $\mu_B \gtrsim 400$ MeV where baryon's are dominate. Roughly speaking, the QGP transition is understood from the Hagedorn transition with the exponentially rising meson-mass spectrum, while the transition at the dense region arises from the Hagedorn transition with the baryon-mass spectrum, and two Hagedorn transition lines cross just around $\sqrt{s_{NN}} \simeq 8$ GeV. In this way, the most baryonic point around $\sqrt{s_{NN}} \simeq 8$ GeV could be regarded as a *QCD triple point* approximately facing baryon-less deconfined matter, baryon-rich deconfined matter, and confined hadronic matter [25].

From the correlations between baryon number and strangeness, the QCD triple point can be a landmark for the realization of the most strangeness matter that contains hyperons. In particular, the interactions between nucleons (N) and hyperons (Y), i.e., Y-N and Y-Y interactions are important parameters for the structure of neutron stars. The most strangeness matter would provide us with chances to constrain those interactions.

Before closing the theory status section, let us mention that the polarization measurements of Λ and $\bar{\Lambda}$ have signified the formation of matter with huge vorticity, and interestingly the polarization increases as $\sqrt{s_{NN}}$ decreases. The theory is still being developed (we cannot fully cover the literature, and see Refs. [26, 27] for reviews) and we will briefly discuss this issue next in the experimental section.

3 Current status—experiment

3.1 QCD critical point search

The latest experimental results on the QCD critical point search are shown in Fig. 3. The left panel (1) and the right panel (2) show the measurements of $S_p\sigma_p$ and $\kappa_p\sigma_p^2$ (where p stands for the proton) for the net-proton number distribution in Au+Au collisions at various $\sqrt{s_{NN}}$. We note that N in Eq. (2) is the baryon number (that is a conserved charge), but neutrons are not electrically charged, and the proton number is used experimentally as a proxy for the baryon number. Results of S_p and κ_p are shown for both

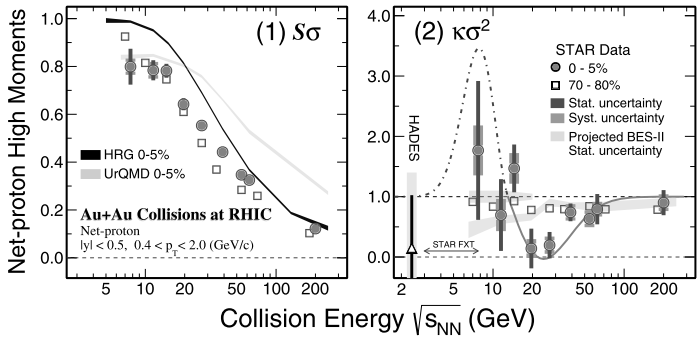

Fig. 3 Experimental results [28] of $\sqrt{s_{NN}}$ dependence of the net-proton $S_p\sigma_p$ (left) and $\kappa_p\sigma_p^2$ (right) from 70–80% peripheral (open squares) and 0–5% central (filled circles) Au+Au collisions. In the figures the subscript, p, is omitted. Projected statistical uncertainty for the second phase of the RHIC BES program is shown by the green-band. The STAR experiments fixed-target program extends the center of the mass collision energy down to 3 GeV. Results of calculations are shown as black and gold bands for the HRG model and transport model (UrQMD), respectively. The solid red and the dashed blue line in plot (2) is a schematic representation of the expectation from a QCD-based model calculation in the presence of a critical point

central ($0-5\%$, small impact parameter) and peripheral ($70-80\%$, large impact parameter) collisions. Also shown are the expectations from the HRG model and a transport based model called Ultra relativistic Quantum Molecular Dynamics (UrQMD), calculations for central Au+Au collisions without including critical fluctuations.

The following conclusions can be drawn: (a) as we go from lower order moments ($S_p\sigma_p$) to higher order moments ($\kappa_p\sigma_p^2$), deviations between central and peripheral collisions for the measured values increase. (b) Central $\kappa_p\sigma_p^2$ data show a non-monotonic variation with collision energy at a significance of $\sim 3\sigma$ [28]. (c) Experimental data show deviation from heavy-ion collision models without a critical point. Although a non-monotonic variation of the experimental data with collision energy looks promising from the point of view of the QCD critical point search, a more robust conclusion can be derived when the uncertainties get reduced and significance above 5σ is reached. The goal of the second phase of the BES program (BES-II) at RHIC and the fixed target (FXT) programs designed to have high precision measurements in the energy range of $\sqrt{s_{NN}} = 3 - 19.6$ GeV.

The data presented in Fig. 3 provides the most relevant measurements over the widest range in μ_B ($20-450$ MeV) to date for the critical point search and for comparison with the baryon number susceptibilities computed from QCD to understand the various features of the QCD phase structure. The deviations of $\kappa_p\sigma_p^2$ below the baseline, shown in Eq. (4), are qualitatively consistent with theoretical considerations including a critical point [29]. However, the conclusions on the experimental confirmation of the QCD critical point might be made only after improving the precision of the measurements at lower collision energies and by comparing the QCD calculations with critical point behavior which includes the dynamics associated with heavy-ion collisions. See Ref. [30] for the latest report.

3.2 High baryon density matter

Figure 4a in the upper panel shows the energy dependence of K/π particle yield ratio. The results are from AGS [31–33], SPS [34, 35], and RHIC [13]. These ratios reflect the strangeness content relative to entropy of the system formed in heavy-ion collisions. The thermal model calculation is shown as yellow band for K^+/π^+ and green band for K^-/π^-. The dot-dashed line represents the net-baryon density at the chemical freeze-out as a function of collision energy, calculated from the thermal model [36].

The following observations can be made. (a) The collision energy dependence of both the ratios is fairly well described by a thermal model calculation. (b) A peak position in energy dependence of K^+/π^+ is observed and has been suggested to be a signature of a change in degrees of freedom (baryon to meson [37] or hadrons to QGP [38]) while going from lower to higher energies. (c) The calculated net baryon density exhibits a maximum value as the collision energy is scanned, with a value of about three-fourth of the normal nuclear saturation density (i.e., $\rho_0 \simeq 0.16$ nucleons/fm^3). The collision energy where the maximum net-baryon density occurs is very close to the peak position of the K^+/π^+ ratio. This way of representating the results of experimental measurements and theory calculations serve to demonstrate clearly that the freeze-out density and K^+/π^+ ratio could be related. (d) The K^-/π^- ratio seems unaffected by the changes in the

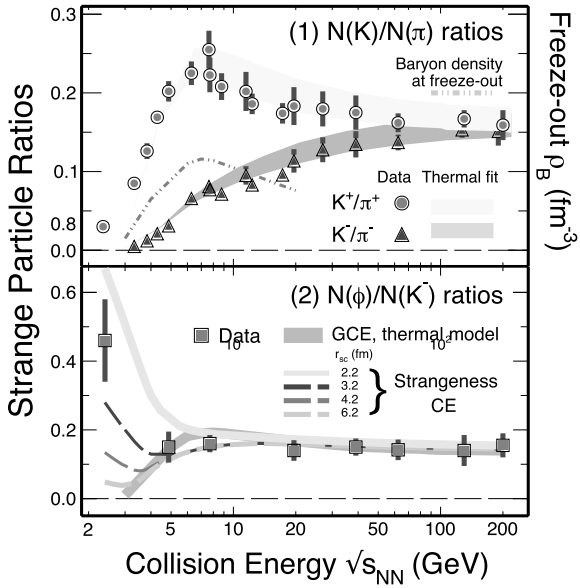

Fig. 4 a Particle yield ratios of kaons to pions as a function of $\sqrt{s_{NN}}$. Thermal fits are also shown as bands in the plot. The dot dashed line represents the net-baryon density at the chemical freeze-out. K^+/π^+ (circles) trace the baryon density at the chemical freeze-out well, while K^-/π^- (triangles) increase smoothly as a function of $\sqrt{s_{NN}}$. **b** Particle yield ratios of ϕ-meson to kaon (ϕ/K^-) as a function of $\sqrt{s_{NN}}$. At energy below 8 GeV, the GCE fit no longer works, and the strangeness CE takes over

net-baryon density with collision energy and shows a smooth increasing trend.

Through these measurements we have the knowledge of regions in collision energy where the maximal net-baryon density is reached. This is an important aspect in the context of planning of experiments that seek to explore compressed baryonic matter.

3.3 Tests of thermal model—GCE vs. CE

Relativistic statistical thermodynamics has been applied to systems ranging from cosmology to heavy-ion collisions in the laboratory. The cosmological applications usually deal with systems having large volumes and matter or radiation; hence, the GCE is a suitable description, as we slightly mentioned in the theory section of this paper. For heavy-ion collisions, the situation is complicated due to the femtometer-scale nature of the systems. Often one assumes (approximate) local thermal equilibrium for such processes. Further, such thermal models based on the GCE employ chemical potentials to account for conservation of quantum numbers on average. These GCE models have been able to explain the particle production successfully for a wide range of collision energies [12]. However, conservation laws do impose restriction on particle production if the available phase space is reduced. Hence, the relativistic statistical thermodynamics provides two choices for the formalisms: a GCE and a CE approaches [39]. In the thermodynamic (large volume) limit, the GCE and the CE formalisms are equivalent, but it is an interesting question to ask where and when the transition from a GCE picture to a CE one occurs for finite volume systems produced in collisions in man made collisions, where the collision energy spans from a few GeV to a few TeV (three orders in magnitude).

Figure 4b in the lower panel shows the energy dependence of ϕ/K^- yield ratio. For most collision energies, the ratio remains constant. Similar to the K^-/π^- ratio, the ϕ/K^- ratios seem not to be affected by the net-baryon density. Below the collision energy where the freeze-out net-baryon density peaks [shown by the dot-dashed line in Fig. 4a] the ϕ/K^- ratio starts to increase. Thermal model calculations, adopting the GCE, which has been quite successful in accounting for the observed yields of the hadrons in heavy-ion collisions, explains the measurements up to collision energy of 5 GeV. Then, the GCE model values decrease, while the increase in ϕ/K^-

at lower energies is explained by using a thermal model within the CE framework for strangeness. Note that a control parameter, r_{sc}, is introduced for strangeness CE results in Fig. 4b. The physical meaning of r_{sc} is a typical spatial size of $s\bar{s}$ correlations. For smaller r_{sc}, pairs of s and $\bar{s}$ stick together and the strangeness free condition is satisfied locally, which suppresses the yield of K^- and thus enhances ϕ/K^-. This makes a quantitative difference from the GCE results. For a given volume of the whole system, r_{sc} determines how close to the GCE/CE situation the strangeness sector in the system should be. Since the r_{sc} reflects the intrinsic properties of matter, the shifting from the GCE to the CE in strangeness signals a considerable change of the medium properties. Future measurements of ϕ/K^- at lower collision energies can be used as an observable to estimate the volume in which the open strangeness is produced (reflected by the value of r_{sc}).

3.4 Lifetime of hypernuclei

Hypernuclei are bound states of nucleons and hyperons; hence, they are natural hyperon-nucleon correlated systems [40]. They can be used as an experimental probe to study the hyperon-nucleon (Y-N) interaction. Studying hypernuclei properties is one of the best ways to investigate the strengths of Y-N interactions. Theoretically, the lifetime of a hypernucleus depends on the strength of the Y-N interactions. Therefore, a precise determination of the lifetime of hypernuclei provides direct information on the Y-N interaction strength. The high energy heavy-ion collisions at RHIC and LHC create favorable conditions to produce hypernuclei in significant quantities. At the moment, the experiments have measured the production of the lightest hypernuclei, i.e., the hypertriton, ${}^{3}_{\Lambda}\mathrm{H}$, which is a bound state of a proton, a neutron and a Λ.

Figure 5 shows a compilation of the measurement of the hypertriton lifetime from various experiments and theory calculations [41, 42]. The lifetime of the (anti-) hypertriton is determined by reconstructing the mesonic decay channels. A statistical combination of all the experimental results yields a global average lifetime of 206^{+15}_{-13} picoseconds. The lifetime is about 22% shorter than the lifetime of a free Λ of 263.2 $\pm$2.0 picoseconds, indicating a possibility of a reasonable hyperon-nucleon interaction in the hypernucleus system. Most calculations predict the hypertriton lifetime to be in the range of $213 - 256$ picoseconds. The Y-N interaction is of fundamental interest, for it controls the onset of strange degrees of freedom in high density nuclear matter, such as matter in the neutron star. The lifetime measurements of hypernuclei thus provides a crucial input for models attempting to understand physics of the neutron star. One should be aware of discrepancies in the measured lifetime of ${}^{3}_{\Lambda}\mathrm{H}$ from RHIC and LHC. High statistics data are called for in order to resolve these discrepancies.

3.5 Polarization and spin alignment

Recently, it was realized that the initial condition of the QGP in relativistic heavy-ion collisions is subjected to two extraordinary parameters. The angular momentum and the magnetic field. The angular momentum of the order of $10^7\hbar$ is theorized to be imparted to the system through the torque generated when two nuclei collide at non-zero impact parameter with center-of-mass energies per nucleon of a few 100 GeV [43]. This leads to a thermal vorticity of the order of 10^{21} per second for QCD matter formed in the collisions [44]. Furthermore, when the two nuclei collide in the LHC, an extremely strong magnetic field of the order of 10^{15} T is generated by the spectator protons, which pass by the collision zone without breaking apart in inelastic collisions. The effect of the angular momentum (which is a conserved quantity) is expected to be felt throughout the evolution of the system. In contrast to that, the magnetic field is transient in nature and stays for a short time of the order of $\sim$ 0.1 fm/c unless the electric conductivity is large (but this is disfavored, see discussions in Ref. [45]). Just to give an idea of the magnitude of these values, the highest angular momentum measured for nuclei (near the Yrast line) is $\sim 70\hbar$ and the strongest magnetic field we have managed to produce in the laboratory is $\sim 10^3$ T using the electromagnetic flux compression technique. Getting experimental signatures of these phenomena is not easy due to the femtoscopic nature of the system (both in space and time) formed in the heavy-ion collisions. Nevertheless, the experiments at RHIC and LHC have been able to address this challenging problem.

It is known that the spin-orbit LS coupling causes the fine structure in atomic physics and the shell structure in nuclear physics, and is a key ingredient in the field of spintronics in materials sciences. The LS coupling is also expected to affect the development of the rotating QGP created in collisions of nuclei at high energies. The extremely large initial value of the orbital angular momentum is expected to lead to the polarization of quark spin along the direction of the angular momentum of the plasma's rotation due to the LS coupling [46]. This should in turn cause the spins of vector (spin = 1) mesons (K^{*0} and ϕ) to align [47] and hyperons like Λ baryons to be polarized [44]. Both hyperon polarization and the spin alignment can be studied by measuring the angular distribution of the decay products of Λ and vector mesons. The hyperon polarization is found to increase with decreases in heavy-ion collision energy. The thermal vorticity values thus show that the QGP formed in the collisions, along with exhibiting the emergent properties of relativistic fluid, is also the most vortical fluid found in nature [44].

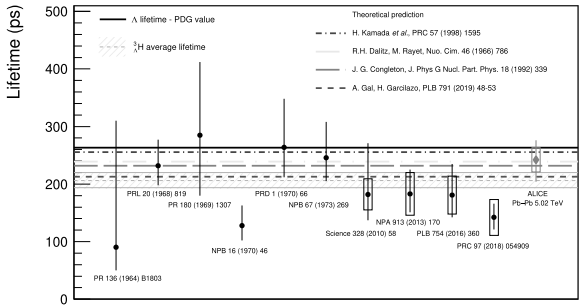

Fig. 5 Collection of the hypertriton lifetime measurements from different experiments [41, 42]. The vertical lines and boxes are the statistical and the systematic uncertainties, respectively. The orange band represents the average of the lifetime values and the lines at the edge correspond to 1σ uncertainty. The dot-dashed lines are four theoretical predictions

Meanwhile, the observed spin alignment of vector mesons (with $J = 1$) was quantified by obtaining the probability of finding a vector meson in a $J_z = 0$ state along the z direction that is the direction of the orbital angular momentum of the rotating QGP. The momentum dependence of these probability values indicated polarization of quarks in the presence of large initial angular momentum in heavy-ion collisions and a subsequent hadronization by the process of recombination [47].

4 Future directions—theory

There remain many theoretical challenges in understanding the physics of dense baryonic/quark matter with magnetic field and rotation. Below we present brief summaries on some of these issues.

4.1 QCD phase structures and quark matter at high baryon density

Theoretically, it is highly nontrivial how quarks can melt from hadrons in cold and dense matter. Unlike hot QCD even an approximate measure for quark deconfinement is still unknown or such an order parameter simply may not exist.

The QCD critical point is a landmark on the QCD phase diagram; the next intriguing question is where we can find quark matter. One might naively think that the asymptotic freedom with a large quark chemical potential, $\mu_q \gg \Lambda_{QCD}$, makes quarks unbound from hadrons, but this is not necessarily true. When μ_q is large, quarks form a Fermi sphere, and the typical energy scale of quarks near the Fermi surface is $\sim \mu_q$. However, gluons can still carry soft momenta, mediating confining forces. Therefore, excitations on top of the Fermi surface are still confined, while the Fermi sphere itself is dominated by quarks, and this refined picture of a dense baryonic state is called quarkyonic matter [48].

One can develop a more precise definition of quarkyonic matter by deforming the fundamental theory; in reality $N_c = 3$ where N_c is the number of colors, and one can significantly simplify theoretical treatments by taking the $N_c \to \infty$ limit. In this special limit, the ground state could have an inhomogeneous crystalline shape [49] (see also a review [4] for comprehensive studies of inhomogeneous phases). In reality, mesonic fluctuations would destroy inhomogeneity, but some remnant correlations can still remain. Those remnants of enhanced spatial correlations would increase the density fluctuation. For experimental detections to discriminate it from bubble formation associated with a first-order transition beyond the QCD critical point, more theoretical work is needed.

4.2 Neutron star phenomenology

We specifically pick two problems here in neutron star phenomenology. One is a question of whether quark matter is found in cores of the neutron star, which is a continued subject from the above problem of the phase diagram, and the other is what is called the hyperon puzzle.

It is an experimental fact that massive neutron stars whose masses are greater than $2M_\odot$ exist, where $M_\odot$ represents the solar mass. This observations is strong enough to constrain the stiffness of the equation of state (EoS) and a strong first-order phase transition has already been excluded. Thus, even if quark matter existed in cores of the neutron star, it is likely that there is only a smooth crossover or a weak first-order transition from nuclear to quark matter.

Matter created in heavy-ion collision is regarded better as hot and dense baryonic matter. Since the physical observables are sensitive to the EoS, the global analysis of experimental data would quantify the most likely regions of EoS parameters. Such a program of global Bayesian analysis has already been successful at large $\sqrt{s_{NN}}$ where

the experimentally inferred EoS is found to be consistent with the lattice-QCD results [50]. The same machinery could in principle constrain the EoS of hot and dense baryonic matter. One of the most interesting EoS parameters is the speed of sound c_s^2, which hints the presence of quark matter as discussed in Ref. [51]. We also mention that the global analysis of the flow measurements could constrain the viscosities of dense matter (apart from leptonic contributions), which should be useful for considerations of the r-mode evolutions of neutron stars [52]. See, for example, Ref. [53] for a theoretical estimate of viscosities of dense nuclear matter.

Let us now turn into the hyperon puzzle that has twofold manifestations. If the baryon density reaches several times ρ_0, inside the neutron star to balance the gravitational force, it is energetically more favorable to activate the strangeness degrees of freedom. One problem is that the introduction of strangeness generally softens the EoS and it would become more difficult to support the neutron stars with a mass $\gtrsim 2M_\odot$. Another problem is that once hyperons are favored, the direct Urca process would shorten the time scale of the neutron star cooling, which would make the neutron star too cold. Thus, the threshold of the neutron star mass to open the direct Urca process is an important parameter, and this is dictated by the Y-N and Y-Y interactions as well as three-body forces involving hyperons.

Theoretically speaking, the most promising approach is the first-principles calculation of the baryon interactions including nontrivial strangeness from lattice-QCD simulations [54]. In the HAL QCD method, the Nambu-Bethe-Salpeter wave functions are computed on the lattice, from which the potential is extracted; see Ref. [55] for a review on the HAL QCD method including hyperon results. For example, $p\Xi^-$ correlation has been theoretically predicted to have attractive interaction [56]; this is an interesting system since $\Xi^- \sim dss$ is a multi-strange baryon, and the experimental signature is reported [57]. Also, the correlations of $\Omega\Omega$ and $N\Omega$ have also been estimated in Ref. [58] based on the lattice-QCD determined potential. For more comprehensive discussions to quantify the potential from the correlations in heavy-ion collisions, see a recent review [59].

4.3 Dibaryons and diquarks

$\Omega\Omega$ is an interesting candidate for one of possible dibaryons [60] are six-quark objects. There is a long history of the dibaryon hunting (see Ref. [61] for a review); the idea is traced back to the conjecture on the H-dibaryon [62]. One might think that the deuteron is also a six-quark bound state, but what is special about the H-dibaryon is that diquark correlation plays an essential role. From the one-gluon exchange interaction, the color-triplet diquarks are favored and the low-energy reduction leads to the Breit interaction involving the color and the spin degrees of freedom. It is an established notion that the energetically most favored channel is the spin-singlet and the flavor-triplet, and diquarks in this channel are called "good diquarks," while the second stable diquarks, i.e., "bad diquark," are found in the spin-triplet and the flavor-sextet channel. The structure of the H-dibaryon is considered to be dominated by three good diquarks, i.e., $H \sim (ud)(ds)(su)$.

It is still challenging to find a direct signature of the strong diquark correlation. From the theoretical point of view, the difficulty lies in the fact that diquarks are not gauge invariant. Nevertheless, the density-density correlation in baryon wave-functions could quantify the diquark correlation in a gauge-invariant way [63]. Interestingly, the diquark correlations would be more prominent at higher baryon density. Actually, it is a solid theoretical prediction that QCD matter at asymptotically high density should be a color superconductor in which the diquarks form condensates. If there is no sharp transition separating baryonic matter from color-superconducting quark matter, as is conjectured in the quark-hadron continuity scenario, one can expect some remnants of the diquark correlations in density regions accessible by the heavy-ion collision. The interesting question is whether diquarks are treated as active thermal degrees of freedom, participating in the thermal model in dense matter; see Ref. [64] for a model with colored thermal excitations like diquarks. Since the lattice-QCD calculation is not functional at finite density, the test can be made only in comparison to experimental data.

4.4 Femto-nova rotating with magnetic fields

One of the profound features of matter created in the heavy-ion collisions is that non-central collisions are accompanied by vorticity and magnetic fields as illustrated in Fig. 1. Such a hot, dense, and rotating object exposed under the magnetic field can be thought of as an emulator of a proto-neutron star after a supernova, and we may well call this heavy-ion system the femto-nova.

The femto-nova investigations have a lot of research potentials. Relativistic rotation and magnetic fields would change the properties of matter, or even the phase diagram should be affected [65]. In numerical simulations of the supernovae and the neutron-star-mergers, effects of rotation and magnetic fields have not been taken into account yet. Thus, the heavy-ion collision experiments can constrain uncertainties in the interplay of rotation and magnetic field in strongly interacting matter. In particular, relativistic formulations of spin- and magneto-hydrodynamics are still in the process of developments.

From the point of view of the topological effects, rotation and magnetic fields are of paramount importance. Once the density (finite μ_B), the rotation (finite angular

velocity $\boldsymbol{\omega}$), and the magnetic field $\boldsymbol{B}$ are coupled together, the QCD theory tells us that the *chiral separation effect* (CSE) and the *chiral vortical effect* (CVE) should appear (see Ref. [66] for a review):

$$\boldsymbol{J}_5 = \sigma_s \boldsymbol{B}\,, \qquad \boldsymbol{J}_5 = \sigma_v \boldsymbol{\omega}\,, \tag{6}$$

where $\sigma_s \propto \mu_{\rm B}$ if the particle masses are negligible. The coefficient σ_v has two components; one is $\propto T^2$ and the other $\propto \mu_{\rm B}^2$. Here, $\boldsymbol{J}_5$ is the axial current, and its physical meaning is the spin expectation value of matter. Therefore, the left equation in Eq. (6) physically represents the spin polarization, and what is nontrivial in relativistic systems is that the spin and the momentum of massless fermions are tightly correlated with a certain handedness. Therefore, global spin polarization results from the CSE leading to the chirality separation associated with a chirality flow along the polarization.

The second equation, i.e., the CVE, looks like a counterpart of the CSE with $\boldsymbol{B}$ replaced by $\boldsymbol{\omega}$, but physical interpretations are rather nontrivial. In this context, the physical meaning of the CVE is the relativistic realization of the *Barnett effect* (see Ref. [67] for a review by Barnett himself); a mechanical rotation yields nonzero magnetization [68]. One might then wonder if the chiral anomaly mechanism could be an independent origin from the conventional *LS* coupling. Actually, in the nonrelativistic Barnett effect, the magnetization is inversely proportional to the gyromagnetic ratio, and so, it is proportional to the mass; this has motivated the nuclear Barnett effect experiment [69]. The CVE is more prominent, however, for massless fermions, and their mass dependences look competing. The theoretical framework is not yet complete to incorporate all those effects consistently for arbitrary masses of fermions. Establishing a firm bridge between nonrelativistic and relativistic (as seen in the heavy-ion collision) Barnett effects is a challenging subject in theory.

5 Future directions—experiment

5.1 More on the QCD critical point

As discussed above, the search for the QCD critical point has been led by the RHIC BES program, where the collision energy has been dialed down from 200 GeV (see Fig. 3). It spans a $\mu_{\rm B}$-range from 20 to 400 MeV of the phase diagram. The fluctuations near the QCD critical point are predicted to make $\kappa_B\sigma_B^2$ swing below its baseline value (= 1.0) as the critical point is approached, then going well above, with both the dip and the rise being significant for head-on nuclear collisions [29]. The data show a substantial drop and intriguing hints of a rise for the lowest energy collisions, although the uncertainties at present are too large to draw definitive conclusions, see panel (2) of Fig. 3. The ongoing phase-II of the BES program and the fixed target program at RHIC aim to gather high statistics data to look for this important landmark in the QCD phase diagram. The lattice-QCD calculations suggest that the QCD critical point, if exists, lies in the region of $\mu_{\rm B}/T \gtrsim 2$ [17]. Thus, the role of the upcoming high baryon density experiments as listed below becomes important in the critical point search program. Not only do they extend the search to high $\mu_{\rm B}$ regions (≈ 750 MeV) of the phase diagram, they also provide a reverse approach of studying the critical point observable by dialing up the beam energy. This approach is complimentary to the current searches and the observable studied from both directions of collision energy (i.e., from both above and below the QCD critical point) is expected to meet at a common point. This would be a complete test of the theoretical prediction of non-monotonic variation of $\kappa_B\sigma_B^2$ with collision energies.

5.2 Light hypernuclei production

Figure 6 shows the yields of light-nuclei and (multi-)hypernuclei at mid-rapidity, from thermal (HRG) model calculations, shown as a function of colliding energy. All of the data points are from Refs. [70, 71] (see also Ref. [72] for a theoretical analysis). As one can see in the figure, all of the light hypernuclei yields peak around the range of $3-8$ GeV that is fully covered by both the STAR fixed target (FXT) program [73] (hatched region) and the future CBM experiment at FAIR [74].

Data of K^+ over pion ratios show a peak at the center-of-mass energy of 8 GeV implying that the baryon density at chemical freeze-out reaches maximum around this colliding energy; see Fig. 4 top panel. Due to the relatively low production threshold, the production of the Λ hyperon becomes abundant. The coalescence process [75] combines these advantages and leads to the copious production of the hypernuclei in this energy region. The strangeness degrees of freedom are therefore introduced into the dense nuclear matter. The cross sections for hypernuclei production in high energy nuclear collisions are much higher than that in either elementary collisions or in Kaon-induced interactions, thus making heavy-ion collision as a hypernuclei factory (HNF). HNFs offer a new opportunity for studying fundamental interactions of hyperon-nucleon (Y-N), hyperon-hyperon (Y-Y) within the many-body baryonic system, and the spectroscopy of nuclear structure with strangeness [76].

In addition, these nuclear collisions could provide the means to study the inner dynamics of compact stars in the laboratory. We should note that most of the studies on hypernuclei so far utilized a "light system" with electron or pion or Kaon beams. In such cases, the hypernuclei were produced in the vacuum. Data on hyperon production in nuclear collisions is scarce [77]. Measurements of hypernuclei collectivity in the truly heavy-ion, Au+Au, collisions, for example, allow us to extract information on the transport properties (crucial for neutron

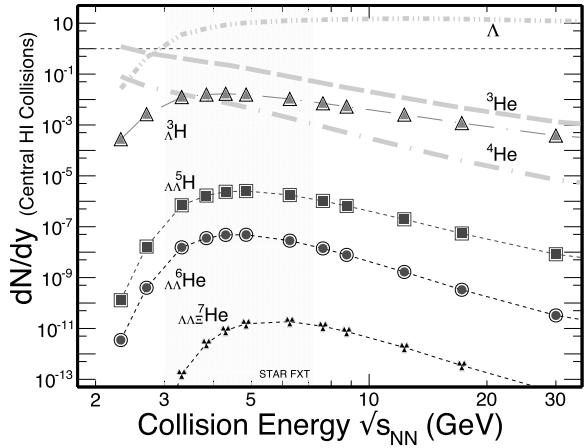

Fig. 6 Heavy nuclei (dashed lines) and (multi-)hypernuclei (symbols) yields calculated in the HRG model [70, 71] for central heavy-ion collisions at mid-rapidity as a function of center-of-mass energy. Also shown for comparison are the yields of Λ hyperon from the same model. The collision energy region of fixed target program in STAR is indicated as a yellow band. Model results from Ref. [71]

star stability, see Ref. [53]) as well as the *Y-N* interaction driven EoS, with the strangeness degrees of freedom, in the hot and dense environment where the baryon density could be very high. Simulations for neutron star inner properties crucially depend on the EoS; see Ref. [78] for the effect of *Y-Y* interactions and also Ref. [79] for the hyperon effects including the possibility of quark mixture. Furthermore, an additional benefit of the unique high baryon density environment is the enhanced production of multi-Λ hypernuclei as already suggested in Fig. 6.

The future fixed target experiments, aimed for high baryon density matter, will collect data in heavy-ion collisions around 2 − 8 GeV, which is within ideal energy range serving as the HNF, see Fig. 6. Hence, these future experiments could make tremendous contributions towards measuring the yields of hypernuclei and their life-time. This would then provide valuable inputs to understanding the hyperon-nucleon (*Y-N*) interactions in heavy-ion collisions and the inner dynamics of the compact stars.

5.3 Fluid vorticity of high baryon density matter

Experiments at RHIC and LHC have observed that the polarization of hyperons and vector mesons have a distinct energy dependence. Their values increase with decrease in collision energy. The physics reasons attributed for the observed energy dependence are twofold. First, the baryon stopping is enhanced and shear flow patterns in the beam direction emerge; second, the shorter lifetime of the fluid phase thereby allows perseverance of the initial vorticity in the system and keeps it from getting diluted [80]. The possibility of high interaction rate experiments in high baryon density matter at the upcoming facilities opens up a unique opportunity to study relativistic effects of the spin, the orbital angular momentum, and the magnetic field in QCD matter. This will guide theoretical developments in the field of relativistic spin- and magneto-hydrodynamics.

5.4 Future experimental facilities for high baryon density matter

The upcoming facilities for studying high baryon density matter includes (a) the Nuclotron-based Ion Collider fAcility (NICA) at the Joint Institute for Nuclear Research (JINR), Dubna, Russia, (b) the Compressed Baryonic Matter (CBM) at Facility for Antiproton and Ion Research (FAIR), Darmstadt, Germany, (c) the Japan Proton Accelerator Research Complex (J-PARC), Ibaraki, Japan, and (d) the CSR External-target Experiment (CEE) at High Intensity heavy-ion Accelerator Facility (HIAF) [81], Huizhou, China. The interaction rates of these upcoming experiments compared to existing and other future facilities are shown in Fig. 7. Note that all the new facilities will focus on the energy region where the baryon density is high. Below, we discuss briefly the salient features of these four experiments.

5.4.1 NICA@JINR

At this new accelerator complex that is under construction, the plan is to provide accelerated particle beams

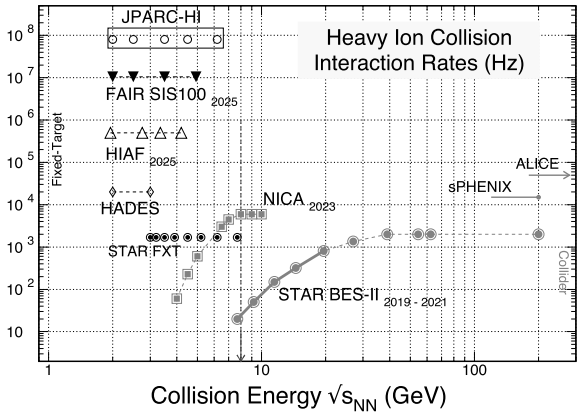

Fig. 7 Interaction rates (in Hz) for high-energy nuclear collision facilities. Collider mode: the second phase RHIC beam energy scan (BES-II) [73] for 7.7 GeV $< \sqrt{s_{NN}} <$ 19.6 GeV (filled-red-circles) and NICA (filled-red-squares) [82]. Fixed target mode: STAR fixed target (FXT) program for 3.0 GeV $< \sqrt{s_{NN}} <$ 7.2 GeV (filled-black-circles), FAIR (CBM, SIS) [74], HADES [83], J-PARC [84], and HIAF [85]. Also shown for reference are the expected collision rates of ALICE at LHC [86] and sPHENIX at RHIC [87]

both in collider (Multi Purpose Detector) and fixed target (Baryonic Matter at Nuclotron) modes [82]. The center of mass collision energies will be in the range of $\sqrt{s_{NN}} = 4-11$ GeV. The dominant physics goals are dominantly to explore the QCD phase diagram through measurements of particle yields, collective flow, femtoscopy, etc. In addition, NICA will also study polarization of hyperons and investigate hyperon-nucleon (Y-N) interactions through hypernuclei production. As seen in Fig. 7, NICA connects the high-energy collider experiments with the FXT experiments nicely.

5.4.2 CBM@FAIR

This facility currently under construction will offer the opportunity to study nuclear collisions at extreme interaction rates. It will initially comprise of the SIS100 ring will provide center of mass energy for gold beams of $\sqrt{s_{NN}} = 2.7 - 4.9$ GeV and $\mu_B > 500$ MeV. The CBM detector at FAIR has been designed as a multi-purpose device that will be capable of measuring hadrons, electrons, and muons in heavy-ion collisions over the above beam energy range at interaction rates up to 10 MHz for selected observables. The physics goals include studying the phase structure of the QCD phase diagram (i.e., the order of the transition, the QCD critical point, and chiral symmetry), the possible modification of properties of hadrons in dense baryonic matter, and the EoS at high density, which is expected to be relevant to the core of neutron stars through measurements of hypernuclei and heavy multi-strange objects.

5.4.3 JPARC-HI@KEK/JAEA

The idea of this facility has been under discussion for quite a few years and the planned J-PARC-HI will provide heavy-ion beams up to uranium for center-of-mass energies of $2 - 6.2$ GeV. This corresponds to exploring the QCD phase diagram in very high baryon densities [84]. The J-PARC-HI experiment will carry out important measurements including dileptons in order to understand QCD transitions, in-medium modifications of ρ, ω, and ϕ mesons decaying into dileptons, and rare particles such as multi-strangeness hadrons, exotic hadrons, and hypernuclei utilizing its high rates capability. According to the plan, the J-PARC-HI would be the experiment with the highest beam rate capability, up to 100MHz, which would allow measurement of rare processes with unprecedented precision in heavy ion collisions.

5.4.4 CEE@HIAF

HIAF's is under construction and it is expected to be in operation in 2025. The machine is designed to deliver bright ion beams of protons and heavy nuclei such as uranium with the center-of-mass energy up to 10 GeV and 4 GeV, respectively. A superconducting dipole magnet spectrometer experiment (CEE) [88] is also under construction. In many respects, this is a simple hadron spectrometer with the main physics focused on the measurements of proton, light nuclei including hypernuclear production and the correlation functions for understanding the QCD phase structure. In addition, meson ratios of pions will be measured with high precision in order

to extract the EoS parameters at the high baryon density region.

Future new experiments are all designed with high rates, large acceptance, and state-of-the-art particle identification, at the center of mass energy region where baryon density is high, i.e., 500 MeV $< \mu_B <$ 800 MeV, see Fig. 7.

6 Conclusions

We reviewed what we have understood so far and what we are trying to understand in the future using relativistic heavy-ion collisions. There are three important physics targets:

1 Scanning the QCD phase diagram and seeking for the QCD critical point.
2 Constraining the Y-N and Y-Y interactions and the EoS in dense baryonic matter including strangeness degrees of freedom.
3 Exploring the effects of large angular momentum and strong magnetic fields.

For (1), the "criticality" is essential to detect the critical point, and the extraction of the EoS as (2) requires global analysis including the "collectivity," and the physics of (3) exhibits topologically nontrivial effects once nonzero "chirality" is involved. These three Cs abbreviate the future directions of the heavy-ion collision physics.

The first-principles calculations from the lattice-QCD simulation have shown tremendous progresses with the cutting-edge computing technologies also toward the high-density region. Now understanding the QCD phase structure requires experimental data together with theoretical approaches. The QCD critical point is a landmark, and the next question is what awaits beyond it. If a first-order phase transition is reached, the spinodal decomposition and the nucleation processes would lead to characteristic patterns of baryon fluctuations.

In the heavy-ion collisions of center-of-mass energy below 15 GeV, one of the important features is that the baryon density is high enough to be above the threshold for strangeness production. An interesting observation is the transitional behavior from the grand canonical to the canonical ensembles in the strangeness sector with different collision energies. Also, with abundant strangeness, N-N, Y-N, and Y-Y interactions can be investigated not only in the vacuum but in an environment with a surrounding baryonic mean field. Under such a situation, measurements of baryon correlations and collectivity involving multi-strange hadrons such as ϕ-meson, Λ, Ξ, and Ω-baryons, and hypernuclei would provide us with the information on the EoS relevant to the neutron star structures and simulations of the supernovae and the neutron star mergers. Although it is not covered in this article, as long as the penetrating observables are concerned, dilepton mass distributions for example give us information on the initial thermal properties for matter created during heavy-ion collision (see a recent review [89]).

The unique property of matter during the heavy-ion collision is the presence of rotation (or the angular momentum) and the external magnetic fields. Such extreme environments at high baryon density, with rapid rotation, and strong magnetic fields can be found not only in heavy-ion collisions but also in astrophysical phenomena. Therefore, revealing those effects in the controlled laboratory experiments could create connerstones for understanding the nature of visible matter, through the femto-nova, in the Universe.

Acknowledgements
The authors thank Drs. A. Andronic, A. Bamba, N. Herrmann, K. Redlich, H. Sako, and S. Samanta for exciting discussions. The authors also thank the colleagues from STAR and ALICE collaborations. K.F. was supported in part by the Japan Society for the Promotion of Science (JSPS) KAKENHI, Nos. 18H01211 and 19K21874. B.M. was supported in part by the Chinese Academy of Sciences President's International Fellowship Initiative and the J C Bose Fellowship from the Department of Science of Technology, Government of India. N.X. was supported in part by the National Science Foundation of China, No. 11927901 and the US DOE grant No. KB0201022.

Authors' contributions
NX,KF and BM equally contributed to all aspects of the manuscript. All authors read and approved the final manuscript.

Competing interests
The authors declare that they have no competing interests.

Author details
[1]Institute of Modern Physics, Chinese Academy of Sciences, 509 Nanchang Road, Lanzhou 730000, China. [2]College of Physical Science and Technology, Central China Normal University, Wuhan 430079, China. [3]Nuclear Science Division, Lawrence Berkeley National Laboratory, Berkeley 94720, CA, USA. [4]Department of Physics, The University of Tokyo, 7-3-1 Hongo, Bunkyo-ku, Tokyo 113-0033, Japan. [5]School of Physical Sciences, National Institute of Science Education and Research, HBNI, Jatni 752050, India.

Published online: 01 February 2021

References

1. F. Sanfilippo, PoS LATTICE2014, 014 (2015). http://arxiv.org/abs/1505.02794 [hep-lat]
2. G. Baym. Nucl. Phys. A. **698**, XXIII (2002). http://arxiv.org/abs/hep-ph/0104138
3. K. Fukushima, C. Sasaki. Prog. Part. Nucl. Phys. **72**, 99 (2013). http://arxiv.org/abs/1301.6377 [hep-ph]
4. M. Buballa, S. Carignano. Prog. Part. Nucl. Phys. **81**(39) (2015). http://arxiv.org/abs/1406.1367 [hep-ph]
5. C. S. Fischer. Prog. Part. Nucl. Phys. **105**(1) (2019). http://arxiv.org/abs/1810.12938 [hep-ph]
6. P. Chomaz, in *AIP Conf. Proc.*, vol. 610, (2002), p. 167. http://arxiv.org/abs/nucl-ex/0410024
7. I. Arsene, L. Bravina, W. Cassing, Y. Ivanov, A. Larionov, J. Randrup, V. Russkikh, V. Toneev, G. Zeeb, D. Zschiesche. Phys. Rev. C. **75**, 034902 (2007). http://arxiv.org/abs/nucl-th/0609042
8. A. Bazavov, *et al*, HotQCD. Phys. Lett. B. **795**, 15 (2019). http://arxiv.org/abs/1812.08235 [hep-lat]
9. R. D. Pisarski, F. Wilczek. Phys. Rev. D. **29**, 338 (1984)
10. S. Ejiri, F. Karsch, E. Laermann, C. Miao, S. Mukherjee, P. Petreczky, C. Schmidt, W. Soeldner, W. Unger. Phys. Rev. D. **80**, 094505 (2009). http://arxiv.org/abs/0909.5122 [hep-lat]

11. P. Braun-Munzinger, J. Stachel, C. Wetterich. Phys. Lett. B. **596**, 61 (2004). http://arxiv.org/abs/nucl-th/0311005
12. A. Andronic, P. Braun-Munzinger, K. Redlich, J. Stachel. Nature. **561**, 321 (2018). http://arxiv.org/abs/1710.09425 [nucl-th]
13. L. Adamczyk, *et al*, STAR. Phys. Rev. C. **96**, 044904 (2017). http://arxiv.org/abs/1701.07065 [nucl-ex]
14. S. Gupta, D. Mallick, D. K. Mishra, B. Mohanty, N. Xu (2020). http://arxiv.org/abs/2004.04681 [hep-ph]
15. J. Cleymans, H. Oeschler, K. Redlich, S. Wheaton. Phys. Rev. C. **73**, 034905 (2006). http://arxiv.org/abs/hep-ph/0511094
16. K. Fukushima, T. Hatsuda. Rept. Prog. Phys. **74**, 014001 (2011). http://arxiv.org/abs/1005.4814 [hep-ph]
17. A. Bazavov, *et al*. Phys. Rev. D. **95**, 054504 (2017). http://arxiv.org/abs/1701.04325 [hep-lat]
18. D. Son, M. Stephanov. Phys. Rev. D. **70**, 056001 (2004). http://arxiv.org/abs/hep-ph/0401052
19. P. C. Hohenberg, B. I. Halperin. Rev. Mod. Phys. **49**, 435 (1977)
20. B. Berdnikov, K. Rajagopal. Phys. Rev. D. **61**, 105017 (2000). http://arxiv.org/abs/hep-ph/9912274
21. H. Fujii. Phys. Rev. D. **67**, 094018 (2003). http://arxiv.org/abs/hep-ph/0302167
22. M. Stephanov. Phys. Rev. Lett. **102**, 032301 (2009). http://arxiv.org/abs/0809.3450 [hep-ph]
23. S. Ejiri, F. Karsch, K. Redlich. Phys. Lett. B. **633**, 275 (2006). http://arxiv.org/abs/hep-ph/0509051
24. F. Karsch, K. Redlich. Phys. Lett. B. **695**, 136 (2011). http://arxiv.org/abs/1007.2581 [hep-ph]
25. A. Andronic, *et al*. Nucl. Phys. A. **837**, 65 (2010). http://arxiv.org/abs/0911.4806 [hep-ph]
26. J.-H. Gao, G.-L. Ma, S. Pu, Q. Wang. Nucl. Sci. Tech. **31**, 90 (2020). http://arxiv.org/abs/2005.10432 [hep-ph]
27. E. Speranza, N. Weickgenannt (2020). http://arxiv.org/abs/2007.00138 [nucl-th]
28. J. Adam, *et al*, STAR (2020). http://arxiv.org/abs/2001.02852 [nucl-ex]
29. M. Stephanov. Phys. Rev. Lett. **107**, 052301 (2011). http://arxiv.org/abs/1104.1627 [hep-ph]
30. M. Bluhm, *et al* (2020). http://arxiv.org/abs/2001.08831 [nucl-th]
31. L. Ahle, *et al*, E866, E917. Phys. Lett. B. **476**, 1 (2000). http://arxiv.org/abs/nucl-ex/9910008
32. L. Ahle, *et al*, E-802, E-866. Phys. Rev. C. **60**, 044904 (1999). http://arxiv.org/abs/nucl-ex/9903009
33. L. Ahle, *et al*, E866, E917. Phys. Lett. B. **490**, 53 (2000). http://arxiv.org/abs/nucl-ex/0008010
34. S. Afanasiev, *et al*, NA49. Phys. Rev. C. **66**, 054902 (2002). http://arxiv.org/abs/nucl-ex/0205002
35. C. Alt, *et al*, NA49. Phys. Rev. C. **77**, 024903 (2008). http://arxiv.org/abs/0710.0118 [nucl-ex]
36. J. Randrup, J. Cleymans. Phys. Rev. C. **74**, 047901 (2006). http://arxiv.org/abs/hep-ph/0607065
37. J. Cleymans, H. Oeschler, K. Redlich, S. Wheaton. Phys. Lett. B. **615**, 50 (2005). http://arxiv.org/abs/hep-ph/0411187
38. M. Gazdzicki, M. I. Gorenstein. Acta Phys. Polon. B. **30**, 2705 (1999). http://arxiv.org/abs/hep-ph/9803462
39. R. Hagedorn, K. Redlich. Z. Phys. C. **27**, 541 (1985)
40. B. Abelev, *et al*, STAR. Science. **328**, 58 (2010). http://arxiv.org/abs/1003.2030 [nucl-ex]
41. S. Acharya, *et al*, ALICE. Phys. Lett. B. **797**, 134905 (2019). http://arxiv.org/abs/1907.06906 [nucl-ex]
42. L. Adamczyk, *et al*, STAR. Phys. Rev. C. **97**, 054909 (2018). http://arxiv.org/abs/1710.00436 [nucl-ex]
43. W.-T. Deng, X.-G. Huang. Phys. Rev. C. **93**, 064907 (2016). http://arxiv.org/abs/1603.06117 [nucl-th]
44. L. Adamczyk, *et al*, STAR. Nature. **548**, 62 (2017). http://arxiv.org/abs/1701.06657 [nucl-ex]
45. L. McLerran, V. Skokov. Nucl. Phys. A. **929**, 184 (2014). http://arxiv.org/abs/1305.0774 [hep-ph]
46. Z.-T. Liang, X.-N. Wang. Phys. Rev. Lett. **94**, 102301 (2005). [Erratum: Phys.Rev.Lett. 96, 039901 (2006)], http://arxiv.org/abs/nucl-th/0410079
47. S. Acharya, *et al*, ALICE. Phys. Rev. Lett. **125**, 012301 (2020). http://arxiv.org/abs/1910.14408 [nucl-ex]
48. L. McLerran, R. D. Pisarski. Nucl. Phys. A. **796**, 83 (2007). http://arxiv.org/abs/0706.2191 [hep-ph]
49. T. Kojo, Y. Hidaka, L. McLerran, R. D. Pisarski. Nucl. Phys. A. **843**, 37 (2010). http://arxiv.org/abs/0912.3800 [hep-ph]
50. S. Pratt, E. Sangaline, P. Sorensen, H. Wang. Phys. Rev. Lett. **114**, 202301 (2015). http://arxiv.org/abs/1501.04042 [nucl-th]
51. E. Annala, T. Gorda, A. Kurkela, J. Nättilä, A. Vuorinen. Nature Phys. (2020). http://arxiv.org/abs/1903.09121 [astro-ph.HE]
52. N. Andersson, K. D. Kokkotas. Int. J. Mod. Phys. D. **10**, 381 (2001). http://arxiv.org/abs/gr-qc/0010102
53. E. Kolomeitsev, D. Voskresensky. Phys. Rev. C. **91**, 025805 (2015). http://arxiv.org/abs/1412.0314 [nucl-th]
54. H. Nemura, *et al*, in *EPJ Web Conf.*, vol. 175, (2018), p. 05030. http://arxiv.org/abs/1711.07003 [hep-lat]
55. S. Aoki, T. Doi. Front. Phys. **8**, 307 (2020). http://arxiv.org/abs/2003.10730 [hep-lat]
56. T. Hatsuda, K. Morita, A. Ohnishi, K. Sasaki. Nucl. Phys. A. **967**, 856 (2017). http://arxiv.org/abs/1704.05225 [nucl-th]
57. S. Acharya, *et al*, ALICE. Phys. Rev. Lett. **123**, 112002 (2019). http://arxiv.org/abs/1904.12198 [nucl-ex]
58. K. Morita, S. Gongyo, T. Hatsuda, T. Hyodo, Y. Kamiya, A. Ohnishi. Phys. Rev. C. **101**, 015201 (2020). http://arxiv.org/abs/1908.05414 [nucl-th]
59. S. Cho, *et al*, ExHIC. Prog. Part. Nucl. Phys. **95**, 279 (2017). http://arxiv.org/abs/1702.00486 [nucl-th]
60. S. Gongyo, *et al*. Phys. Rev. Lett. **120**, 212001 (2018). http://arxiv.org/abs/1709.00654 [hep-lat]
61. H. Clement. Prog. Part. Nucl. Phys. **93**, 195 (2017). http://arxiv.org/abs/1610.05591 [nucl-ex]
62. R. L. Jaffe. Phys. Rev. Lett. **38**, 195 (1977)
63. C. Alexandrou, P. de Forcrand, B. Lucini. Phys. Rev. Lett. **97**, 222002 (2006). http://arxiv.org/abs/hep-lat/0609004
64. E. V. Shuryak, I. Zahed. Phys. Rev. D. **70**, 054507 (2004). http://arxiv.org/abs/hep-ph/0403127
65. Y. Jiang, J. Liao. Phys. Rev. Lett. **117**, 192302 (2016). http://arxiv.org/abs/1606.03808 [hep-ph]
66. D. Kharzeev, J. Liao, S. Voloshin, G. Wang. Prog. Part. Nucl. Phys. **88**, 1 (2016). http://arxiv.org/abs/1511.04050 [hep-ph]
67. S. J. Barnett. Rev. Mod. Phys. **7**, 129 (1935)
68. J.-H. Gao, Z.-T. Liang, S. Pu, Q. Wang, X.-N. Wang. Phys. Rev. Lett. **109**, 232301 (2012). http://arxiv.org/abs/1203.0725 [hep-ph]
69. M. Arabgol, T. Sleator. Phys. Rev. Lett. **122**, 177202 (2019)
70. A. Andronic, P. Braun-Munzinger, J. Stachel. Nucl. Phys. A. **772**, 167 (2006). http://arxiv.org/abs/nucl-th/0511071
71. A. Andronic, P. Braun-Munzinger, J. Stachel, H. Stocker. Phys. Lett. B. **697**, 203 (2011). http://arxiv.org/abs/1010.2995 [nucl-th]
72. J. Steinheimer, K. Gudima, A. Botvina, I. Mishustin, M. Bleicher, H. Stocker. Phys. Lett. B. **714**, 85 (2012). http://arxiv.org/abs/1203.2547 [nucl-th]
73. SN0598: Studying the Phase Diagram of QCD Matter at RHIC. https://drupal.star.bnl.gov/STAR/starnotes/public/sn0598
74. T. Ablyazimov, *et al*, CBM. Eur. Phys. J. A. **53**, 60 (2017). http://arxiv.org/abs/1607.01487 [nucl-ex]
75. A. Baltz, C. Dover, S. Kahana, Y. Pang, T. Schlagel, E. Schnedermann. Phys. Lett. B. **325**, 7 (1994)
76. O. Hashimoto, H. Tamura. Prog. Part. Nucl. Phys. **57**, 564 (2006)
77. C. Rappold, *et al*, HypHI. Phys. Rev. C. **88**, 041001 (2013)
78. I. Vidana, A. Polls, A. Ramos, L. Engvik, M. Hjorth-Jensen. Phys. Rev. **C62**, 035801 (2000). http://arxiv.org/abs/nucl-th/0004031 [nucl-th]
79. T. Maruyama, S. Chiba, H.-J. Schulze, T. Tatsumi. Phys. Rev. D. **76**, 123015 (2007). http://arxiv.org/abs/0708.3277 [nucl-th]
80. I. Karpenko, F. Becattini. Eur. Phys. J. C. **77**, 213 (2017). http://arxiv.org/abs/1610.04717 [nucl-th]
81. HIAF at IMP. http://english.imp.cas.cn/Work2017/HI2017/
82. N. Geraksiev, NICA/MPD. J. Phys. Conf. Ser. **1390**, 012121 (2019)
83. G. Agakishiev, *et al*, HADES. Eur. Phys. J. A. **41**, 243 (2009). http://arxiv.org/abs/0902.3478 [nucl-ex]
84. Letter of Intent for the J-PARC Heavy-Ion Program. https://j-parc.jp/researcher/Hadron/en/Proposal_e.html#1707
85. S. Ruan, *et al*. Nucl. Instrum. Meth. A. **892**, 53 (2018)
86. CERN Yellow Reports: Monographs(A. Dainese, M. Mangano, A. B. Meyer, A. Nisati, G. Salam, M. A. Vesterinen, eds.), *Report on the Physics at the HL-LHC,and Perspectives for the HE-LHC*, vol. 7/2019. (CERN, Geneva, Switzerland, 2019). ISBN 978-92-9083-549-3
87. G. Roland, Sphenix. PoS. **HardProbes2018**, 013 (2019)
88. L. Lü, H. Yi, Z. Xiao, M. Shao, S. Zhang, G. Xiao, N. Xu. Sci. China Phys. Mech. Astron. **60**, 012021 (2017)
89. P. Salabura, J. Stroth (2020). http://arxiv.org/abs/2005.14589 [nucl-ex]

Tipărit la Tipografia E.U.B.–B.U.P.
Editura Universității din București–*Bucharest University Press*

2023

2023
UNIVERSITATEA DIN BUCUREȘTI
Virtute et Sapientia

Șoseaua Panduri nr. 90, București, România
www.unibuc.ro